VYSOKÉ UČENÍ TECHNICKÉ V BRNĚ
BRNO UNIVERSITY OF TECHNOLOGY

FAKULTA STAVEBNÍ
FACULTY OF CIVIL ENGINEERING

ÚSTAV TECHNOLOGIE STAVEBNÍCH HMOT A DÍLCŮ
INSTITUTE OF TECHNOLOGY OF BUILDING MATERIALS AND COMPONENTS

STUDIUM CHOVÁNÍ VYSOKOPEVNOSTNÍCH BETONŮ PŘI PŮSOBENÍ VYSOKÝCH TEPLOT
STUDYING THE BEHAVIOR OF HIGH STRENGTH CONCRETE AT HIGH TEMPERATURES

DIPLOMOVÁ PRÁCE
DIPLOMA THESIS

AUTOR PRÁCE
AUTHOR
Bc. Kateřina Sovová

VEDOUCÍ PRÁCE
SUPERVISOR
Ing. LENKA BODNÁROVÁ, Ph.D.

BRNO 2017

VYSOKÉ UČENÍ TECHNICKÉ V BRNĚ
FAKULTA STAVEBNÍ

Studijní program	N3607 Stavební inženýrství
Typ studijního programu	Navazující magisterský studijní program s prezenční formou studia
Studijní obor	3607T020 Stavebně materiálové inženýrství
Pracoviště	Ústav technologie stavebních hmot a dílců

ZADÁNÍ DIPLOMOVÉ PRÁCE

Student	Bc. Kateřina Sovová
Název	Studium chování vysokopevnostních betonů při působení vysokých teplot
Vedoucí práce	Ing. Lenka Bodnárová, Ph.D.
Datum zadání	31. 3. 2016
Datum odevzdání	13. 1. 2017

V Brně dne 31. 3. 2016

prof. Ing. Rostislav Drochytka, CSc., MBA	prof. Ing. Rostislav Drochytka, CSc., MBA
Vedoucí ústavu	Děkan Fakulty stavební VUT

PODKLADY A LITERATURA

ČSN EN 1992-1-2 Eurokód 2: Navrhování betonových konstrukcí – Část 1-2: Obecná pravidla – Navrhování konstrukcí na účinky požáru.
Designing Concrete Structures for Fire Safety, ACI, SP-255
Bradáčová, I. Stavby z hlediska požární bezpečnosti. ERA group, s.r.o. Brno 2007. ISBN 978-80-7366-090-1.
Bodnárová, L. Kompozitní materiály, učební opora VUT Brno, FAST, 2007
Drochytka, R. Trvanlivost stavebních materiálů, učební opora VUT Brno, FAST, 2008
Sborníky z tuzemských a zahraničních konferencí (r. 2010-2015).
České a zahraniční normy. Internetové zdroje.

ZÁSADY PRO VYPRACOVÁNÍ

Vysokopevnostní betony se vyznačují řadou unikátních vlastností, zejména vysokou pevností, vysokou hutností a vysokou trvanlivostí. Vysoká hutnost betonu může být ale rizikovým faktorem při působení vysokých teplot na beton.
V teoretické části práce proveďte rešerši literatury z oblasti chování vysokopevnostních betonů vůči působení vysokých teplot.
Vyhledejte možnosti pro zvýšení odolnosti vysokopevnostních betonů vůči působení vysokých teplot.
V experimentální části diplomové navrhněte recepturu vysokopevnostního betonu a vyrobte zkušební tělesa.
Realizujte zatížení betonových zkušebních vzorků vysokou teplotou - ověřte chování zkušebních vzorků z vysokopevnostního betonu a vzorků z betonu třídy C 25/30.
Navrhněte složení vysokopevnostního betonu s vyšší odolností vůči působení vysokých teplot a ověřte, zda navržené úpravy složení betonu měly pozitivní efekt.
Zhodnoťte změny fyzikálních vlastností betonů a změny vzhledu betonů po teplotním zatížení.
Diplomová práce bude zpracována ve spolupráci s Technische Universität Wien, Institut für Hochbau und Technologie.
Doporučený rozsah diplomové práce min. 80 stran.

STRUKTURA DIPLOMOVÉ PRÁCE

VŠKP vypracujte a rozčleňte podle dále uvedené struktury:
1. Textová část VŠKP zpracovaná podle Směrnice rektora "Úprava, odevzdávání, zveřejňování a uchovávání vysokoškolských kvalifikačních prací" a Směrnice děkana "Úprava, odevzdávání, zveřejňování a uchovávání vysokoškolských kvalifikačních prací na FAST VUT" (povinná součást VŠKP).
2. Přílohy textové části VŠKP zpracované podle Směrnice rektora "Úprava, odevzdávání, zveřejňování a uchovávání vysokoškolských kvalifikačních prací" a Směrnice děkana "Úprava, odevzdávání, zveřejňování a uchovávání vysokoškolských kvalifikačních prací na FAST VUT" (nepovinná součást VŠKP v případě, že přílohy nejsou součástí textové části VŠKP, ale textovou část doplňují).

Ing. Lenka Bodnárová, Ph.D.
Vedoucí diplomové práce

ABSTRAKT

Diplomová práce se skládá ze dvou částí, teoretické a praktické. V teoretické části této studie jsou popsány vlivy vysokých teplot na strukturu betonu a chemické, mechanické fyzikální změny probíhající při tepelném zatížení. Dále je popsán jev odprýskávání betonu a metody, jak tomuto jevu zabránit. Také je popsána funkce polypropylenových a celulózových vláken v betonu. Praktická část se zabývá s návrhem, výrobou a testováním betonu na bázi cementu s použitím rozdílných vláken (polypropylenové a celulózové vlákna). Vlastnosti a aplikace ve vysokých teplotách je také zahrnuta. Je posouzen vliv zvýšené teploty na pevnost, porositu, viditelné změny vzorků, změny povrchu a degradace vzorků zatěžováním dle normové teplotní křivky (ISO 834) a křivky uhlovodíková. Samotný experiment je pro přehlednost rozdělen do dvou částí a na konci každé části jsou posouzeny výsledky z naměřených hodnot. Závěrem jsou shrnuty veškeré poznatky a vyhodnocena nejvhodnější receptura včetně návrhu postupu pro další výzkum.

KLÍČOVÁ SLOVA

explosivní odprýskávání, polypropylenová vlákna, celulózová vlákna, teplotní zatížení, normová teplotní křivka (ISO 834), uhlovodíková teplotní křivka, vysokopevnostní beton

ABSTRACT

This master's thesis is divided into two parts; practical and theoretical. The theoretical part of this study describes the influence of high temperature on concrete structure and chemical, mechanical and physical changes, which take place during the exposure to high temperatures. The thesis also evaluates spalling of concrete and the methods to prevent it, as well as the function of polypropylene and cellulose fibers in the concrete. The practical part deals with design, production and testing of the cement-based concrete with the use of different fibers (polypropylene fibers and cellulose fibers). The properties and the means of applications in high temperatures are also included. The practical part also assesses the influence of high temperature on strength, porosity, visual changes of specimens, changes of surface and degradation of testing specimens due to heat loads according to normative heat curve (ISO 834) and also according to hydrocarbon curve. For clearer arrangement, the experimental tests are divided into two parts and the measured values are evaluated at the end of each part. The conclusion resumes all data obtained by testing and evaluates what is the most suitable formulation. The approach for further research is also discussed.

KEYWORDS

explossive spalling, polypropylene fibers, cellulose fibers, thermal load, normative heat curve (ISO 834), hydrocarbon curve, high performance concrete

BIBLIOGRAFICKÁ CITACE VŠKP

Bc. Kateřina Sovová *Studium chování vysokopevnostních betonů při působení vysokých teplot.* Brno, 2017. 112 s. Diplomová práce. Vysoké učení technické v Brně, Fakulta stavební, Ústav technologie stavebních hmot a dílců. Vedoucí práce Ing. Lenka Bodnárová, Ph.D.

PROHLÁŠENÍ

Prohlašuji, že jsem diplomovou práci zpracoval(a) samostatně a že jsem uvedl(a) všechny použité informační zdroje.

V Brně dne 8. 1. 2017

Bc. Kateřina Sovová
autor práce

Acknowledgement

I would like to express my gratitude to my supervisor Ing. Lenka Bodnárová, Ph.D. for the useful comments, remarks and engagement through the learning process of this master thesis. Furthermore I would like to particularly thank Dipl.-Ing. Dr.techn. Johannes Kirnbauer for the help with experimental part of this thesis and for his patience, time, and immense knowledge.

Finally, I must express my very profound gratitude to my parents and to my friends for providing me with unfailing support and continuous encouragement throughout my years of study and through the process of researching and writing this thesis. This accomplishment would not have been possible without them. Thank you.

CONTENT

INTRODUCTION 9

AIM OF THE STUDY 11

1 THEORETICAL PART 12

1.1. Fire protection standards for tunnels 12

1.1.1 Superior European Directives for tunnel safety 13

1.1.2 Relevant Eurocodes for fire protection design 13

1.1.3 Fire curves 14

1.2. Behavior of concrete at high temperature 17

1.2.1 Influence of high temperature on cement paste 19

1.2.2 Influence of high temperatures on aggregate 21

1.2.3 Influence of high temperatures on mechanical properties of concrete 22

1.3. Spalling of concrete 24

1.3.1 Definition of spalling 24

1.3.2 Types of spalling 24

1.3.3 Mechanism of spalling 27

1.3.4 Factors influencing spalling 29

1.3.5 Methods to prevent explosive spalling 31

2 EXPERIMENTAL PART 38

2.1. Introduction of experimental part 38

2.2. Methodology 39

2.3. Preparation of the experiment 40

2.3.1 Preparation of the concrete mix 40

2.3.2 Preparation of specimens 44

2.3.3 Mixture 45

2.3.4 Concrete properties 47
2.4. Experiment 50
2.4.1 ISO – 834 curve 51
2.4.2 Hydrocarbon curve 75
2.4.3 Discussion of results 100
CONCLUSION 103
LIST OF REFERENCES 104
LIST OF FIGURES 108
LIST OF TABLES 111
LIST OF ACRONYMS AND SYMBOLS 112

INTRODUCTION

In today's world, the population keeps getting bigger and so are getting the fire hazards. This can be caused by the intensive increase in road transport, as well as in train transport, which leads to more frequent accidents in tunnels. Therefore, there is a great importance put on the building products' heat resistance and durability, especially those for concrete constructions. A big emphasis is also placed on the components themselves, in particular on the type of cement used, aggregate, additions and also on the type of fibers used (usually polypropylene, steel, glass or cellulose). During a fire, the concrete constructions are withstanding temperatures which can come up to 1200 °C, which can lead to diminishing of the quality of the concrete and can later even result in a complete destruction of the concrete.

Concrete is a high-quality, reliable building element, which serves many functions, such as static function, but also a resistance against the effect of aggressive waters, durability and waterproofness. From the fire point of view, concrete has certain advantages, where one of the biggest ones definitely is that it is fireproof and has a low thermal conductivity. The importance of concrete's resistance to high temperatures was proven in many accidents, specifically in areas where a tunnel is, namely the fire in a tunnel under Mont Blanc, where the temperature in the epicenter rose up to 1000 °C. This incident resulted in stricter norms about the safety in motorway tunnels. Nowadays, concrete mixture is adjusted to meet the special requirements of its composition. For example, polypropylene fibers are especially helpful in this case. The very first tunnel in the Czech Republic, which was built with the addition of polypropylene fibers was the tunnel near Klimkovice in the stretch of the highway D47.

Noticeable deterioration of the quality can be observed with the concrete that is not designed with the resistance against fire in mind. This deterioration is accompanied by explosive spalling that is caused by the increasing pressure in the inner pores in the concrete and in the inner pressure tension which occurs due to the expansion of the materials in higher temperatures. This results in the loss of load bearing capacity function of concrete, accompanied by spalling of cover layer of the construction, which leads to exposing of the reinforcement to the higher temperatures, which are higher than their critical value. The issue of the explosive spalling occurs with the high-performance

concretes, since they have denser and thus less permeable structure of concrete, which prevents the water vaporing out. Therefore, during a fire, the pore pressure increases, which results in explosive spalling of concrete. Furthermore, during the heating, the concrete (depending on the used mixture) can significantly lose its strength even in temperatures higher than 300 °C.

AIM OF THE STUDY

The aim of the diploma thesis is to focus on the resistance of concrete exposed to high temperatures with focus of resistance against explosive spalling. Special attention is paid of action of polypropylene and cellulose fibers. In theoretical part is an introduction to the issues of behavior of concrete at high temperature, fire protection of tunnels and explosive spalling. The main aim of experimental part is to compare the behavior of high performance concrete modified by polypropylene and cellulose fibers and the behavior of ordinary concrete C 30/37 and verify function of fibers in concrete. The concrete specimens are, in the first case, exposed to thermal load of temperatures 1100 °C reached in 30 min and subsequent isothermal dwell for 30 minutes. In the second case, the specimens are exposed to thermal load of temperatures 900 °C. The experimental work focuses on different behaviors and physical mechanical properties without any fibers, with polypropylene fibers and cellulose fibers. In addition, the specimens of high-performance concrete are compared to ordinary concrete.

1 THEORETICAL PART

1.1. Fire protection standards for tunnels

Several serious fires have already occurred in European tunnels, during which human lives have perished, serious damages of the constructions have occurred which led to long-termed shutdowns of traffic. Nowadays, methods of construction fire safety are being researched in Europe, to ensure the safety for operating the tunnels. Passive and active systems of protections against fire are considered to be a necessary part of fire safety of the tunnels, to prevent the devastating consequences of fire. The concrete, used in number of constructions of public facilities, is used as a fireproof material and if designed right, it can resist the fire for a very long time. The suggested load imitating the fire in these constructions corresponds with the cellulosic ISO-834 fire curve in the following chapter. The situation in tunnels compared to the situation in the constructions of public facilities is completely different, especially because of the presence of trucks. These vehicles often carry combustible materials, which can in the case of an accident start a fire, which means there is a larger fire strain and therefore higher maximum temperatures, as well as faster spreading of the fire [1].

In these conditions, the behavior of the concrete will be of course different. The methods of assessment are still evolving to prove the ability of the materials to protect the concrete against spalling and the steel and metal components against melting as a result of the fast increase of temperature in the conditions of the fire and to reduce the constructional as well as the economic consequences of a fire. These curves compared to the cellulosic curve can reach the maximum temperature already after 5 to 10 minutes.

An important research was HRR (Heat Release Rates, during a real fire in a tunnel), which showed the proposal curves that were closer to reality. In European research programs of the tunnel safety, complex range of fire tests were carried out. One of the big test fires took place in 2003 in abandoned motorway tunnel in Norway, it was the so-called Runehammer test. Four tests with four fires of a large scale with different types of cargo in the semitrailers were carried out. The cargo was not labeled as dangerous or flammable, it was mostly common wooden plates or plastic cups. The result was that some of the proposal curves used till that time did not correspond with the real value of speed of release of heat HRR measured during those fires. This value was higher than 200 MW and

the temperature of gasses in the surroundings of the fire was higher than 1350 °C. Based on these tests, an example of the result given was that norm ISO 834 can be used only in the case where either empty trucks or no trucks go through the tunnel [1].

In this chapter, the main European standards and guidelines for the fire protection of tunnel linings and their specific criteria are summarized as well as the most common general temperature-time curves will be showed and briefly described.

1.1.1 Superior European Directives for tunnel safety

EU Tunnel Directive 2004/54/EC [2]

The document provides minimum general requirements and specifications for the safety of road tunnels with the trans-European road network.

Directives include mainly the tunnel general layout, escape routes and emergency exits, safety installations, water supply, monitoring system, etc. with no specific requirements for structural fire resistance, except for the requirement of no collapse of important neighboring structures (cascading effect).

EU 2008/163/EC (TSI-Guideline) [2]

Technical specification in term of International multi-system operability relating to safety in railway tunnels in the trans-European conventional and high-speed rail system provides minimum safety requirements including structural requirements under fire.

Requirement of no collapse of the structure during evacuation. Fire resistance of the tunnel surface to fire impact for a time of 170 min. 17

1.1.2 Relevant Eurocodes for fire protection design

Eurocode EN 1991-1-2: Actions on structures [3]

Defines general loading assumption and general rules for the analysis of structures under the high temperature

Eurocode EN 1992-1-2: Design of concrete structures [4]

Provides general material requirements of concrete and steel reinforcement that vary with increasing temperature and detailed and simplified methodologies for the design of concrete structures under the impact of fire.

Eurocode EN 13501-1:2007+A1:2009: Fire classification of construction products and building elements [5]

Fire classification of construction products and building elements

1.1.3 Fire curves

Large deal of research of international scale has been undertaken with the aim to specify the types of fire which could occur in tunnel and underground spaces. It has been tested in both real, disused tunnels and laboratory conditions. As a result of the data gained from these experiments, a series of temperature-time curves for the various exposures have been developed ([5]-[6]). The most common general temperature-time curves are showed in Figure.

Figure 1: Temperature- time curves for fire [6]

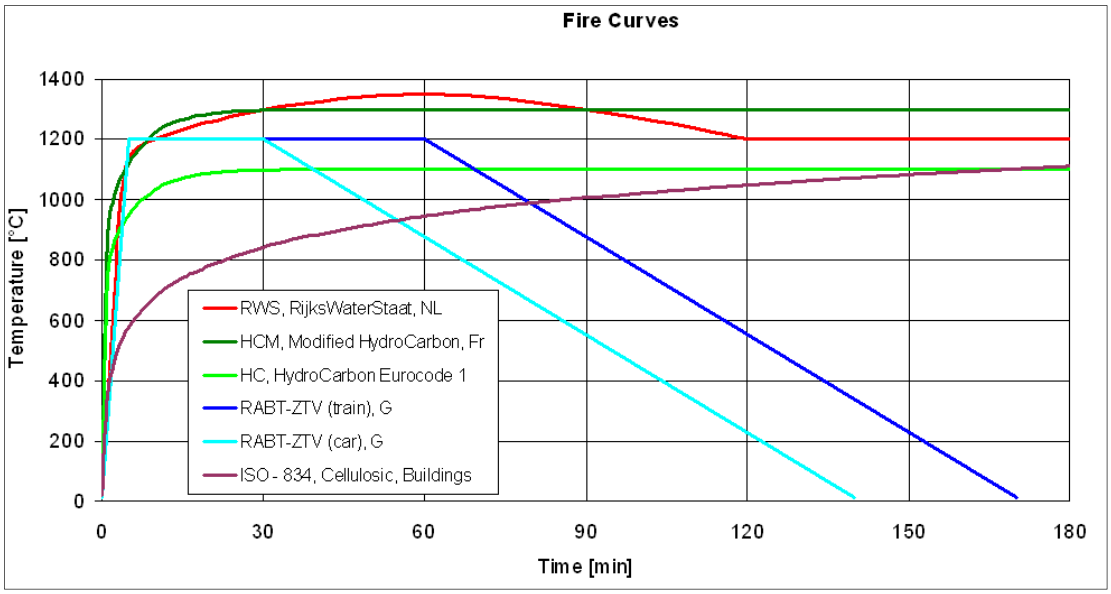

Cellulosic ISO-834 curve

This cellulosic ISO-based curve is based on the burning rate of the materials found in general building materials and contents and it is used in standards throughout the world. It is a model of a ventilated controlled natural fire, i.e. fires in a normal building. The increase of temperature after 30 minutes is 842 °C and temperature increase up to 1110 °C in 180 minutes [6].

ISO 834 specifies the temperature T [°C] as:

$T = 345 \cdot \log_{10} \cdot (8t+1) + T_0$

t … time [min]

T_0 … ambient temperature [°C]

Hydrocarbon curve

Although the Cellulosic curve has been in use for many years, it soon became apparent that the burning rates for materials such a petrol gas, chemicals and etc. have a different temperature-time load. Therefore, there was a need to develop an alternative exposure for the purpose of carrying out the experiments on structures and materials used within the petrochemical industry. The Hydrocarbon temperatute-time curve was determined as a simulation of a ventilated oil fire with a high initial temperature increase of 1100 °C after 30 minutes and then constant temperature 1100 °C hold up to 180 minutes [6].

The temperature development of the Hydrocarbon (HC) fire curve is described by the following equation:

$$T = 1080 \cdot (1 - 0{,}325 \cdot e^{-0{,}167t} - 0{,}675 \cdot e^{-2{,}5t}) + T_0$$

t … time [min]

T_0 … ambient temperature [°C]

Hydrocarbon Modified curve

Derived from the above-mentioned Hydrocarbon curve, the French regulation asks for an increased version of that Hydrocarbon curve, the so called HydroCarbon Modified curve (HCM).

The maximum temperature of the HCM curve is 1300°C instead of the 1100 °C, standard HC curve.

However, the temperature gradient in the first few minutes of the HCM fire is as severe as all Hydrocarbon based fires (RWS, HCM, HC), possibly causing a temperature shock to the surrounding concrete structure and concrete spalling as a result of it.

The temperature T (°C) in hydrocarbon fire curve is given by:

$$T = 20 + 1280 \cdot (1 - 0{,}325 \cdot e^{-0{,}167t} - 0{,}675 \cdot e^{-2{,}5t})$$

t … time [min]

T_0 … ambient temperature [°C]

RABT curve ZTV

RABT curve (Figure 1-1) was developed in Germany as a result of series of test programs such as the Eureka Project EU 499: Firetun [7]. In the RABT Curve (car, train), the temperature rise is very rapid up to 1200 °C within 5 minutes. The duration of the 1200 °C exposure is shorter than other curves with the temperature drop off starting to occur at 60 minutes for cars and 30 minutes for trains [6].

RWS curve

RWS curve, model of petroleum based fire of 300 MW fire load in an enclosed area developed by the Rijkswaterstaat, Ministry of Transport in the Netherlands is specified for use in tunnels (Figure 1-5). This curve is based on the assumption that in a worst case scenario, a 50 m³ fuel, oil or petrol tanker fire with a fire load of 300 MW could occur, lasting up to 120 minutes. It is internationally accepted. The temperature increases after 30 minutes is 1300 °C. Temperature reaches 1350 °C (melting point of concrete) for short duration in 60 minutes and then the drop off starts to occur after 60 minutes. After 120 minutes temperature is constant up to 180 minutes [6].

1.2. Behavior of concrete at high temperature

Concrete is a flexible material, which has many advantages over other construction materials. Moreover, it has good characteristics from the fire safety point of view. It can be classified on the scale of flammability as A – inflammable [8].

Nevertheless, during the exposure to high temperatures, there are physical, chemical and mechanical processes taking place in the concrete, which can be reversible or irreversible. These processes are described in Table 1. These changes can manifest themselves in a collapse of the structure of cement putty, which can lead to the loss of the load bearing capacity of the concrete. The safety and durability depends on the concrete's strength for the duration of the fire and the strength during the cooling process. Crucial are temperatures from 300 °C to 1000 °C or up to 1300 °C and the duration of the heating. In the beginning, one can expect that by heating of the concrete to high temperatures, the strength of the concrete decreases, because the putty, as well as the aggregate are changed by the heat. The changes are going to differ with each composition of the concrete and the solid components, depending on the level of heat and its duration [9].

Table 1: Changes of concrete related to temperature [10]

Temperature of concrete θ [°C]	Changes in concrete	
20 - 100	Formation of CSH gel and portlandite.	**Explossive spalling**
100	Disintegration of hydrates and loss of free water.	
150	Degradation of gypsum $CaSO_4 . 2H_2O$; decomposition of CSH gel 170 °C melting of PP-fibers.	
200 >	Evaporation of chemisorbed bounded water.	
300 >	Dehydration and degradation of CSH gels and CAH. Degradation of portlandite: $Ca(OH)_2 \rightarrow CaO + H_2O$.	
550 - 600	Phase transition of quartz takes place from triclinic crystal structure to hexagonal crystal structure (573°C). This leads to breaking of bonding between aggregate and cement paste thanks to different thermal expansion.	**Cracks formation**
700 - 750	Climax of second phase decomposition of CSH. Decomposition of carbonate $CaCO_3$: $CaCO_3 \rightarrow CaO + CO_2$	
800 >	Hydraulic bond transforms to ceramic bond. It happens to decarbonation of limestone aggregate and releases carbon dioxide, gaseous substance damaging the concrete.	
900	Absolute decomposition of cement paste.	
1000 >	Beginning of melting of cement stone. Formation of wollastonite β ($CaO.SiO_2$).	
1200 >	Cement stone is available as vitreous glasses.	

Figure 2: The structure of HPC composed of silicate-lime aggregates heated up to 600 °C (SEM, 50x) [11]

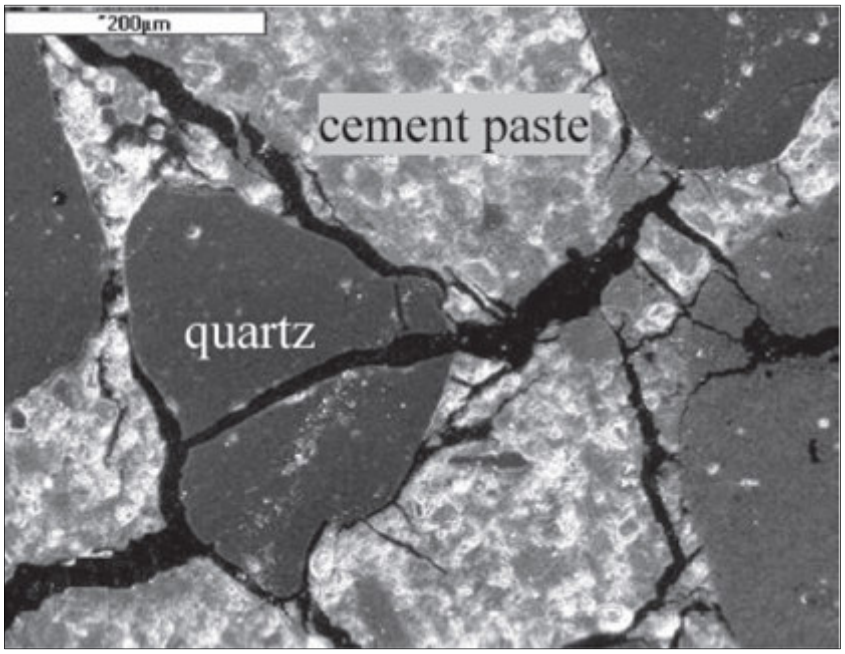

1.2.1 Influence of high temperature on cement paste

Warming of the cement paste leads to evaporation of physically and chemically bonded water which is present in the material. At first, it causes evaporation of physically bonded water from cement paste via capillaries and after heating to higher temperature, it starts to release chemically bonded water. However, during hydrothermal reaction, which can occur during autoclave (closed and moist environment), this can lead to significant changes in microstructure. The character of these changes depends on several aspects:

- mineralogical composition,
- ratio CaO/SiO2,
- amount of ultrafine powder (silica fume),
- level of reached temperature and pressure.

The mechanical properties of cement paste are strongly influenced by the chemical bond and the layers between CSH gel. It is assumed that around 50 % of the cement paste strength is provided by cohesive forces between the layers which are in CSH gel. Evaporation of water between layers of CSH, highly influences the mechanical properties of the cement paste.

Figure 3: Model of CSH phase [10]

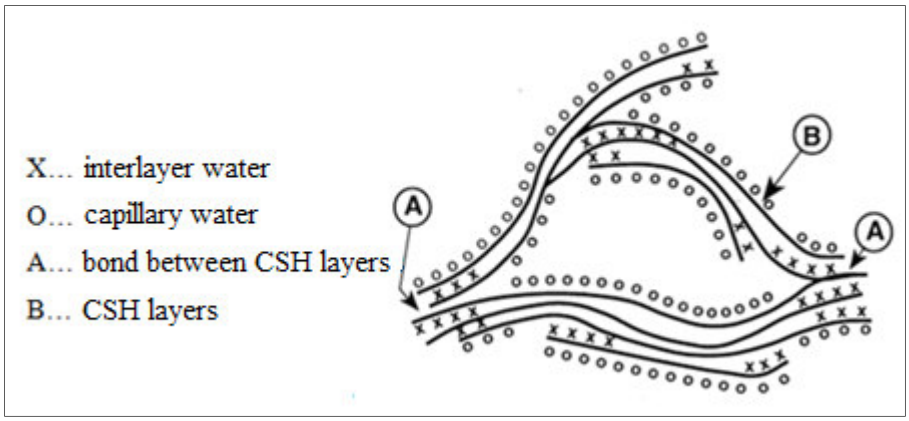

Dehydration process of GSH gel causes a decrease of cement hydrate volume and this effect leads to increasing of the cement matrix porosity. Total volume of pores rises; therefore, an increase of the average pore size occurs. Cement paste expands around 200 °C. This is a result of vapor coming out of the structure.

The least suitable hydraulic binder for dealing with a high temperature is ordinary Portland cement (CEM I), because it yields degradation after the loss of chemically bonded water in hydration products. The effect of dehydration leads to decomposition of portlandite at temperatures 450 – 550 °C to CaO and water vapor. This reaction can be described by following equation:

$$\boldsymbol{Ca(OH)_2 \rightarrow CaO + H_2O}$$

This reaction of the decomposition of portlandite increases the porosity of the cement matrix and decreasing of mechanical properties. However, this process can be changed if the admixtures with pozzolanic activity properties are used. This leads to the creation of CSH gel during the hydration. These phases decompose within a wide range of high temperatures. The rest of CSH gel can be identified in the matrix which is exposed to temperatures 500 – 600 °C. Because of this, it is better to use blended cement with lower amount of Portland clinker and more admixtures on basis of fly ash or slag. Calcium aluminate cement shows the highest resistance against the impact of high temperatures. Nevertheless, it is not suitable for construction concrete and is even prohibited in the Czech Republic. This is because the metastable phase CAH_{10} and C_2AH_8 transforms into stable cubic form C_3AH_6 at temperatures 20 °C:

$$3CAH_{10} \rightarrow C_3AH_6 + 2AH_3 + 18H$$

This reaction can take place for several years depending on the temperature. Consequence of this reaction is increase of the porosity and simultaneously decrease of the strength [12].

1.2.2 Influence of high temperatures on aggregate

Aggregates occupy 60-80 % of volume in concrete, and that is why it is necessary to pay attention to this issue. Aggregate, just as all the other solid substances, increases its volume with higher temperature, therefore the thermal expansion is important. The rate of thermal expansion is given in aggregates by mineralogical and chemical composition. Table 2 shows values of coefficient of linear thermal expansion of selected rocks. Mineralogical composition decides on total thermal reshaping of the aggregate. Apart from thermal reshaping, there are also metamorphic changes of minerals taking place. For example, trigonal quartz (α-quartz) will transform into hexagonal β-quartz at 573°C. This change results in increase of the substance's volume of 0,84 %. Carbonate aggregate, for example limestone and dolomite, decompose around temperatures 700 °C. Decomposition of $CaCO_3$ is to CaO and CO_2. During the extinguishing of fire and the access of water, hydration of CaO can occur which results in formation of $Ca(OH)_2$. Formation of $Ca(OH)_2$ leads to expansion up to 40 %. In Table 3 one can see processes which occur by increasing of high temperature at different sort of rocks [12].

Table 2: Coefficient of linear thermal expansion for different types of rocks [9]

Type of rock	**Coefficient of linear thermal expansion [10^{-6}m.C^{-1}]**		
Basalt	3,9	-	9,7
Dolomite	6,7	-	8,6
Sandstone	4,3	-	13,9
Limestone	0,9	-	12,2
Granite	1,8	-	11,9

Table 3: Processes in aggregates during thermal load [13]

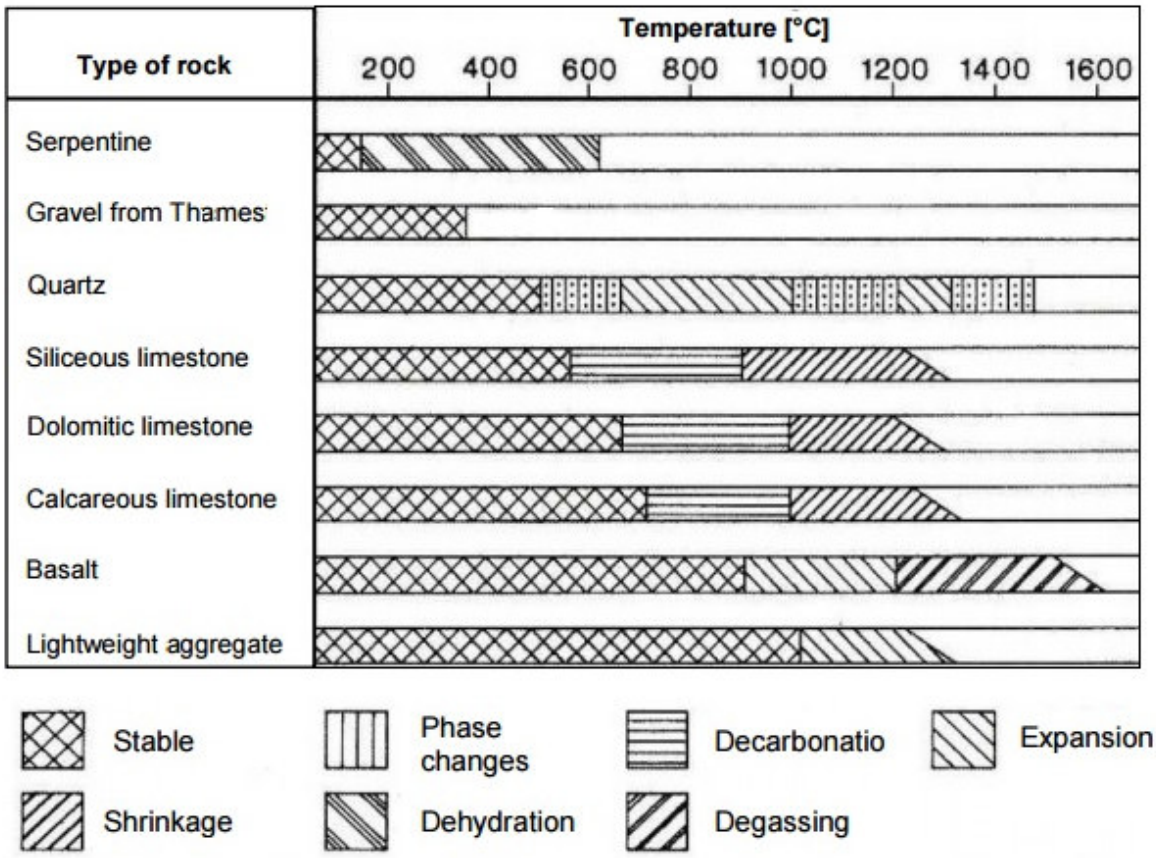

Taking the reaction into consideration, it is suitable to use aggregate with low coefficient of linear thermal expansion and low reshaping during cooling at high temperatures. Moreover, it cannot change its mechanical properties, primary compressive strength. Recommended natural aggregates are basalt, diabase and andesite. Basalt contains only minimum of quartz part so it is still stable. Improper aggregates are especially quartz based rocks. For extreme temperatures over 1000 °C, it is possible to use aggregate corundum or crushed bauxite [12].

1.2.3 Influence of high temperatures on mechanical properties of concrete

Higher temperatures influence not just its compressive strength but also other properties, such as modulus of elasticity. Compressive strength to 300 °C decreases slightly, at temperatures around 400 – 500 °C, chemically bonded water leaves and this leads to disruption of concrete structure (Figure 4). It effects also the modulus of elasticity. Another

effect which influences mechanical properties is a change of quartz as was mentioned in the previous chapter [13].

Figure 4: Diagram of compressive strength related to temperature [14]

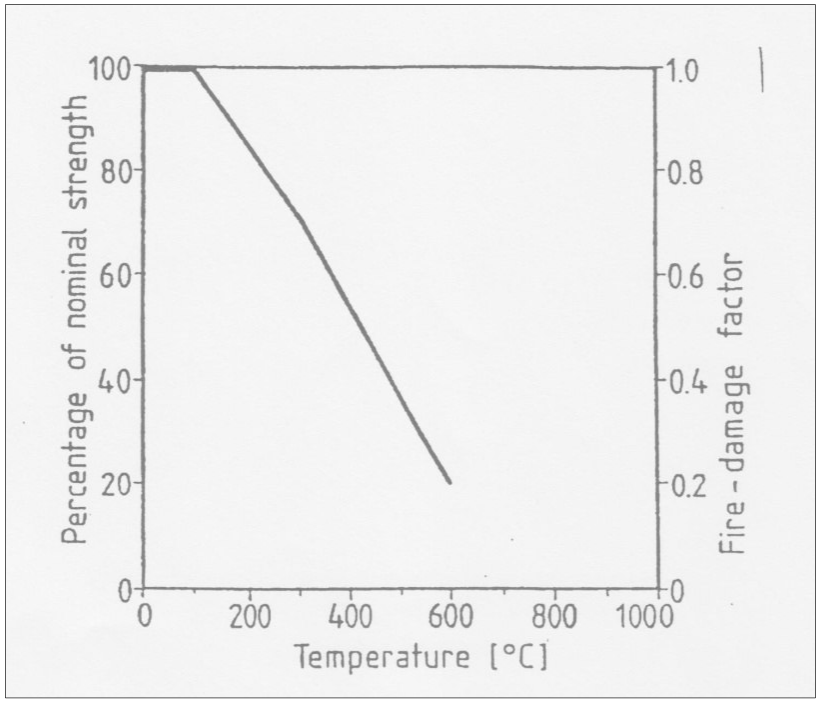

1.3. Spalling of concrete

1.3.1 Definition of spalling

Spalling of concrete was defined as "the violent or non-violent breaking off of layers or pieces of concrete from the surface of a structural element, when it is exposed to high and rapidly rising temperatures as experienced in fires" [15].

This general definition of explosive spalling covers the entire range of observations and observations made in tests for over a century for all types of spalling at high temperature (see following chapter) and is still valid today even with the rapid development of new types of concrete and materials.

However, tests on concrete cylinders [16] showed that even if no spalling was observed at high temperatures, significant post-cooling spalling including complete deterioration of the concrete may occur weeks after cooling to ambient temperatures with significant influences on the structural performance. Since this delayed spalling might occur even a long time after the actual exposure to high temperatures, the second part of the definition by Khoury [15] should be extended to "*during or after it is exposed to high and rapidly rising temperatures as experienced in fires"*.

1.3.2 Types of spalling

In terms of categorizing types of spalling, Gary [17] already noted four main categories of spalling in his tests in 1916. Over the next decades two additional groups were mentioned. Post cooling spalling and sloughing off spalling were noticed the ongoing research on explosive spalling. Today, according to Khoury [15], spalling of concrete at high temperatures may be grouped in the following categories:

- explosive spalling
- surface spalling
- aggregate spalling
- corner spalling
- post cooling spalling
- sloughing off spalling.

In the case of fire, usually several of these different types of spalling occur at the same time; depending on the duration, the concrete is exposed to high temperatures. It is very

difficult to distinguish between some of these types of spalling, explosive and surface spalling in particular.

According to the literature [15], it is noted that explosive, surface and aggregate spalling usually occurs within the first few minutes after the concrete member has been exposed to high temperatures, e.g. according to the ISO fire curve [18]. Corner spalling is usually observed after t = 30 - 90 min exposure to high temperatures, since a certain temperature gradient is required. The risk of corner spalling is increased when reinforcement bars close to the concrete edges are heated [19].

In contrast to these four categories of spalling, post cooling and sloughing off spalling are a rather rare occurrence. They usually take place after concrete has been exposed to high temperatures for a very long time or even some time after the concrete has cooled again to ambient temperatures.

Table 4 summarizes the different forms of spalling and their main characteristics. These six categories are briefly described and discussed in the following, with the main focus being on the explosive spalling of concrete [15].

The difference between violent and non-violent spalling is based on the energy released during spalling. The expression “violent spalling” is frequently used in the literature; however it has not been clearly defined so far. Explosive spalling due to the sudden release of high internal stresses is considered as violent, since a high amount of energy is required to cause these required stresses leading to spalling. This high amount of energy is released at once.

In contrast, sloughing-off and post cooling spalling usually start when the concrete begins to weaken or even after cooling. Since concrete parts simply fall off or ripple the structure, the nature of these types of spalling is considered to be non-violent due to their rather low energy demand. However, no quantitative criterion is given to distinguish between a violent and non-violent type of spalling.

Table 4: Spalling characteristics by Khoury [15].

Spalling	Usual time of occurrence[1)]	Nature[2)]	Sound	Influence on structure	Governing factors leading to spalling
Explosive	7-30 min	violent	loud bang	very serious	material, structural / mechanical and temperature related
Surface	7-30 min	violent	cracking	can be serious	mainly material related
Aggregate	7-30 min	splitting	popping	superficial	mainly material related
Corner	30-90 min	non-violent	none	can be serious	mainly structural / mechanical related
Post-cooling	after cooling	non-violent	none	can be serious	structural / mechanical and material related
Sloughing-off	when concrete weakens	non-violent	none	can be serious	mainly structural / mechanical related

1) In standard fire (i.e. ISO fire exposure [18])

2) Based on energy release upon spalling (boundaries not defined in the literature)

Figure 5: Explosive spalling [25]

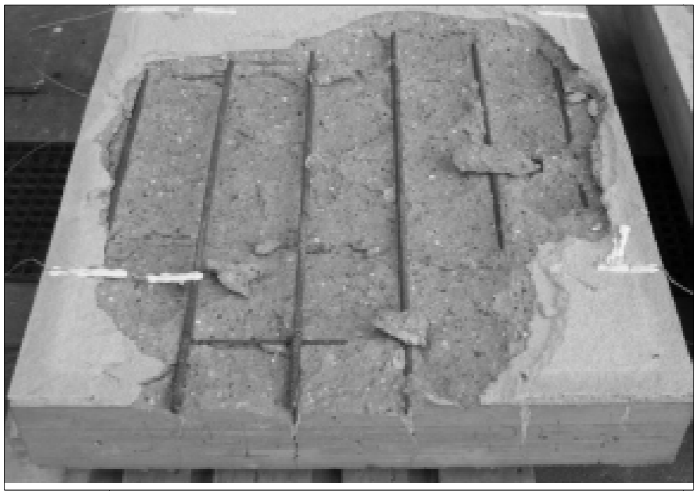

Figure 6: Corner spalling [20]

Figure 7: Post cooling spalling [21]

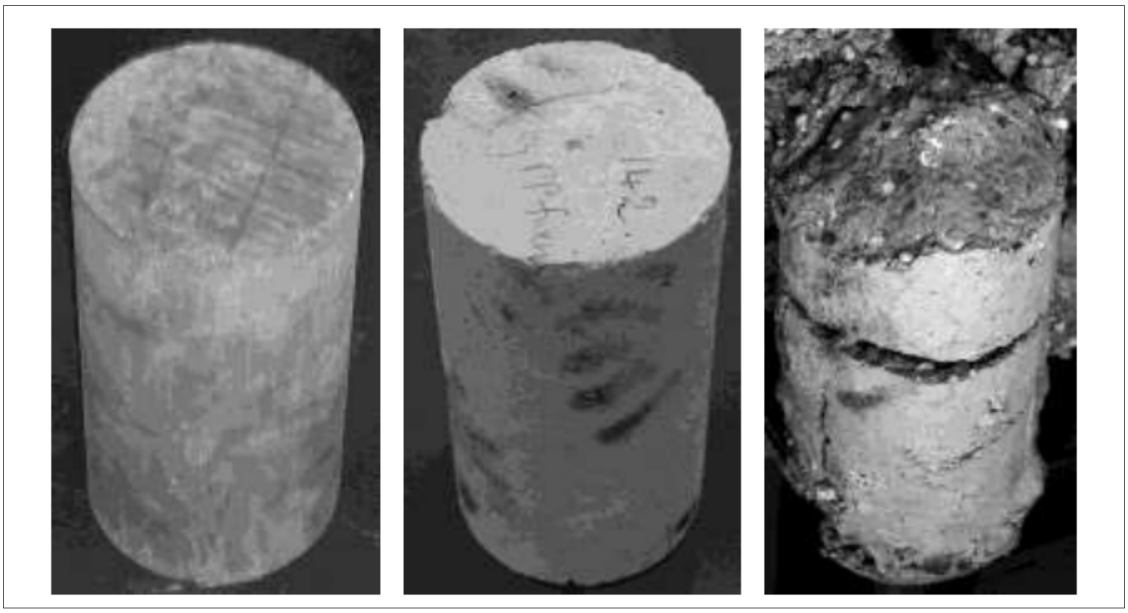

Before test *120 min after test* *Storage of 7 days*

1.3.3 Mechanism of spalling

Spalling may occur for concrete at high temperature, which will greatly reduce mechanical properties of concrete structure and even cause collapse of the structure. The mechanisms of spalling of concrete at high temperature could be mainly explained from vapor pressure in pores and thermal stresses of these two aspects [22].

Hardened concrete is saturated with water in its pores to different extents. The moisture content in concrete is dependent on w/c, age of concrete and environment. When concrete surface is subjected to sufficiently high temperature, a portion of water will be vaporized and move out from concrete into atmosphere. There is also certain amount of water that will be vaporized and will move in the opposite direction to the inner part of concrete. Due to thermal gradient, the inner part of concrete is cooler and the vapor will be condensed there. With the accumulation of the condensed water, a saturated layer is gradually formed. This layer will resist the further movement of vapor into the inner part of the concrete, but will move towards the dry region of the concrete surface with an attempt to escape out of the concrete into atmosphere. If the pore structure of the concrete is sufficiently dense and/or the heating rate is sufficiently high, the escape of the vapor layer would be not fast enough, resulting in a large increase of pore pressure in the concrete. If the tensile stress of concrete could not resist the pore pressure, spalling of concrete would occur [23]. Figure 8

illustrates the whole process of the thermal spalling of concrete as a result of the pore vapor pressure.

Figure 8: Spalling of concrete induced by pore vapor pressure [22]

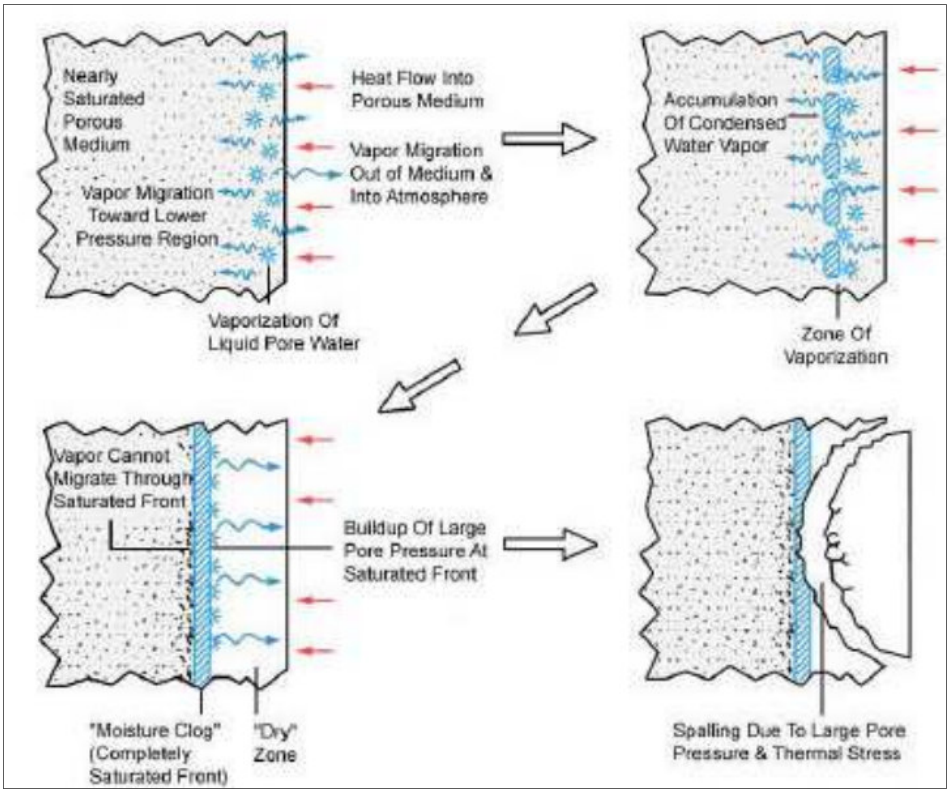

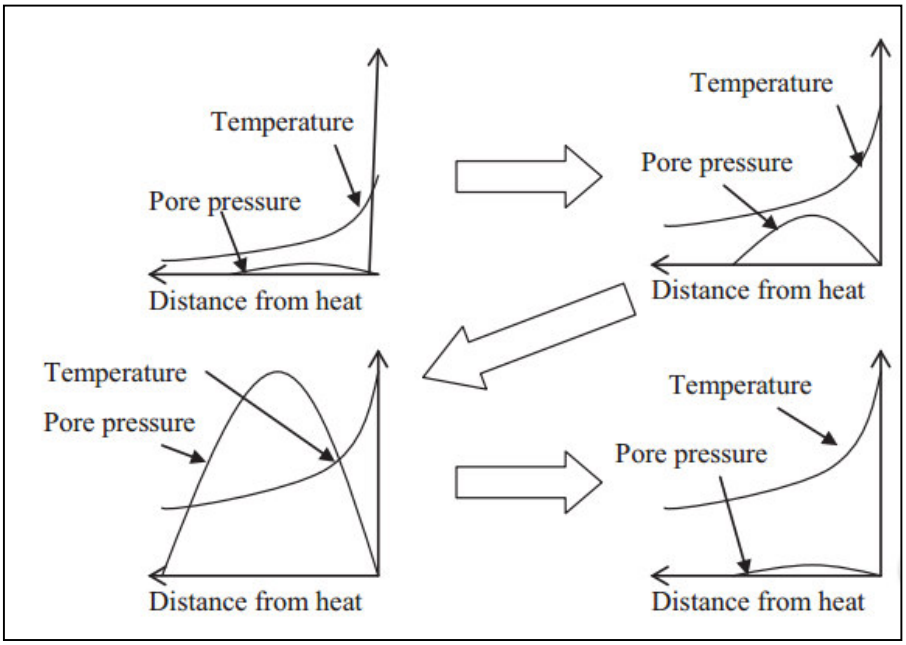

The total pore pressure is a result of the summarization of the partial pressures of all phases involved, i.e. water, vapor, air and melted fibers [24]:

$$P_{tot}(T) = P_W(T) + P_V(T) + P_A(T) + [P_F(T)]$$

Due to dense impermeable structure of high performance concrete, the saturated front is formed near to the surface which leads to the faster heating of the water zone and faster increase of build-up pore pressure (Figure 9). Probability of explosive spalling is therefore higher than in ordinary concrete.

Figure 9: Difference of pressure and moisture distribution in ordinary concrete and high performance concrete [24]

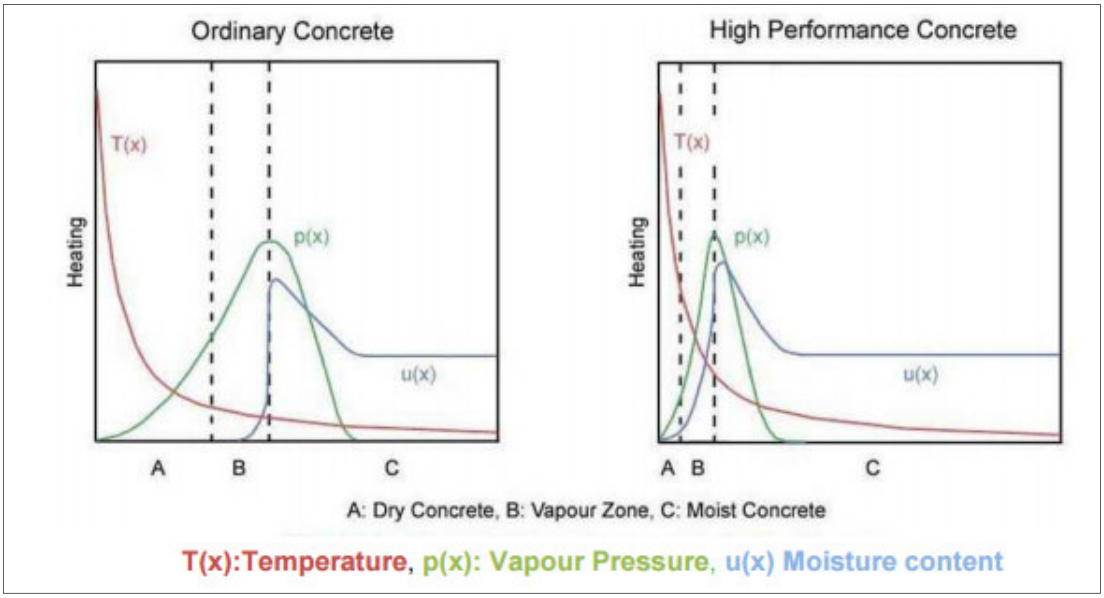

1.3.4 Factors influencing spalling

The main factors leading to the explosive spalling of concrete at high temperatures can be divided into three main categories:

- material related parameters,
- structural /mechanical parameters,
- heating characteristics.

However, some of these parameters could be put into more than one category [25].

Material related parameters

The research on concrete spalling at high temperatures identifies several material related parameters with a big influence on spalling. Table 5 gives an overview of these main parameters in relation to the concrete mix design or the choice of materials used for the concrete [25].

Table 5: Material related parameters [25]

material related parameter	increasing risk of spalling	influence on spalling
silica fume	very high	Silica fume lowers the permeability and increases the possibility of explosive spalling due to the reduced release of high vapor pressure.
limestone filler	high	Lowers permeability, similar behavior compared to silica fume.
permeability	high	Low permeability and insufficient temperature-dependent increase in permeability increases the risk of spalling due to insufficient release of pore pressure.
porous / lightweight aggregates	variable	Higher porosity and permeability enables the release of high pore pressure and decreases the risk of spalling. The higher moisture content of lightweight aggregates promotes the risk of spalling.
quartzite aggregates	high	Can increase the risk of spalling due to a change in the quartzite phase at T = 573°C.
carbonate aggregates	lowering risk	Remains stable even at very high temperatures, have a very low thermal expansion.
aggregate size	moderate	Larger aggregates increase the risk of explosive spalling due to a poor surface to mass ratio.
internal cracks	variable	Two opposing effects. Small cracks might promote the release of high pressure and reduce the risk of spalling. However, parallel cracking close to the heated surface (i.e. due to loads) might increase the risk of spalling.
compressive strength	high	Higher strength grade usually increases risk of explosive spalling, mainly due to the lower w/c ratio and permeability.
moisture content	very high	Higher moisture content (mainly free water) significantly increases the risk of explosive spalling, since more vapor pressure must be released depending on the permeability of the concrete. Critical moisture content is difficult to obtain, in particular for HPC.
cement content	high	High cement content increases the total amount of water added to the concrete, even with low w/c ratios.

Structural /mechanical parameters

The main structural / mechanical parameters with a significant influence on spalling are summarized in Table 6. In some cases it is difficult to distinguish between pure material and pure structural / mechanical parameters leading to spalling, since some parameters can be attributed to both categories. For example, the compressive strength of the concrete is one of these parameters, since several individual material related parameters have an influence on the compressive strength of concrete [25].

Table 6: Structural /mechanical parameters related to influence on spalling [25]

Structural / mech. parameter	increasing risk of spalling	influence on spalling
tensile strength	lowering risk	A high tensile strength is considered as lowering the risk of explosive spalling since it offers a higher resistance: - against spalling due to a high pore pressure. - of high thermal gradients, stresses and expansion. - of corner spalling or thermal stresses from two sides.
applied load	high	The risk of spalling increases with applied higher load levels. Preload as low as 5% of the cold strength increases the risk of spalling. It remains unknown if a low preload minimizes the risk of spalling, since small cracks used for the release of vapor are pressed together.
hindered thermal expansion	high	Fixed ends as boundary conditions, eccentric load or bending increases risk.
cross section geometry	high	Round cross section, rounded corners, sufficient reinforcement cover and spacing and modified tie design lowers the likelihood of spalling or increases the remaining load bearing capacity of concrete members after spalling.

Heating characteristics

In terms of the parameters that depend on heating characteristics, the heating rate and the hereby caused temperature gradients have a strong influence on explosive spalling. High heating rates and thermal gradients increase spalling. Table 7 summarizes the governing parameters depending on the heating characteristics that influence spalling in general [25].

Table 7: Heatings parameters related to influence on spalling [25]

heating characteristic parameter	increasing risk of spalling	influence on spalling
high heating rate	very high	Higher heating rates usually lead to explosive spalling with HPC mixes.
temperature gradient	high	Closely related to the heating rate. Higher temperature gradients ($\Delta T > 1.0$ K/mm) promote the risk of explosive spalling due to thermal stresses.
absolute temperature	moderate	Explosive spalling might occur with temperatures as low as T = 300 - 350°C. Very high temperatures T > 1000°C increase the risk of post cooling spalling.
exposure on multiple surface	high	Heat exposure on more than one side increases the risk of corner or explosive spalling due to higher temperature gradients and thermal stresses.

1.3.5 Methods to prevent explosive spalling

The aim of the fire protection system is to allow safe evacuation of the users as well as allow the rescue units to enter the scene and to limit damages to the tunnel. These systems are constantly being developed with the goal to prevent concrete spalling and heating and melting of steel and metal elements.

Methods are divided into active and passive protections.

Active methods or active fire protection is a group of systems that requires some amount of action in order to work efficiently in the event of a fire. These actions may be manually operated, like a fire extinguisher or automatic, like a sprinkler. Therefore, when fire and smoke is detected in a facility, a fire/smoke alarm will alert those who are inside the building and work to actively put out or slow the fire. Sprinkler systems and fire extinguishers help slow the growth of the fire until firefighter have a chance to get there. Once firefighters arrive, they use fire extinguishers and fire hoses to put out the fire altogether.

Passive methods of passive fire protection is a group of systems that compartmentalize a building through the use of fire-resistance rated walls and floors, keeping the fire from spreading quickly and providing time to escape for people in the building. Dampers are used in a facilities ducts to prevent the spread of fire/smoke throughout the building's ductwork system. Fire doors help compartmentalize a building, while giving its occupants means of escape. Fire walls and floors help separate the building into compartments to stop the spread of fire/smoke from room to room. For building with multiple floors, photoluminescent egress path markers help light the way to safety in dark and smoky stairwells [26].

Concerning fire protection in material science, polypropylene fiber modified concrete, sprayed mortars and pre-fabricated boards are especially important.

Polypropylene fibers

Polypropylene fibers are used as dispersed reinforcement of concrete. Polypropylene is created by polymerization isotactic polypropylene molecules. In comparison with other polymers, polypropylene is harder, solid and has higher melting temperature. Chemical formula of polypropylene is C_3H_6. [27]

Polypropylene fibers are used in concrete to prevent propagation of shrinkage microcracks. This effect is happening in early phases of concrete hydration. Fibers bound water on its surface, which releases gradually and that is why it leads to hydration of concrete. If cracks will appear, then fibers begin to carry tensile stress. After that, hardening of concrete has not another higher influence on physical-mechanical properties. Usual recommended dosage of PP-fibers to prevent explosive spalling is 2 kg per m^3 of concrete.

Another and the main use lies in increasing resistance of concrete at high temperature. The PP-fibers melt at about 170°C, thus creating micro channels for transport of water vapor and thereby decrease pore pressure build-up in the concrete element. Melted fibers due to thermo-oxidative decomposition are partly absorbed by cement matrix and therefore create network more permeable than cement matrix itself and results in the reduction of pore pressure. The important points are melting point at 171°C, vaporization point at 341°C and the burning point at 457°C showed in Figure [28].

Figure 10: DTA, TGA and differential thermo-gravimetric analysis (DTG) [29]

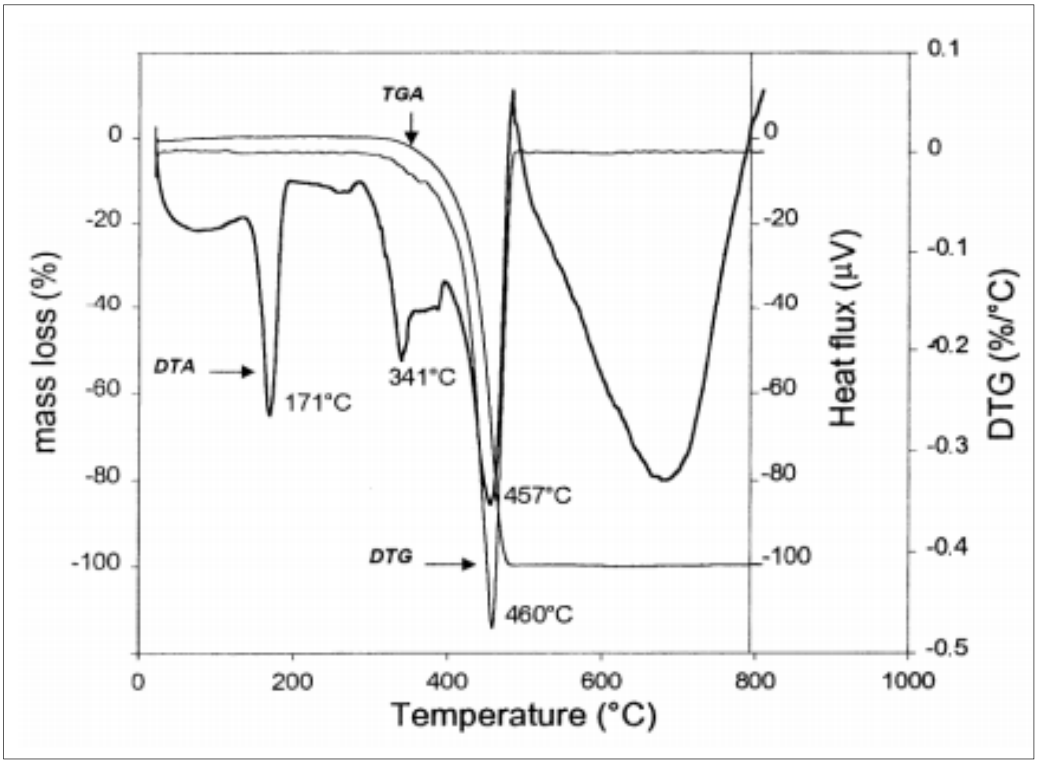

Types of PP-fibers:

- Monofilament polypropylene fibers - are produced by fiberizing (shredding) from the melt with length 5-15mm (32 mm) and a diameter of 10-20 µm
- Fibrillated polypropylene fibers - are produced by fiberizing of modified prestressed plastic foil with thickness about 40-200 mm.
- United fibers – mixed monofilament and fibrillated fibers [28]

Figure 11: a) monofilament fibers b) fibrillated fibers [28]

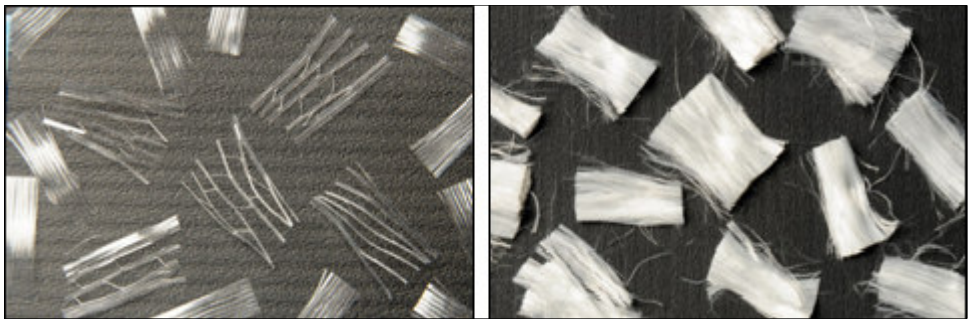

Classification according to dimension [28]:

- Microfibers
- Macrofibers

Effect of polypropylene fibers

Addition of polypropylene fibers has essentially 4 effects on permeation improvement [24]:

Additional micro pores are created during the addition and mixing of fibers in the fresh concrete mix. Addition of PP fibers influences the porosity due to so called "foaming effect" developed during the mixing of the fresh concrete. The higher amount of fibers, the higher porosity (Figures 12-14). It has been observed that thin and small fibers are more effective than the larger ones. Therefore, monofilament PP fibers which are finer than fibrillated fibers are used to avoid spalling.

Figure 12: The air content of fresh concrete related to dosage of PP fibers [30]

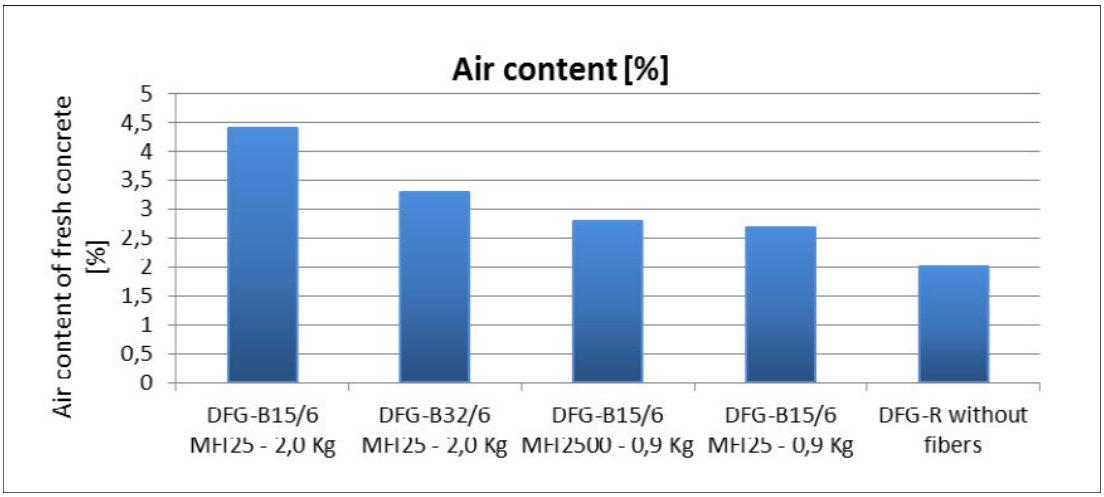

Figure 13: Density of concrete related to dosage of PP fibers [30]

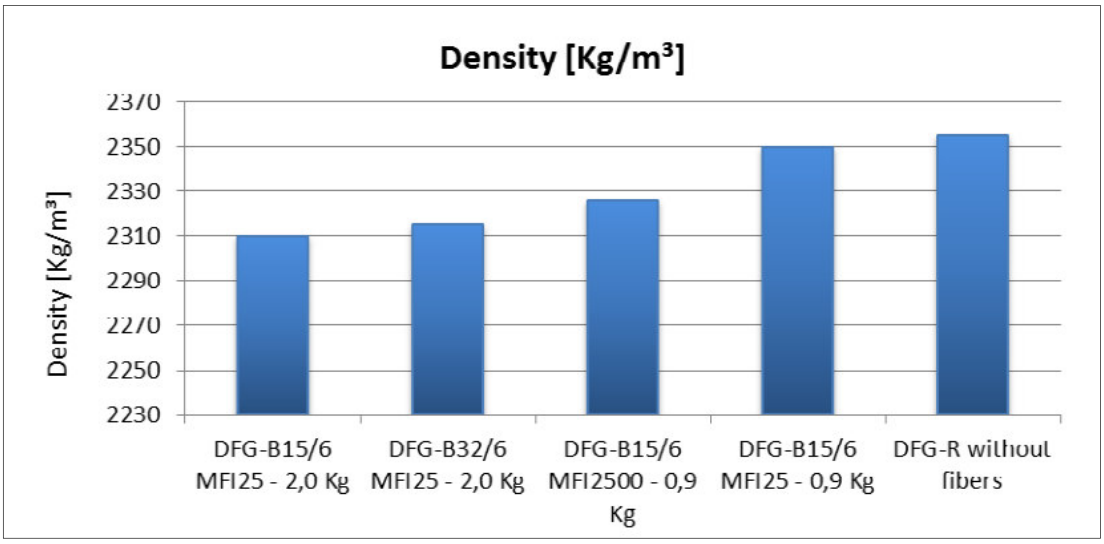

Figure 14: Compressive strength related to dosage of PP fibers [30]

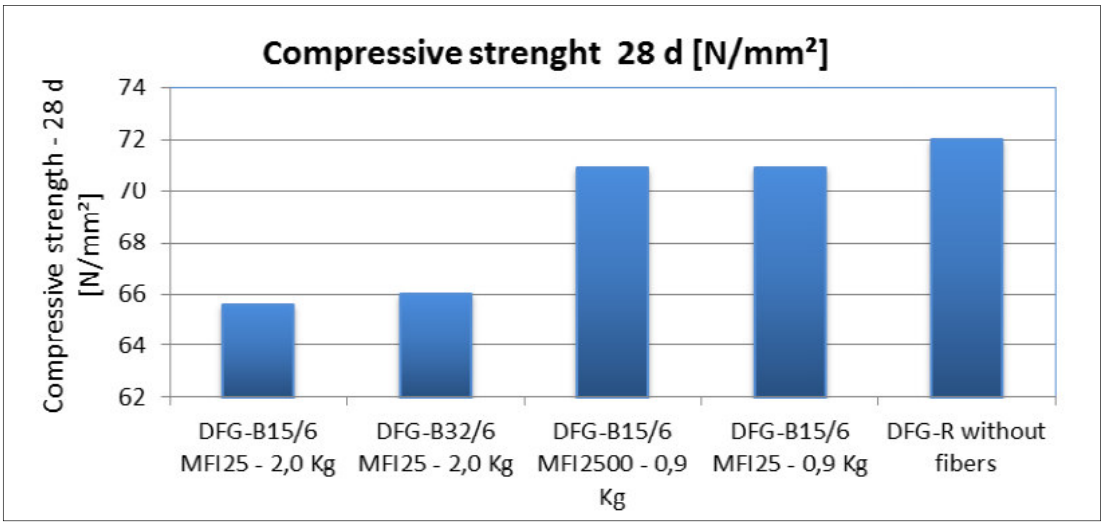

Development of diffusion-open transition zones between aggregate and cement matrix. Transition zones around aggregate allow higher transport of vapor and the addition of PP fibers improves this imperfectly connected system and thus causes the increase the filtration. Schematic description of this theory is illustrated on Figure. Thickness of this transition zone is dependent on w/c ratio, cement type and content of micro silica [24].

Figure 15: Schematic description of "Theory of Permeation" [24]

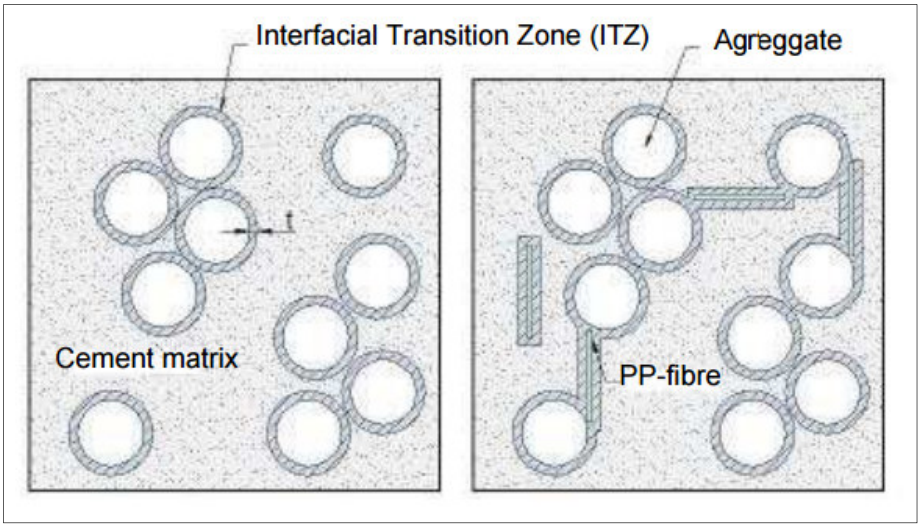

Formation of capillary pores during melting and burning of the fibers. Micro channels for transport of vapor are developed at temperature 171 °C which is the melting point of PP fibers and creation of micro channels continues to the temperature 341- 457°C when fibers vaporize and burn. Kalifa et al. observed that PP fibers are partially absorbed by cement matrix and therefore create a network more permeable than cement matrix itself [29].

Micro cracks formation at the tip of the PP fibers created during heating up and melting.

Cellulose fibers

Cellulose is an organic compound with the formula $C_6H_{10}O_5$, a polysaccharide consisting of a linear chain of several hundred to many thousands of β(1→4) linked D-glucose units. Cellulose is an important structural component of the primary cell wall of green plants, many forms of algae and the oomycetes [31].

Main reason to use cellulose fibers is to prevent shrinkage crack in early part of the concrete hydration. The principle of preventing shrinkage cracks is that the fibers soak in water and act as a water reservoir to the hydration process. As the silicate bonds breakdown in contact with the water, hydroxide ions precipitate out and then recombine with the calcium and attach themselves to the fiber. The calcium hydroxide crystal now starts to grow near to and on the surface of the fiber growing outwards away from the fiber. The crystals do not initially cover the entire fiber surface thus allowing more water to be released to hydrate more cement particles. Eventually, these large fibers, when compared to the crystal size, are completely covered by crystals, and now are also getting locked off

and are supplying no more water, except by diffusion. However, by now they have already hydrated more cement particles than if they were not present in the concrete [32].

Cellulose fibers are also used for increasing the fire resistance of concrete. The fibers give a larger surface area for moisture transfer. As heat is applied, moisture begins to expand in the concrete and in the fiber. Moisture moves out from the fiber, the initial thermal pressures below 250 °C are taken by the fiber, resisting bursting pressures that ordinary concrete would begin to spall at, with a smaller loss of concrete strength or cover. Now with the temperature at or above carbonation point of the fiber, the fiber structure breaks down allowing the moisture to escape more freely. This reduces internal pressure and as a result prevents explosive spalling [32].

Minimum dosage of cellulose fibers is recommended 0,9 kg per m^3. Cellulose fibers used in concrete are in a square form. Larger fraction of aggregate is suggested for mixing, so that fibers can be evenly disperse in the entire concrete volume.

Figure 16: Cellulose fibers [32]

2 EXPERIMENTAL PART

2.1. Introduction of experimental part

The aim of the experimental work is to compare the behavior of high performance concrete modified by polypropylene and cellulose fibers and the behavior of ordinary concrete C 30/37. The concrete specimens were, in the first case, exposed to thermal load of temperatures 1100 °C reached in 30 min and subsequent isothermal dwell for 30 minutes. In the second case, the specimens were exposed to thermal load of temperatures 900 °C. The experimental work focuses on different behaviors and physical mechanical properties without any fibers, with polypropylene fibers and cellulose fibers. In addition, the specimens of high-performance concrete were compared to ordinary concrete. The experimental part is divided into two main parts: the preparation of the experiment and the experiment itself.

The preparation of the experiment is describing the preparation of a suitable mixture of concrete and the preparation of molds for fire spalling test. This part also includes other tests before the fire test, namely the tests of compressive strength, tensile strength and volume density.

The second part of the experimental work was dedicated to testing of the prepared specimens in the oven. The heating rates were reached according to ISO curve and hydrocarbon curve. After the fire test, different properties were evaluated, such as compressive strength, mercury porosimetry and spalling depths.

2.2. Methodology

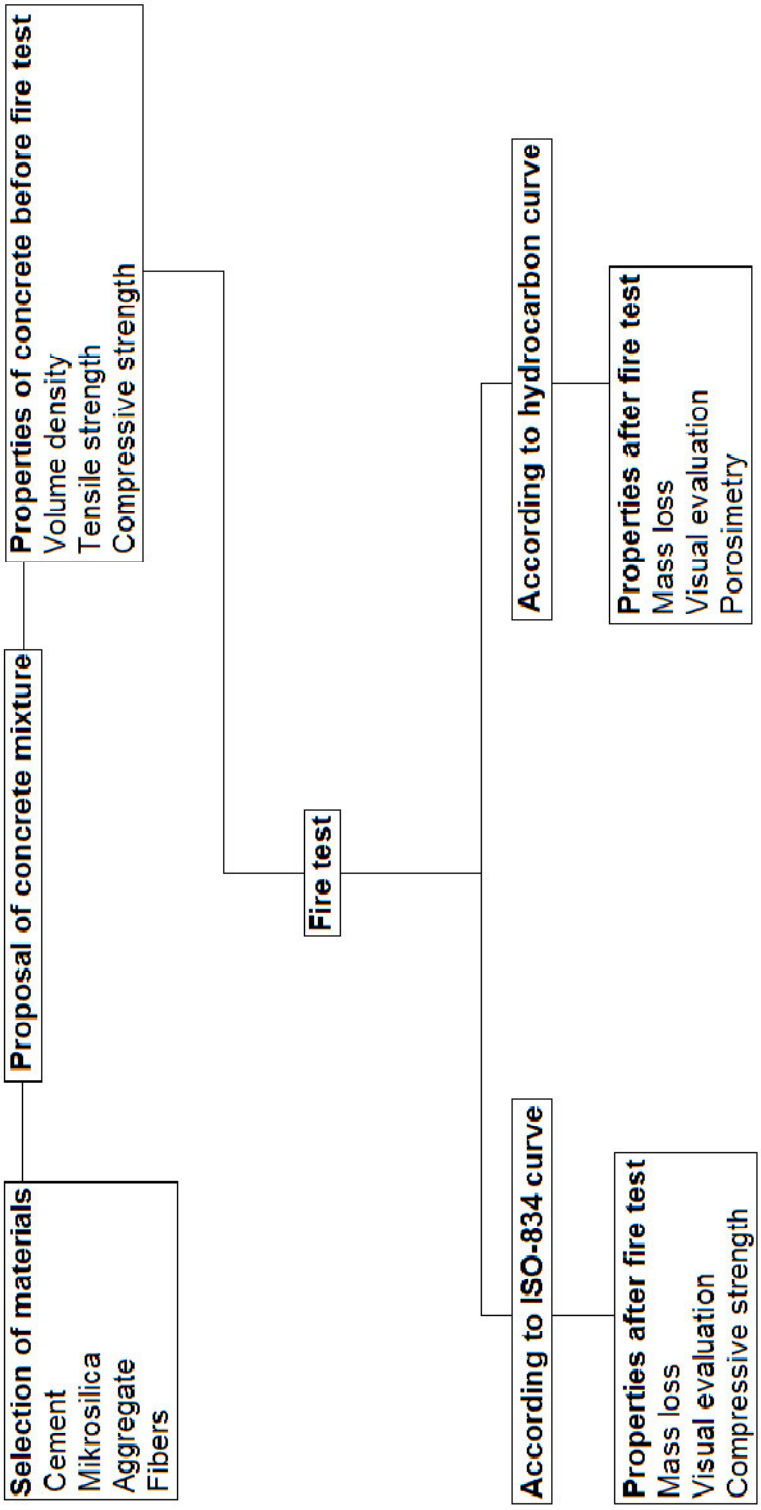

2.3. Preparation of the experiment

Considering the wide scale of the experiment, it was first of all necessary to ensure the required materials, the persons responsible for the implementation of the specimens, to schedule testing dates and to book testing laboratories and equipment.

2.3.1 Preparation of the concrete mix

Proposal of the concrete mix design was based on theoretical knowledge and recommendations from current literature research. The mixtures have been modified by adding two types of dispersed reinforcement in the form of polypropylene fibers and cellulose fibers. There were five proposed mix designs all together, including a reference.

Materials

Cement

For the experimental work, cement CEM I 42, 5 N C_3A frei Mannersdorf of company Lafarge was used. The cement has a low amount of C_3A. The C_3A is connected to the initial setting and hardening of the cement, and hydration heat release. Another important aspect is the fact that the C_3A is linked to sulphate attack resistance when the sulphate is coming from the environment. Properties of the cement are in the following Table 8.

Table 8: Properties of cement CEM I 42,5 N C3A frei [33]

	Guide values	Standard requirement	
		ÖN EN 197-1	**ÖN B 3327-1**
Density [kg/dm^3]	3,14	-	-
Compressive strenght [N/mm^2]- 1 day	12	-	≥ 6
2 days	24	≥ 10	-
7 days	-	-	-
28 days	51	≥ 42,5 ≤ 62,5	-
Tensile strenght [N/mm^2]- 28 days	-	-	-
Grinding fineness [cm^2/g]	3200	-	-
Bleeding [cm^3] after 120 minutes	15	-	≤ 25
Heat development [J/g] after 15 hours	200	-	≤ 210
Initial setting time [min]	160	≥ 60	≥ 90

Microsilica

Another important part of the mix design is Microsilica Grade 940 Undesified. In use, it acts physically as a filler and chemically as a highly reactive pozzolan. It is a key ingredient in many construction materials. It is used in fiber cement products as a process aid, to improve ingredient dispersion and to improve hardening properties and overall durability.

Table 9: Chemical and physical properties of microsilica Elkem 940 U [34]

Properties	**Specificaition**
SiO_2 [%]	> 90
Retention on 45µm sieve [%]	< 1,5
H_2O [%]	< 1,0
Bulk Density [kg/m^3]	200 - 350

Powdered Limestone

Limestone powder was used from company Molln Kalksteinmehl KSM H 100. Residues on sieve 63 µm are more than 17 % (Figure 17).

Figure 17: Particle size distribution of limestone powder KSM H 100 [35]

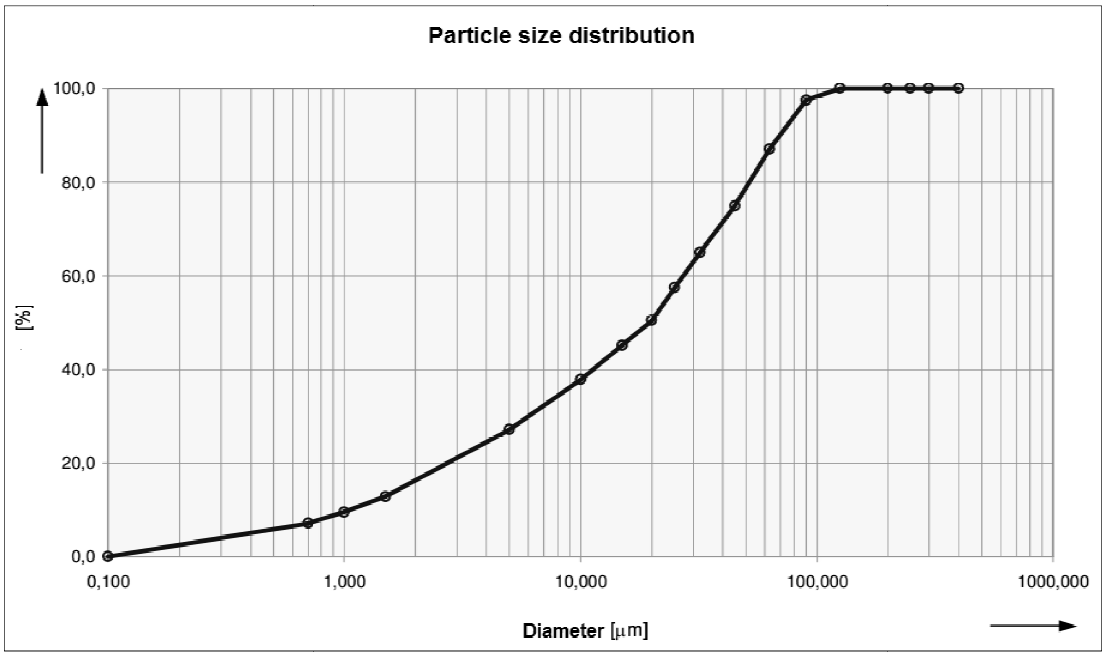

Table 10: Chemical analysis of limestone powder KSM H 100 [35]

$CaCO_3$	> 96 %
$MgCO_3$	< 3,0 %
Fe_2O_3	< 0,2 %
HCl (insoluble)	< 1,0 %

Aggregate

All fractions of aggregate come from area Bad Fischau near Wiener Neustadt and the main part is dolomitic limestone.

Table 11:Mineralogical analysis of aggregate

Dolomitic limestone $MgCa(CO_3)_2$	30 - 40 %
Calcite $CaCO_3$	30 - 40 %
Clay minerals	23 %
Mica	14 %
Quartz	9 %
Feldspar	3 %

Fibers

Polypropylene fibers

In the study, standard and modified polypropylene fibers have been used. The standard PP fibers used have a length of 6 mm, diameter 32 and 15 µm with a melt flow index 25. The modified fibers treated with radiation have length of 6 mm, diameter 15 µm and melt flow index 2500.

A/ HPR modified fibers

PB EUROFIBER HPR is the new, patented PP special fiber to maximize the fire resistance of concrete and minimize concrete spalling. New modified PP fibers provide the required fire protection at a highly reduced fiber dosage (50 - 70 % minimized fiber dosage of PB EUROFIBER HPR achieves the stipulated protection against fire), thereby simplifying the manufacturing process of the concrete. Based on the recommendation of manufacturer's dosage, 0.5 – 0.9 kg/m³ of concrete is generally enough which leads to savings of fiber dosage costs (dosage 0.9 kg/m³ is considered to be effective [36].The reduction of fiber dosage leads to reduction of air void content and consequently to optimizing the concrete

quality, which is significant for achieving the desired properties of the high performance concrete (HPC).

PB EUROFIBER HPR has a significantly faster ease of flow when melted when compared to all other PP fibers available on the market. This special feature works in fire and allows the fiber to melt much faster within the concrete matrix, leading to a rapid creation of the important micro channels needed to discharge the vapor pressure from the concrete. PB

EUROFIBER HPR is distinguished by the low viscosity and oily consistence of its melts.

Table 12: Characteristics PB EUROFIBER HPR

Color	White
Fiber class	Polypropylene
Fiber geometry	1.7 dtex (15.4 mic), 6 mm cutting length
Fiber quantity per kg	Approx. 1 billion
Fiber length per kg	Approx. 6 million km
Melt flow index (230°C/2,16 kg)	> 1000 (PP-standard fibers= approx. 30)

B/ Standard PP-fibers PB EUROFIBRES

PB EUROFIBRES of standard PP-fibers with recommended dosage 2 kg per m^3 produced by BAUMHÜTER, the same company as PB EUROFIBER HPR, were used in tests.

Table 13: Characteristics PB EUROFIBER

Color	White
Fiber class	Polypropylene
Fiber geometry	Diameter 15 µm and 31 µm, 6 mm cutting
Fiber count	1-150 dtex (g/10000 m)
Melt flow index (230°C/2,16 kg)	25
Melting point	Approx. 165°C

Cellulose fibers

In addition to polypropylene fibers, cellulose fibers by company CHRYSO® (CHRYSO® Fibre UF-500) were used. CHRYSO® Fibre UF-500 are natural alkaline resistant fibers, that have a good adhesion to cement putty. The main reason for using cellulose fibers is to

prevent cracks from shrinkage and to increase fire resistance of the concrete. Producer suggests basic dosage 450 g/m^3 [38].

Table 14: Charakteristics CHRYSO® Fibre UF-500 [37]

Color	White
Fiber class	Cellulose
Fiber geometry	Diameter 14 - 17 µm, lenght 1,9 - 2,3 mm
Fiber count	Approx. 1,6 million per 1 g
Melting point	135°C

Superplasticizing additive

The superplasticizing additive ACE 430 is on the basis of polycarboxylats, providing high early and final durability. The new generation of this kind of admixtures is represented by polycarboxylate ether-based superplasticizers (PCEs). With a relatively low dosage (0,15 – 0,3 % by cement weight), they allow water reduction up to 40%. This is due to their chemical structure which enables good particle dispersion. PCE's backbone, which is negatively charged, permits the adsorption on the positively charged colloidal particles. As a consequence of PCE adsorption, the zeta potential of the suspended particles changes due to the adsorption of the COO- groups on the colloid surface. This displacement of the polymer on the particle surface ensures to the side chains the possibility to exert repulsion forces which disperse the particles of the suspension and avoid friction.

2.3.2 Preparation of specimens

Before mixing concrete, molds were prepared for a fire tests. These special molds of size 300 x 250 x 100 mm had thermocouples inside to measure temperature and they were in distance 1, 3, 5, 7, 9 cm from the heated surface of the specimen (Figure 18-20). Another thermocouple was placed directly on the heated surface.

Figure 18: Prepared thermocouple

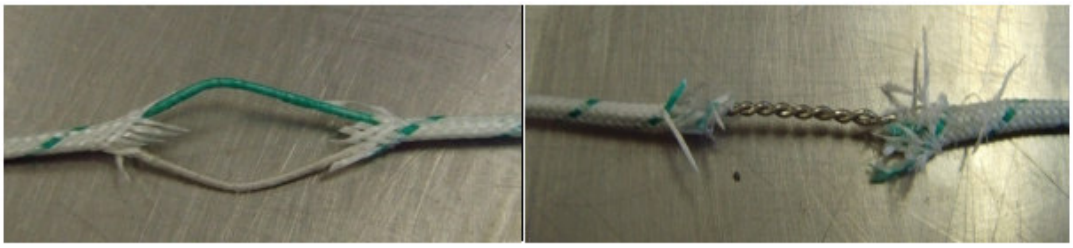

Figure 19: Scheme of thermocouples D1-D9 in mold

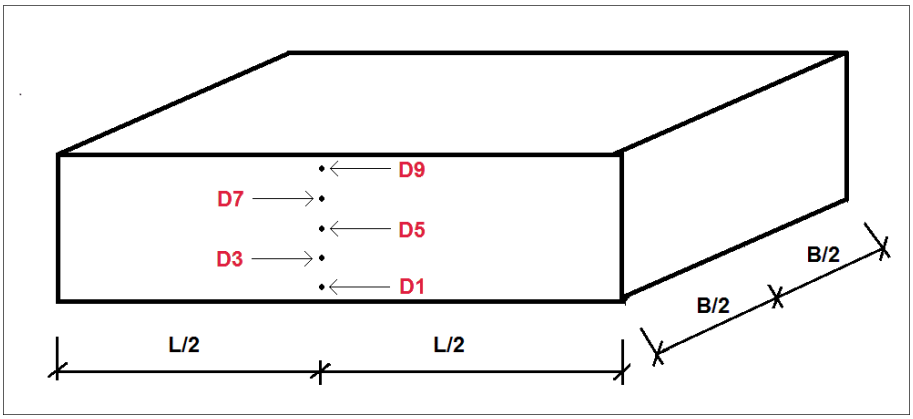

Figure 20: Prepared mold with thermocouples

2.3.3 Mixture

Introduced materials were used in the final mix design. The first mixture was a high-performance concrete with and without the addition of fibers (Table 15) and the second mixture was a concrete class C30/37 (Table 16).

Table 15: Mix design of high performance concrete

Component [kg/m3]	**HPC-WF**	**HPC-HPR**	**HPC-PP**	**HPC-CEL**
Cement I 42,5 N without C3A	508,2			
Mikrosilica Elkem 940 U	50,8			
Powdered limestone KSM H 100	127,0			
Aggregate 0 - 1 mm	862,1			
Aggregate 1 - 4 mm	313,5			
Aggregate 4 - 8 mm	391,9			
Water	154,0			
Additive ACE 430	15,3			
Additive Sky 911	10,2			
Polypropylene fibers PB EUROFIBRE HPR	-	2	-	-
Polypropylene fibers PB EUROFIBRE	-	-	2	-
Celullose fibers CHRYSO® Fibre UF-500	-	-	-	2

Table 16: Mix design of concrete C30/37

Component [kg/m3]	**OC**
Cement I 42,5 N C3A-frei	320,0
Aggregate 04 mm	1396,9
Aggregate 48 mm	465,6
Water	192,0

Each mixture was mixed in intensive mixer Eirich R08W. After filling all the aggregate, binder and other dry components, the mixture was mixed for 300 seconds. As a next step, all liquid components were added in 30 seconds and the mixture was being mixed for another 120 seconds.

Figure 21: Intensive mixer Eirich R08W

In total, 2 specimens were made for each mixture for fore fire test (mold 300 x 250 x 100 mm), 4 specimens for compressive strength (mold 100 x 100 x 100 mm) and 2 specimens for tensile strength (mold 100 x 100 x 350 mm). After demolding, all specimens were left in standard conditions of temperature and pressure and were tested after 28 days.

2.3.4 Concrete properties

Table 17: Characteristics before the fire test

	Volume density	Water content	Tensile strength	Compressive strength
	[kg/m^3]	[%]	[N/mm^2]	[N/mm^2]
OC1	2280	4,6	7,0	44,8
HPC-WF	2400	4,3	9,2	121,9
HPC-REF	2380	4,4	7,2	109,9
HPC-HPR	2380	4,5	7,2	108,8
HPC-CEL	2400	4,4	6,3	106,8

Figure 22: Volume density of concrete related to the mixture

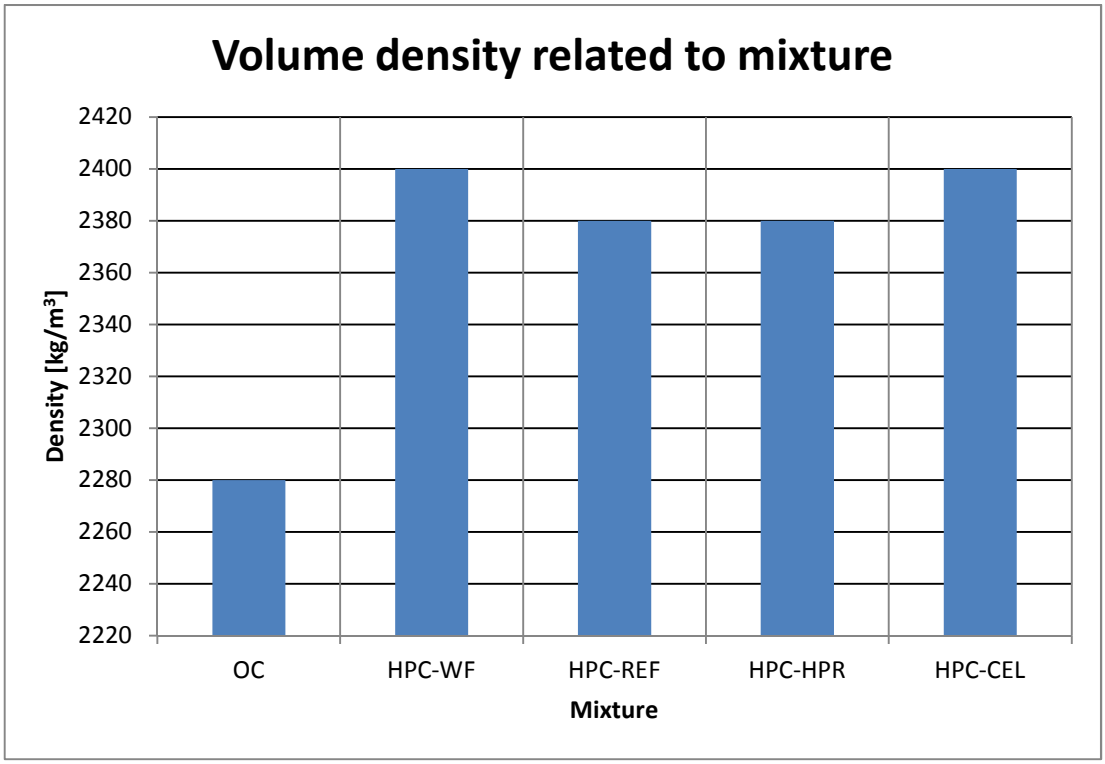

Figure 23: Compressive strength after 28 days related to the mixture

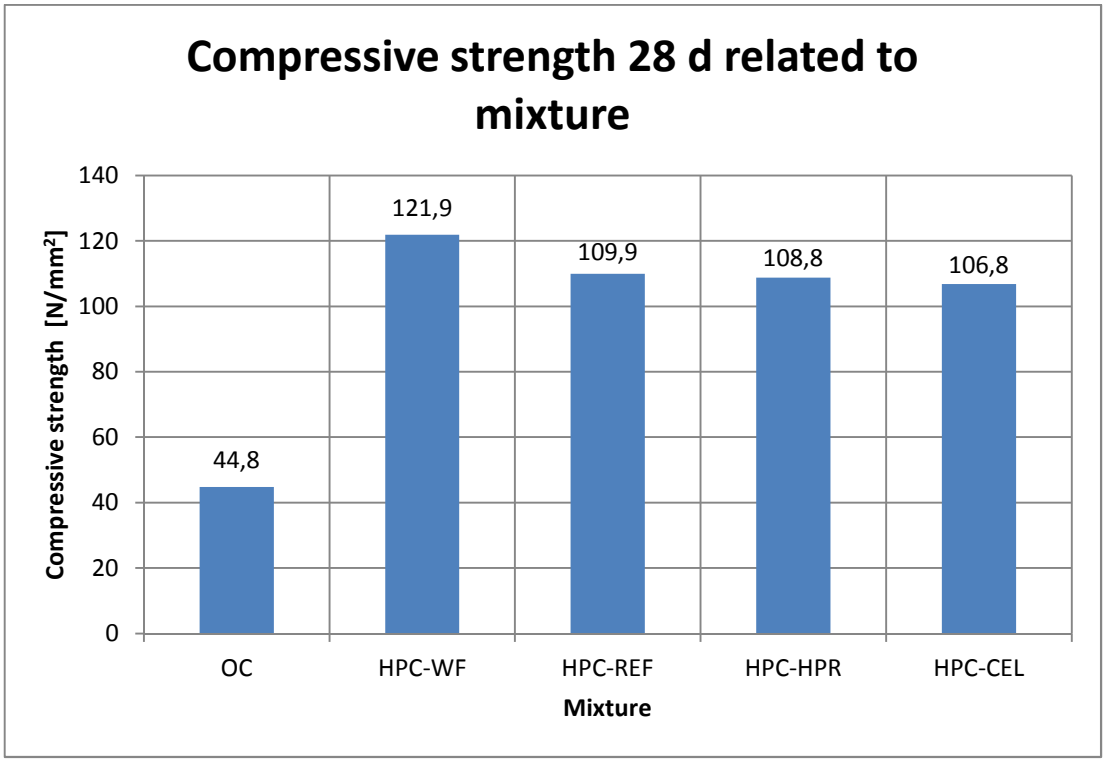

Figure 24: Tensile strength after 28 days related to the mixture

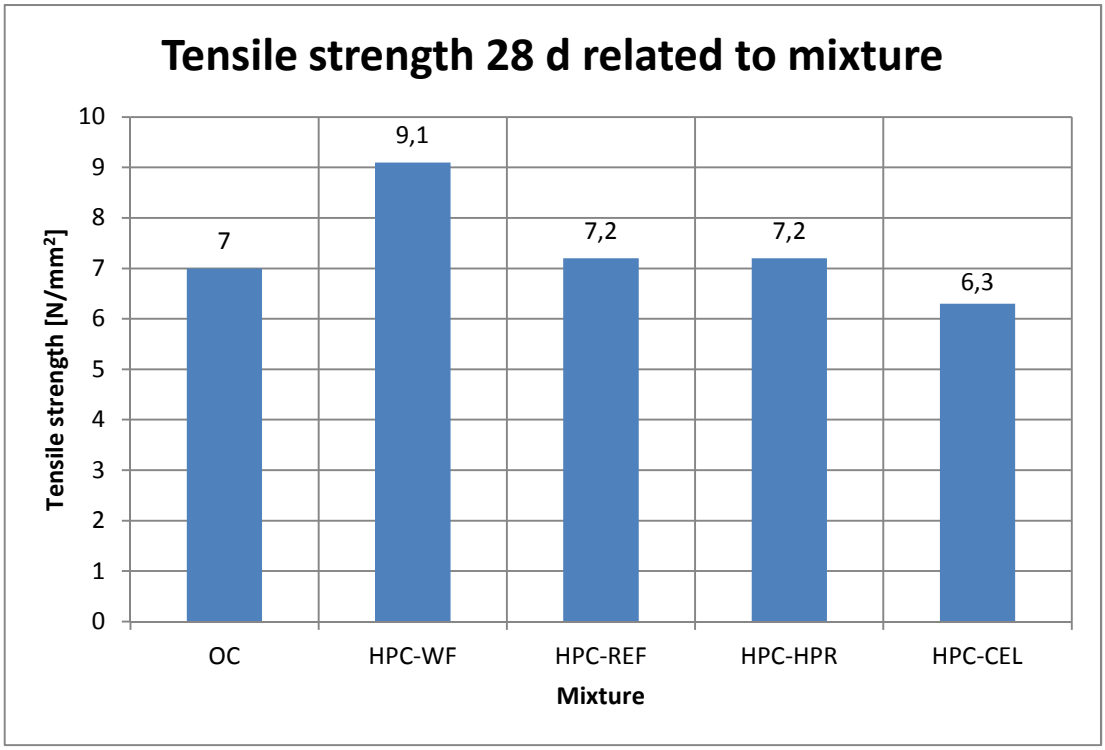

2.4. Experiment

In this experimental part, specimen of each mixture was loaded by two different methods – hydrocarbon curve and ISO – 834 curve. Before the fire test, all specimens were weighed to gain knowledge of mass loss, which includes water and material loss. Thermal loading was performed by oven with two thermocouples inside to measure temperature (see Figure 25).

Figure 25: Oven

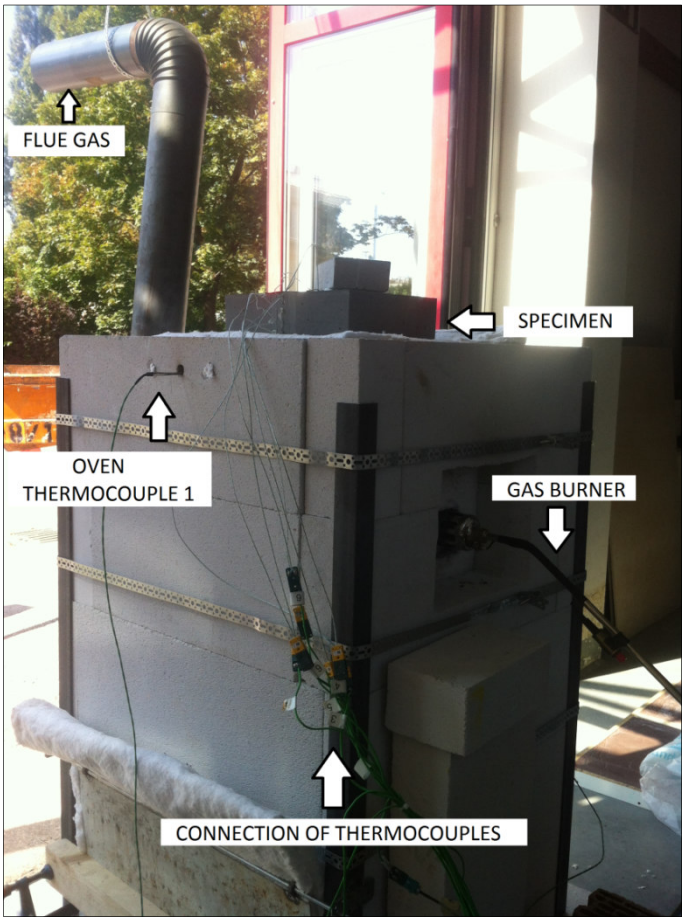

2.4.1 ISO – 834 curve

Specimens of each mixture were heated for 60 minutes according to ISO – 834 curve (Figure 26) and afterwards the measuring continued for 30 minutes. Specimens were left to cool down to room temperature and cut into 4 cubes 100 x 100 x 100 mm to test compressive strength after the fire test.

Figure 26: Time-temperature curve ISO – 834 [6]

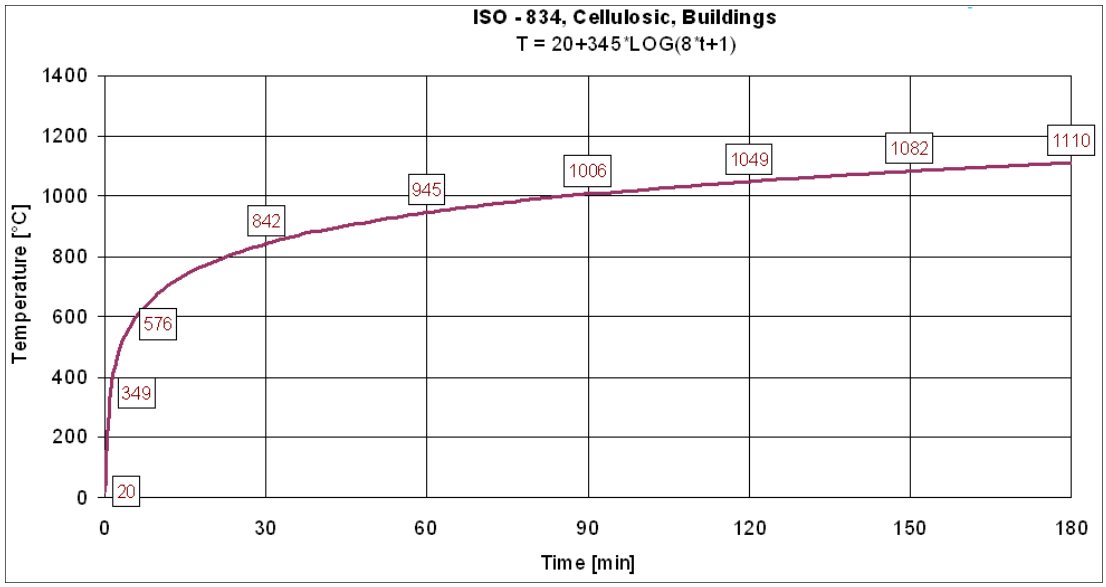

Specimen OC1

Table 18: Characteristics of specimen OC1 before the fire test

OC1		
Characteristics	**Unit**	**Value**
Weight m_1	[kg]	17,585
Water content	[%]	4,6
Compressive strength σ_1	[N/mm^2]	44,8

Observation of the fire test

- Room temperature: 25 °C Oven temperature: 190 °C
- 12 min. Water vapor started coming out
- 13 min. First bigger crack in place of wires
- 17 min. Appearance of other cracks
- 60 min. End of the fire tests

Figure 27: Time-temperature curves of specimen OC1

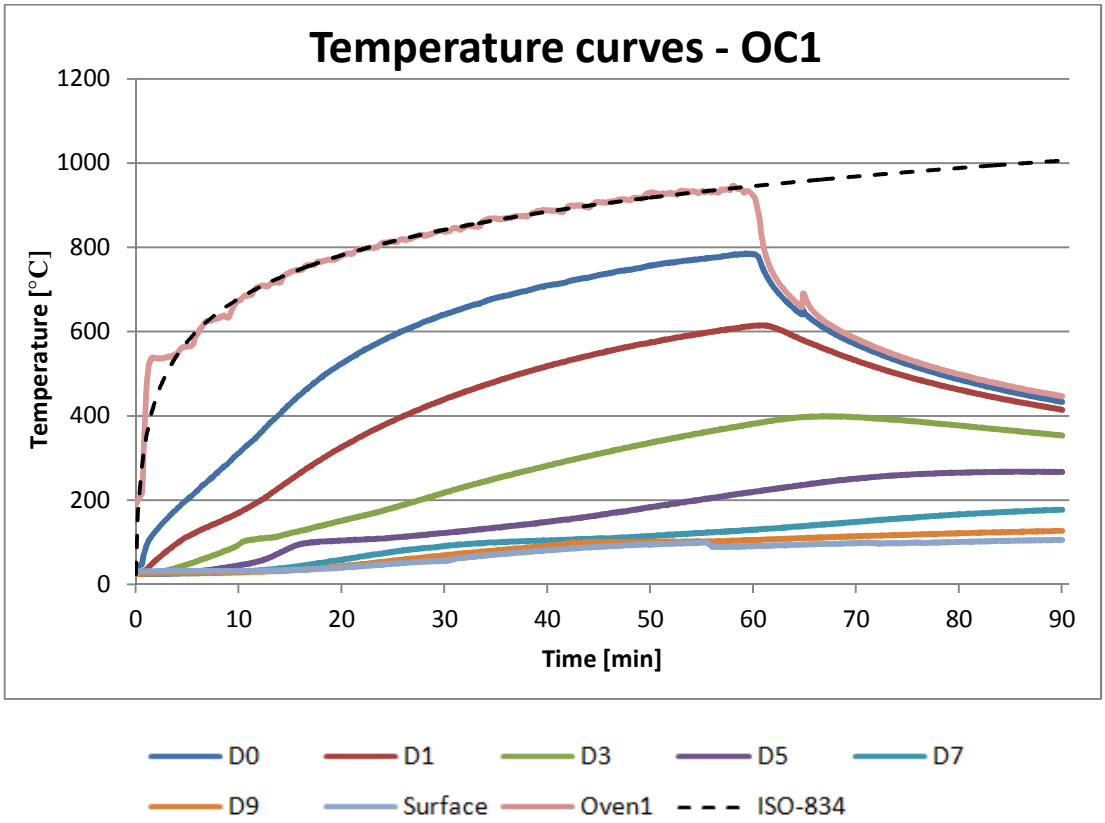

Figure 27: Maximum temperature of specimen was recorded at depth D0 784 °C in time 60 min which responds to the end of the heating. At 100 °C by depth D9, there is a

small plateau as a result of spending the heat on evaporation of water, therefore temperature was not rising. Plateau indicates also possibility of almost no spalling of concrete. After finishing the heating, the temperature at depth 3 cm was increasing for another 10 minutes, before the temperature started to go down. The temperature curve in the depths D3, D5, D7, D9 and on the surface, was still increasing. Both effects (depths D3, D5, D7, D9 and surface) were caused by residual heat coming out of the specimen.

Temperatures at 60 minutes (the end of the fire test)

- D 0 ca. 784 °C
- D1 ca. 615 °C
- D3 ca. 385 °C
- D5 ca. 223 °C
- D7 ca. 131 °C
- D9 ca. 106 °C
- Surface ca. 92 °C

Figure 28: Specimen OC1 24 hours after the fire test

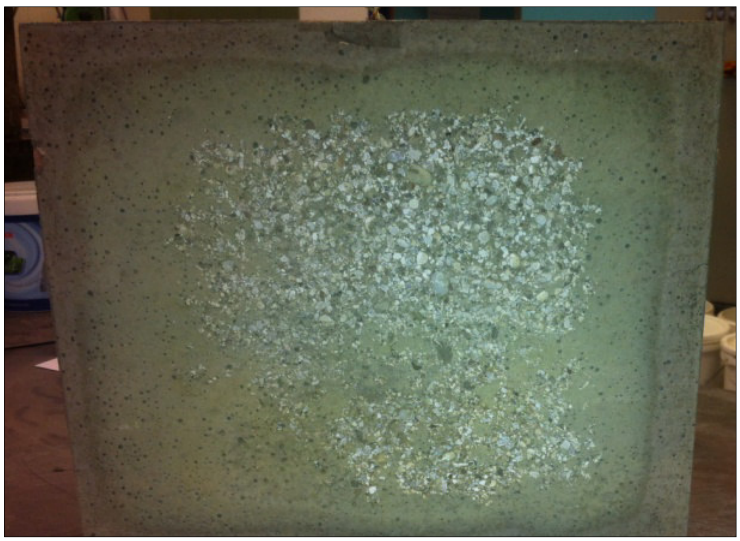

Table 19: Characteristics of specimen OC1 after the fire test

OC1		
Characteristics	**Unit**	**Value**
Weight m_2	[kg]	16,913
Water content	[%]	-
Compressive strength σ_2	[N/mm^2]	28,1

Specimen HPC-WF1

Table 20: Characteristics of specimen HPC-WF1 before the fire test

HPC-WF1		
Characteristics	**Unit**	**Value**
Weight m_1	[kg]	19,361
Water content	[%]	4,3
Compressive strength σ_1	[N/mm^2]	121,9

Observation of the fire test

- Room temperature: 27 °C Oven temperature: 50 °C
- 7 min. Appearance of the first cracks
- 12 min. First spalling, water coming out of the cracks
- 14 min. Second spalling and after that, spalling every minute
- 23 min. Last spalling leading to complete cracking of the specimen
- 24 min. Early ending of the fire test

Figure 29: Time-temperature curves of the specimen HPC-WF1

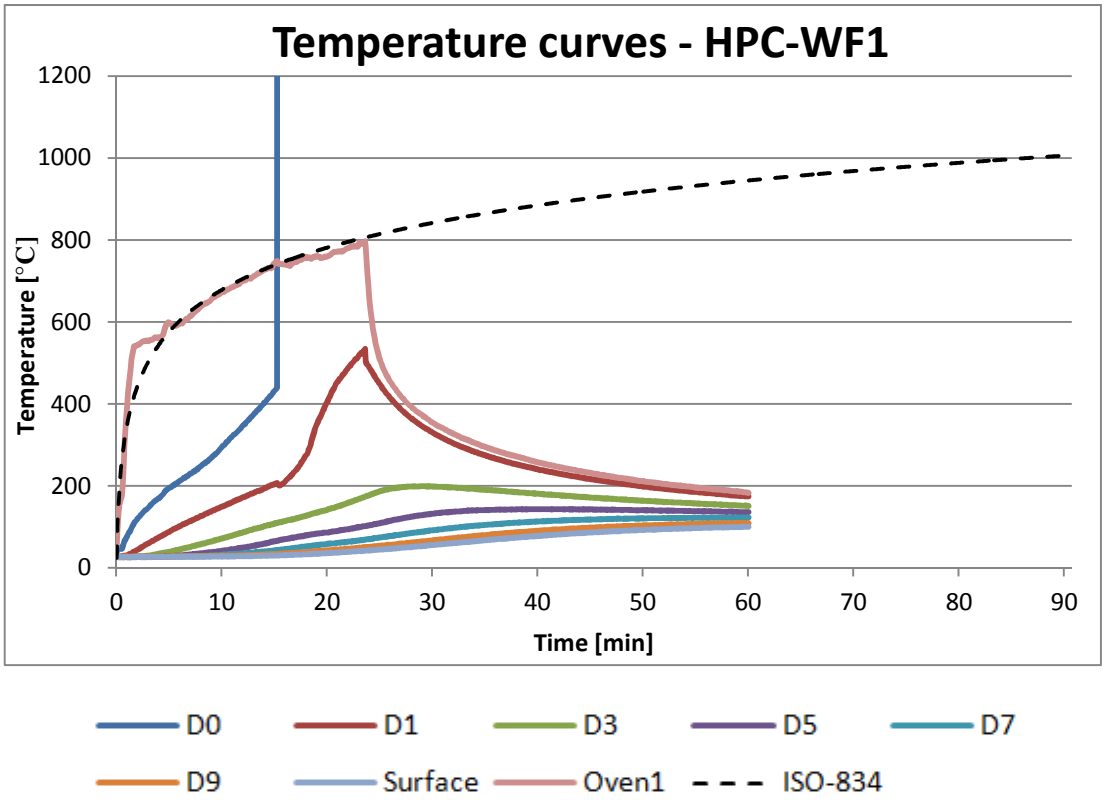

Figure 29: Thermocouple D0 was destroyed 15 minutes after the beginning of the fire test (the last measured temperature 439 °C) after spalling. In the same time, a small decrease of temperature was recorded in the oven and at depth D1. This is a result of spending the heat for heating the new layer of concrete, which was exposed thanks to spalling. A small decrease of temperature can be seen during each spalling. The fire test of the specimen HPC-WF1 lasted only 24 minutes, because the specimen was destroyed by the last spalling. Therefore, maximum temperature was measured in depth D1 534 °C at the early ending of the fire test. Afterwards, temperatures of D5, D7, D9 and the surface were rising from the residual heat.

Temperatures at the time 24 minutes (end of the fire test)

- D0 ca. -
- D1 ca. 534 °C
- D3 ca. 175 °C
- D5 ca. 103 °C
- D7 ca. 70 °C
- D9 ca. 51 °C
- Surface ca. 42 °C

Figure 30: Specimen HPC-WF1 - after last spalling

Figure 30: On picture can be seen cracks formed by last spalling in 24 minutes. These cracks led to destruction of specimen.

Figure 31: Specimen HPC-WF1 – Detail of crack

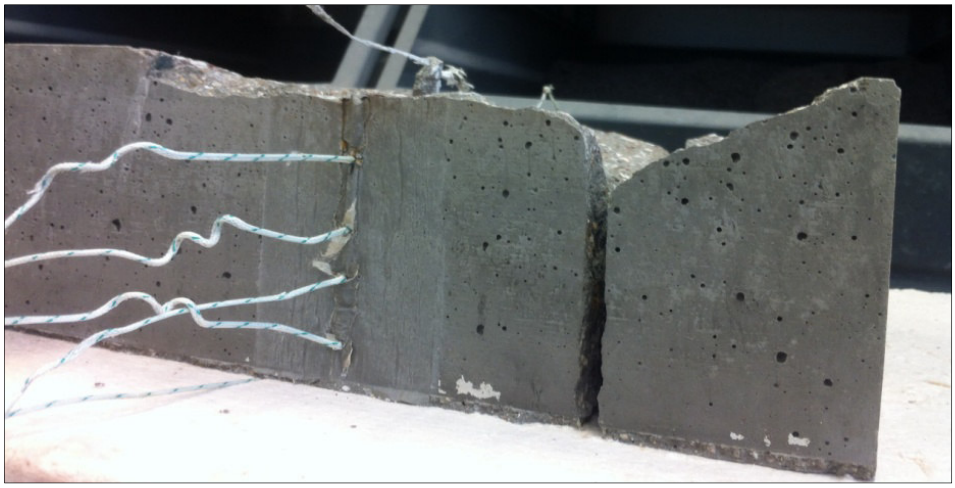

Figure 32: Specimen HPC-WF1 - 24 hours after the fire test

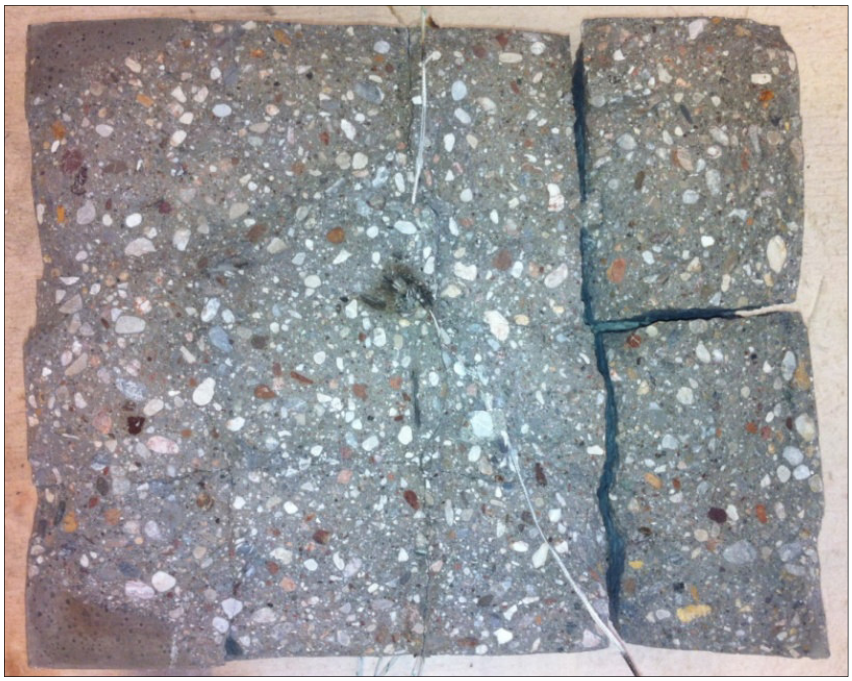

Figure 33: Spalling depths of the specimen HPC-WF1

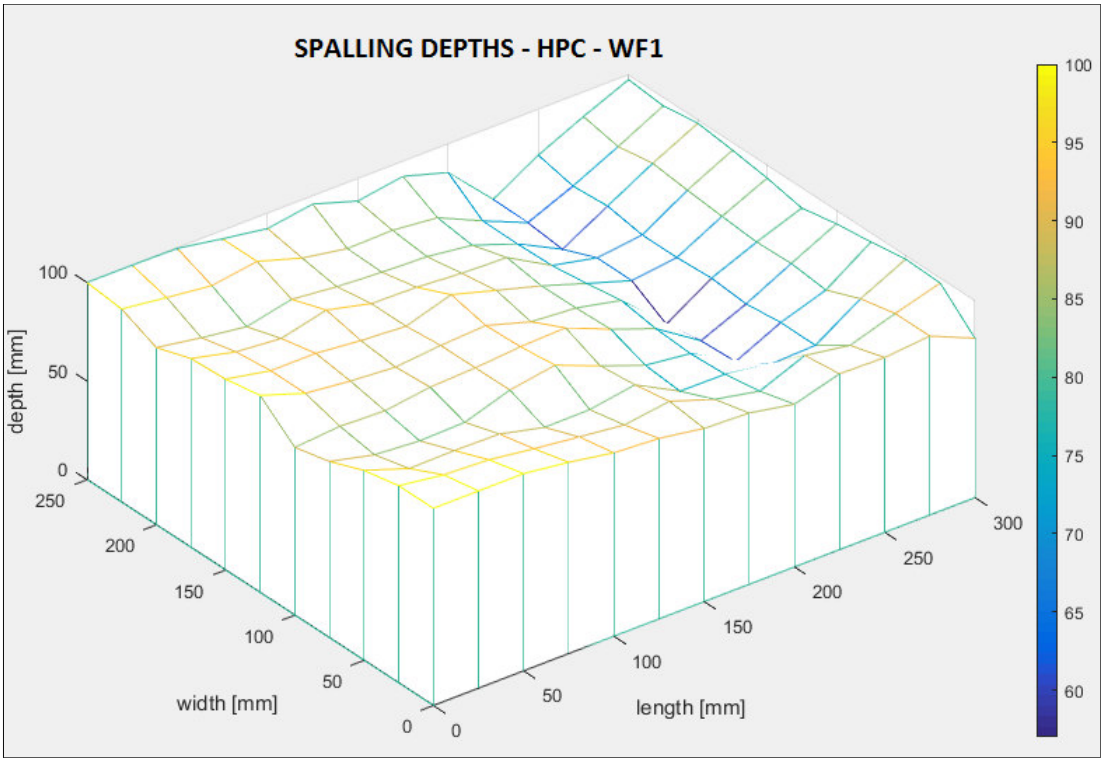

Figure 33: According to the graph, the highest spalling depth is 43 mm. The average spalling depth was around 2 cm. Area with highest spalling depths were on opposite side of burner, where heat was more accumulated.

Table 21: Characteristics of specimen HPC-WF1 after the fire test

HPC-WF1		
Characteristics	**Unit**	**Value**
Weight m_2	[kg]	16,231
Water content	[%]	-
Compressive strength σ_2	[N/mm^2]	-

Specimen HPC-REF1

Table 22: Characteristics of specimen HPC-REF1 before the fire test

HPC-REF1		
Characteristics	**Unit**	**Value**
Weight m_1	[kg]	18,219
Water content	[%]	4,4
Compressive strength σ_1	[N/mm^2]	109,9

Observation of the fire test

- Room temperature: 28 °C Oven temperature: 100 °C
- 14 min. First small cracks in frontal part of the specimen
- 15 min. Water vapor coming out; water coming out of the cracks
- 29 min. Bluish smoke from PP fibers
- 60 min. End of the fire test

Figure 34: Time-temperature curves of the specimen HPC-REF1

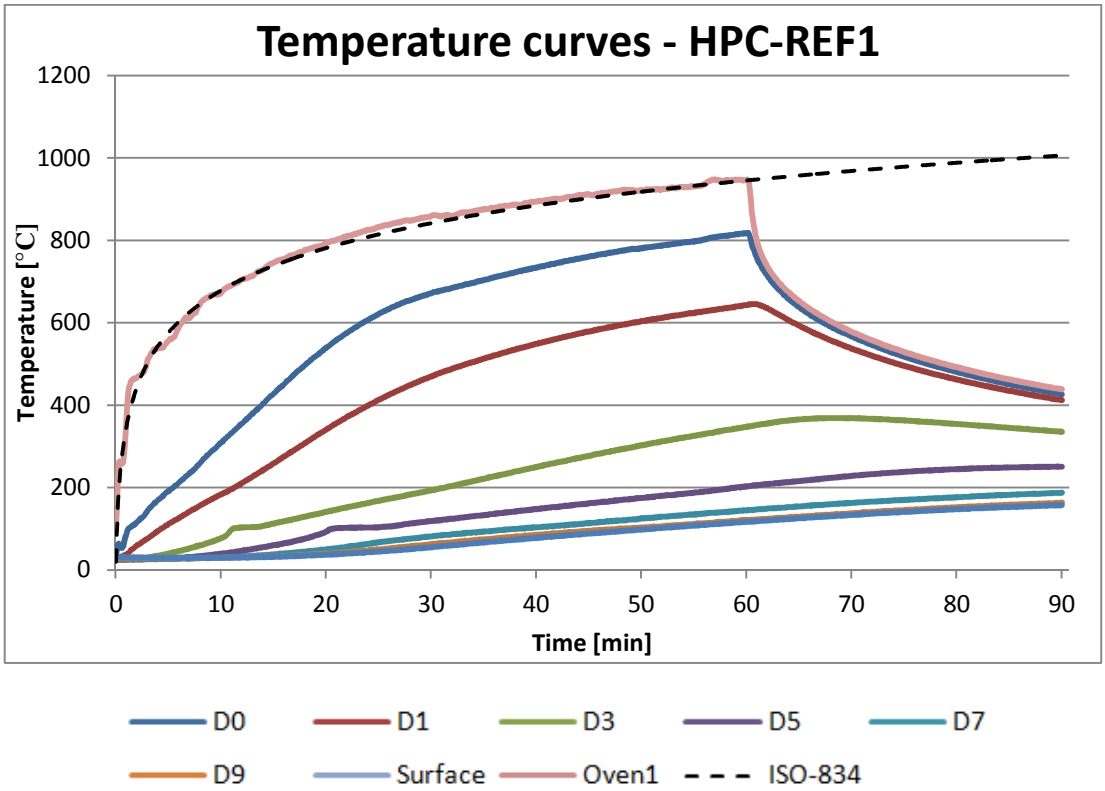

Figure 34: In the graph, there is an obvious appearance of the plateau at 100 °C by depths 3 and 5 cm. The highest temperature 818 °C was measured again after 60 minutes on the

heated surface of the concrete. After the end of the fire test, the temperature was increasing in depths D5, D7, D9 and on the surface of the concrete.

Temperatures at time 60 minutes (end of the fire test)

- D0 ca. 818 °C
- D1 ca. 646 °C
- D3 ca. 351 °C
- D5 ca. 206 °C
- D7 ca. 147 °C
- D9 ca. 122 °C
- Surface ca. 118 °C

Figure 35: Specimen HPC-REF1 during the fire test

Figure 35: On both pictures are visible cracks on side with water coming out. Water coming out of the specimen decrease water content and so it decreases vapor pressure and possibility of spalling. On the right picture (in 25 minutes of fire test) water stopped coming out of the lower part of crack, because specimen was already in that part dried.

Figure 36: Specimen HPC-REF1 24 hours after the fire test

Table 23 : Characteristics of the specimen HPC-REF1 after the fire test

HPC-REF1		
Characteristics	**Unit**	**Value**
Weight m_2	[kg]	17,507
Water content	[%]	-
Compressive strength σ_2	[N/mm^2]	72,8

Specimen HPC-HPR1

Table 24: Characteristics of the specimen HPC-REF1 before the fire test

HPC-HPR1		
Characteristics	**Unit**	**Value**
Weight m_1	[kg]	18,329
Water content	[%]	4,5
Compressive strength σ_1	[N/mm^2]	108,8

Observation of the fire test

- Room temperature: 23 °C Oven temperature: 41 °C
- 4 min. First cracks
- 5min. Other cracks
- 15 min. Water coming out of cracks
- 60 min. End of the test

Figure 37: Time-temperature curves of the specimen HPC-HPR1

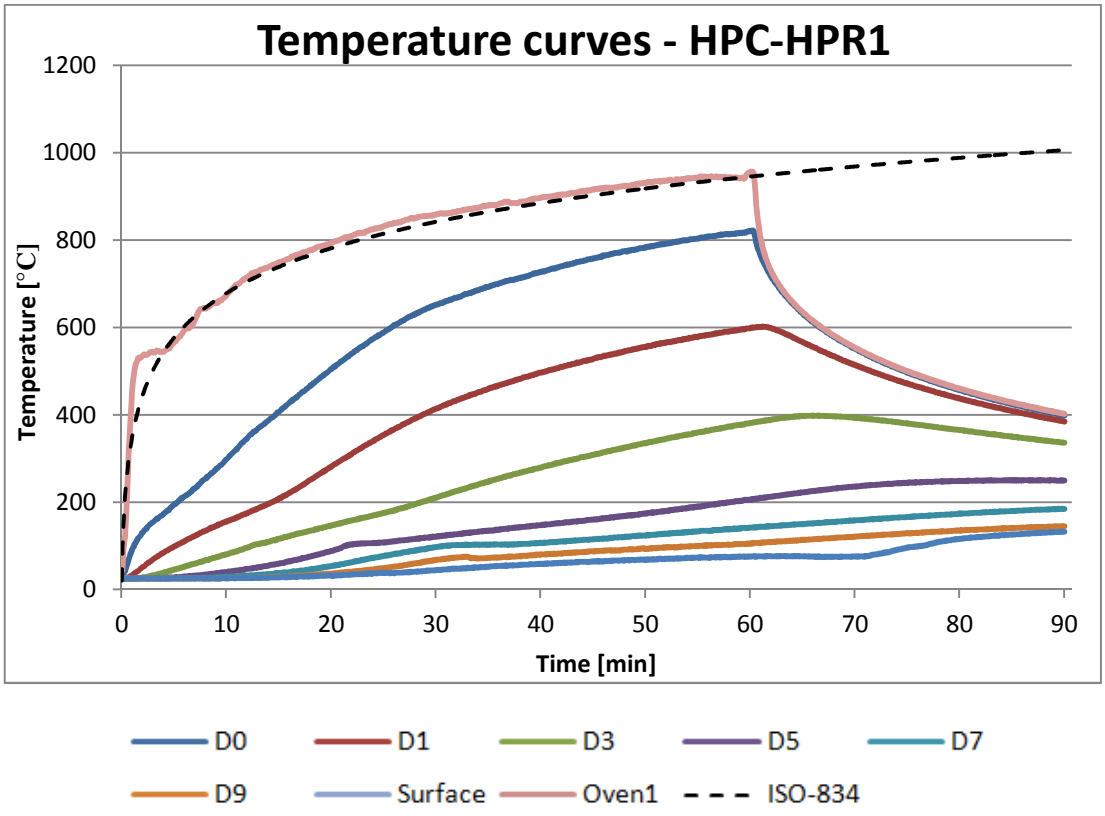

Figure 37: At 100 °C, there are noticeable plateaus in 5 and 7 cm and on the surface of the specimen. The maximum temperature that was measured on heated surface of concrete was 822 °C.

Temperatures at time 60 minutes

- D0 ca. 822 °C
- D1 ca. 601 °C
- D3 ca. 385 °C
- D5 ca. 210 °C
- D7 ca. 143 °C
- D9 ca. 107 °C
- Surface ca. 76 °C

Figure 38: Specimen HPC-HPR1 24 hours after the fire test

Specimen HPC-CEL1

Table 25 : Characteristics of the specimen HPC-CEL1 before the fire test

HPC-CEL1		
Characteristics	**Unit**	**Value**
Weight m_1	[kg]	18,337
Water content	[%]	4,4
Compressive strength σ_1	[N/mm^2]	106,8

Observation of the fire test

- Room temperature: 24 °C Oven temperature: 115 °C
- 2 min. First cracks
- 4 min. Appearance of more cracks
- 10 min. Water coming from the cracks
- 60 min. End of the fire test

Figure 39: Time-temperature curves of specimen HPC-CEL1

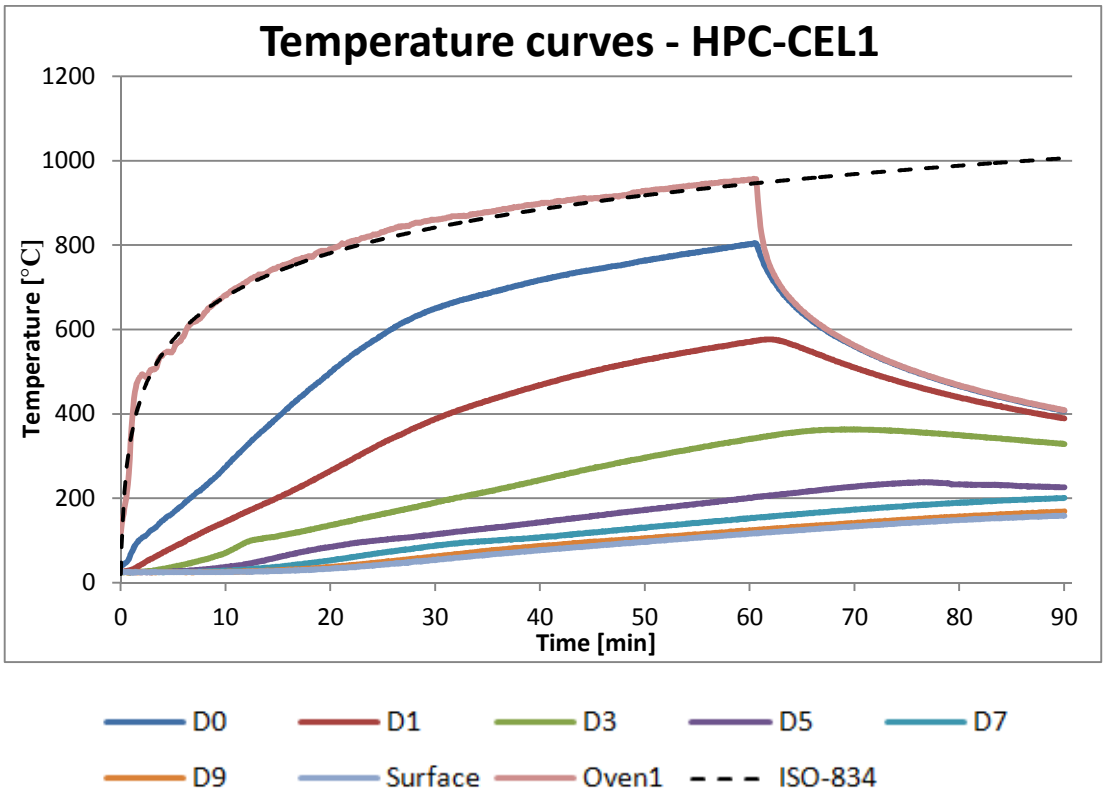

Figure 39: In the graph, there are no plateaus at temperature 100 °C. The maximum temperature was 804 °C at the end of the fire test.

Temperatures at time 60 minutes (end of the fire test)

- D0 ca. 804°C
- D1 ca. 575°C
- D3 ca. 344°C
- D5 ca. 204°C
- D7 ca. 155°C
- D9 ca. 126°C
- Surface ca. 118°C

Figure 40: Specimen HPC-CEL during fire test

Figure 41: Specimen HPC-CEL 24 hours after the fire test

Table 26: Characteristics of the specimen HPC-CEL1 after the fire test

HPC-CEL1		
Characteristics	**Unit**	**Value**
Weight m_2	[kg]	17,621
Water content	[%]	-
Compressive strength σ_2	[N/mm^2]	75,1

Evaluation

Figure 42: Time-temperature curves in depth 0 cm

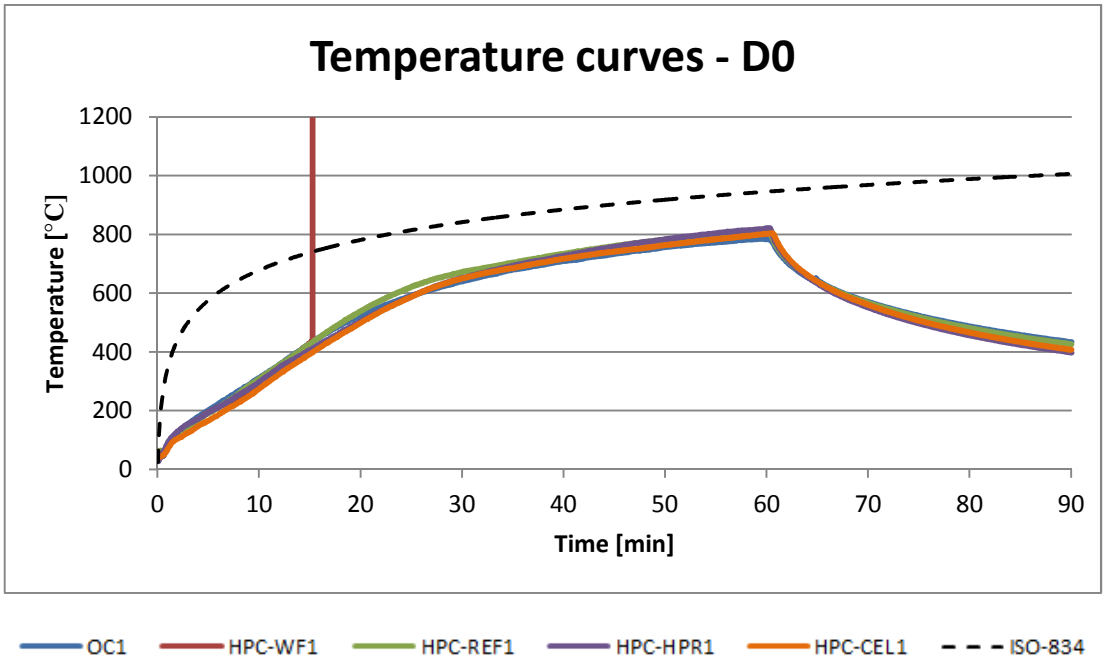

Figure 43: All curves had similar progress on the heated surface of the specimens. The highest temperature on the heated surface of the concrete was reached by the mixture HPC-HPR1 822 °C. Thermocouple of the specimen HPC-WF1 was destroyed at 439 °C in 15 minutes after beginning of the test. The lowest temperature was recorded with the mixture OC1 (ca. 785 °C).

Figure 43: Time-temperature curves in depth 1 cm

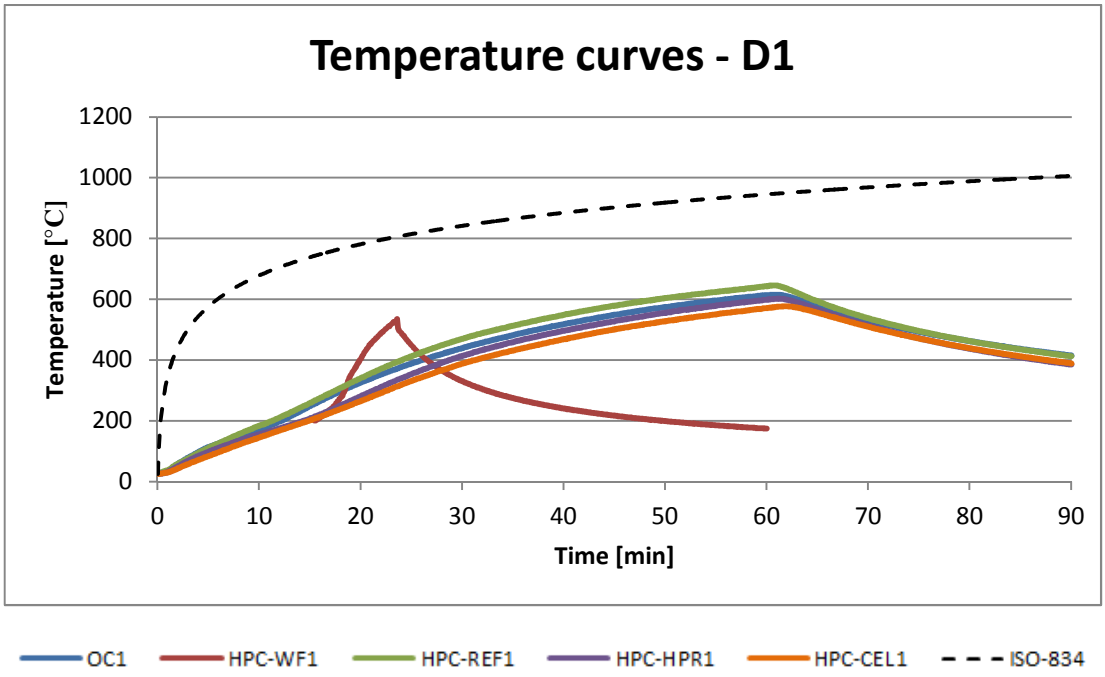

Figure 44: In the graph of temperature curves in depth 1 cm, there is a noticeable peak of HPC-WF1, which had the highest temperature in time 24 minutes out of all the specimens which was the consequence of the explosive spalling. Due to the explosive spalling, a new layer of concrete was exposed to the direct heat of the burner. The highest temperature was recorded with the mixture HPC-REF1 and the lowest with OC1. The temperatures were fluctuating around 600 °C.

Figure 44: Time-temperature curves in depth 3 cm

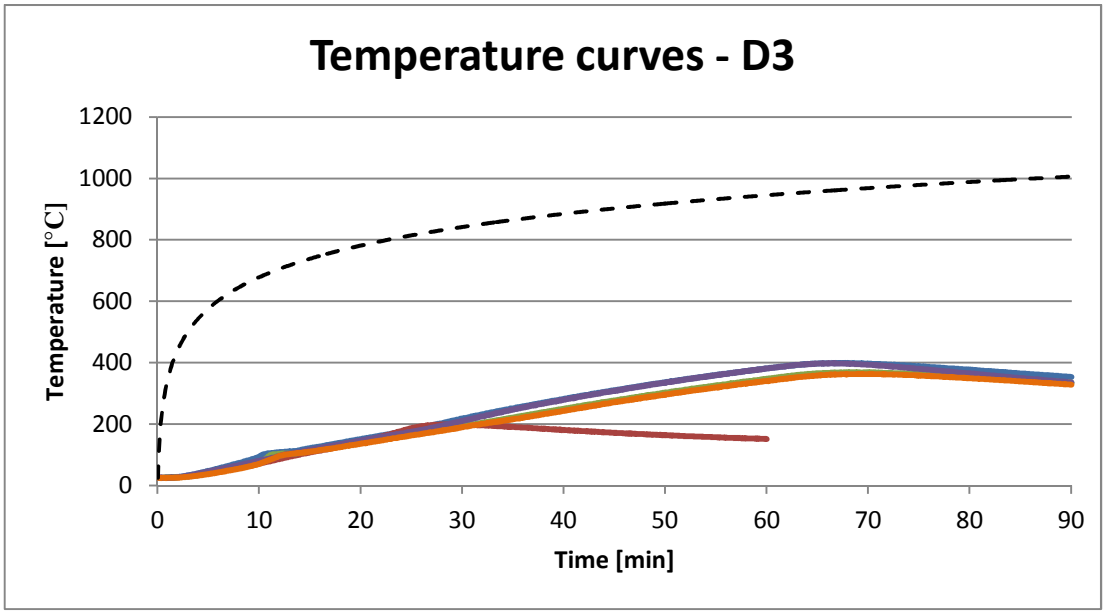

Figure 45: Time-temperature curves in depth 3 cm - detail

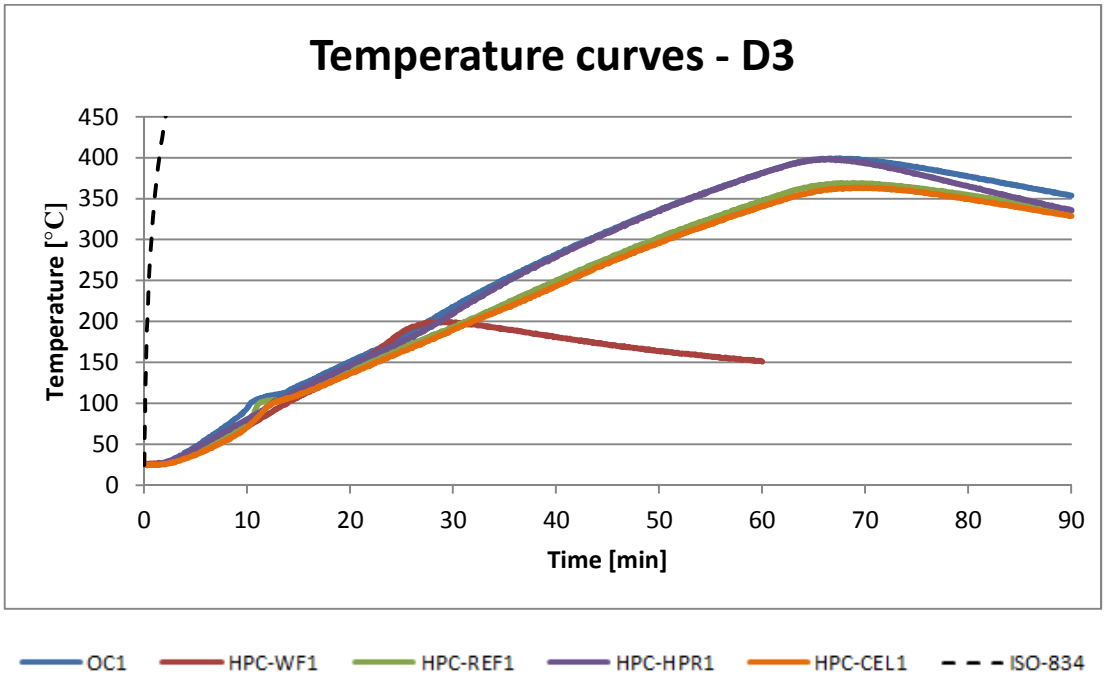

Figure 45, 46: The temperature curves in depth D3 are different after 30 minutes. At the end, the temperatures of OC1 and HPC-HPR1 were fluctuating around 400 °C. The mixtures HPC-CEL1 and HPC-REF1 were ranging with difference ca. 40 °C. HPC-WF1 had the highest temperature around 200 °C, due to the early end of the fire test. Already here, one can notice a slight increase of all specimens' temperature, specifically after the fire test, as a result of the residual heat emitting from the specimens.

Figure 46: Time-temperature curves in depth 5 cm

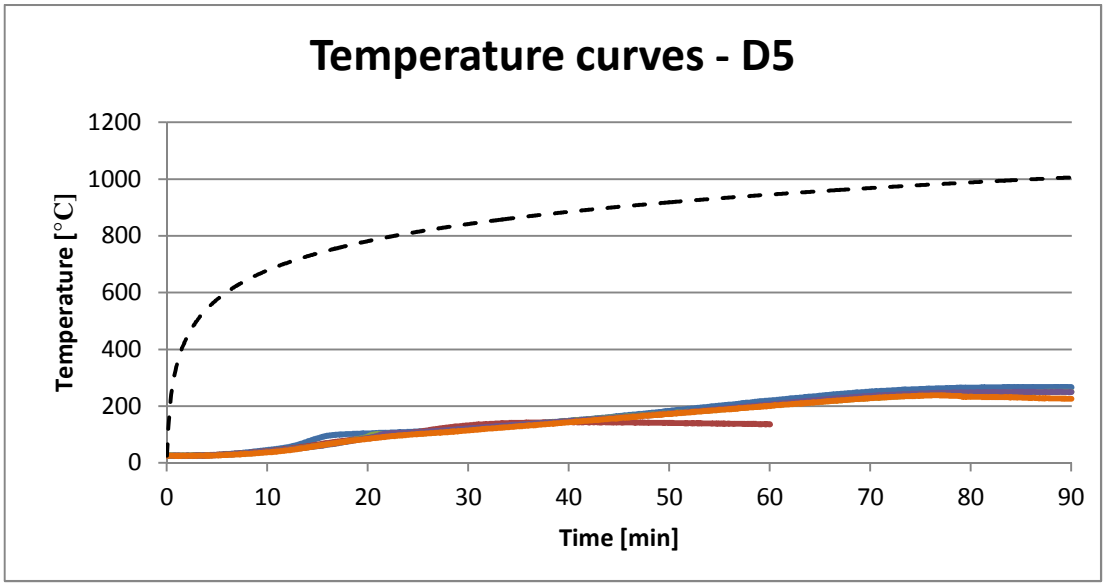

Figure 47: Time-temperature curves in depth 5 cm - detail

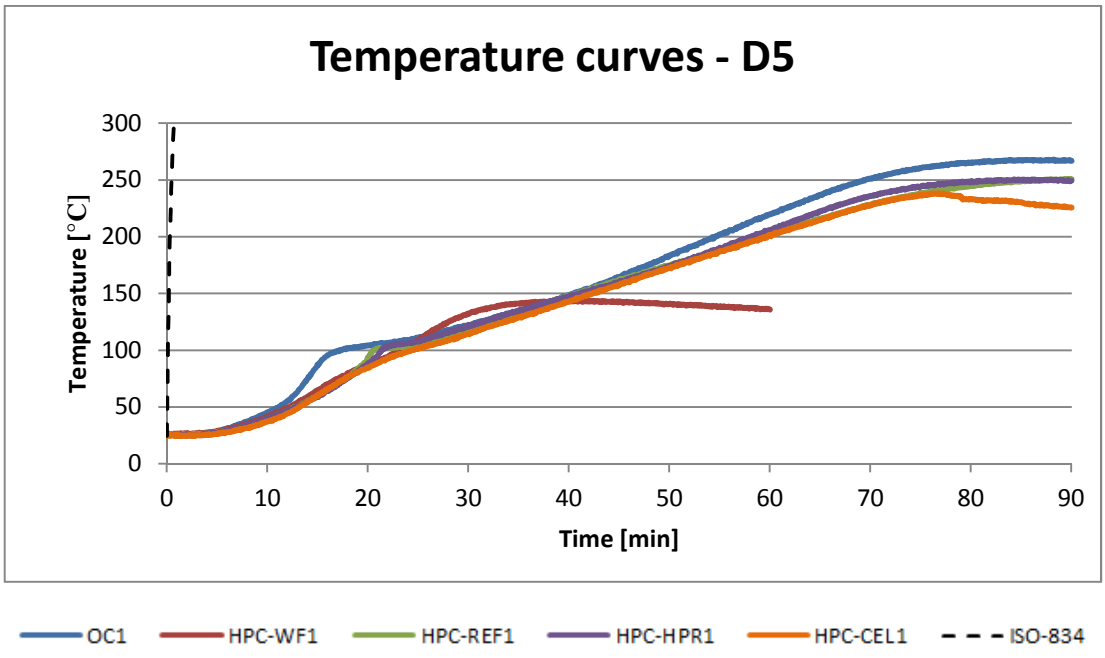

Figure 47, 48: The progress of the temperature curve of the specimens with polypropylene fibers (HPC-REF1 and HPC-HPR1) is similar. Temperature curve OC1 has in 13-17 minutes steeper progress and highest reached temperature was 250 °C at the end of the measuring (90 minutes). The mixture HPC-HPR1 and OC1 have plateaus at 100 °C at depth 5 cm.

Figure 48: Time-temperature curves in depth 7cm

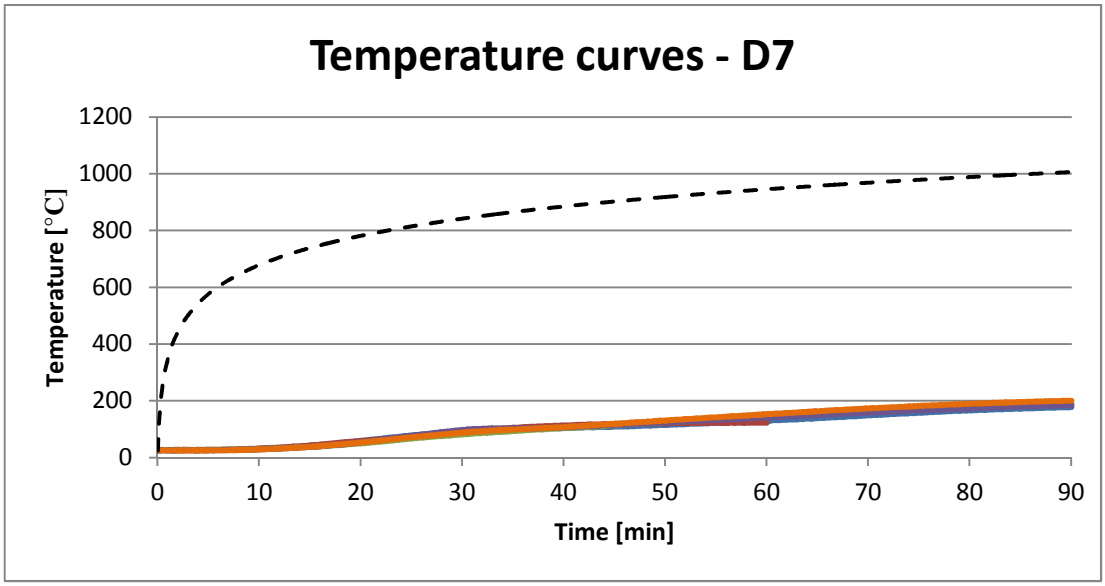

Figure 49: Time-temperature curves in depth 7cm - detail

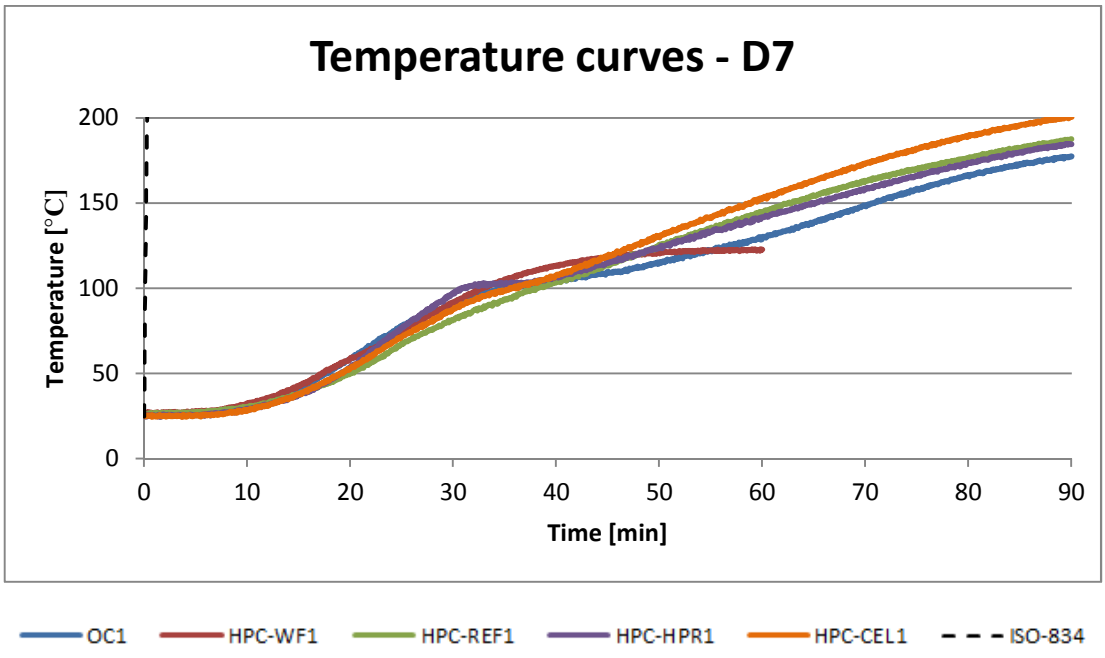

Figure 49, 50: The mixture HPC-HPR1 shows a plateau at 100 °C, which lasted approx. 5 minutes. All curves were rising steadily, except for the curve HPC-WF1. The residual heat of the specimen HPC-WF1 was not that intense to increase the temperature curve as with the other mixture which was heated for the whole 60 minutes. The maximum temperature was reached after the heating. The highest temperature was recorded with HPC-CEL1 (ca. 200 °C).

Figure 50: Time-temperature curves in depth 9 cm

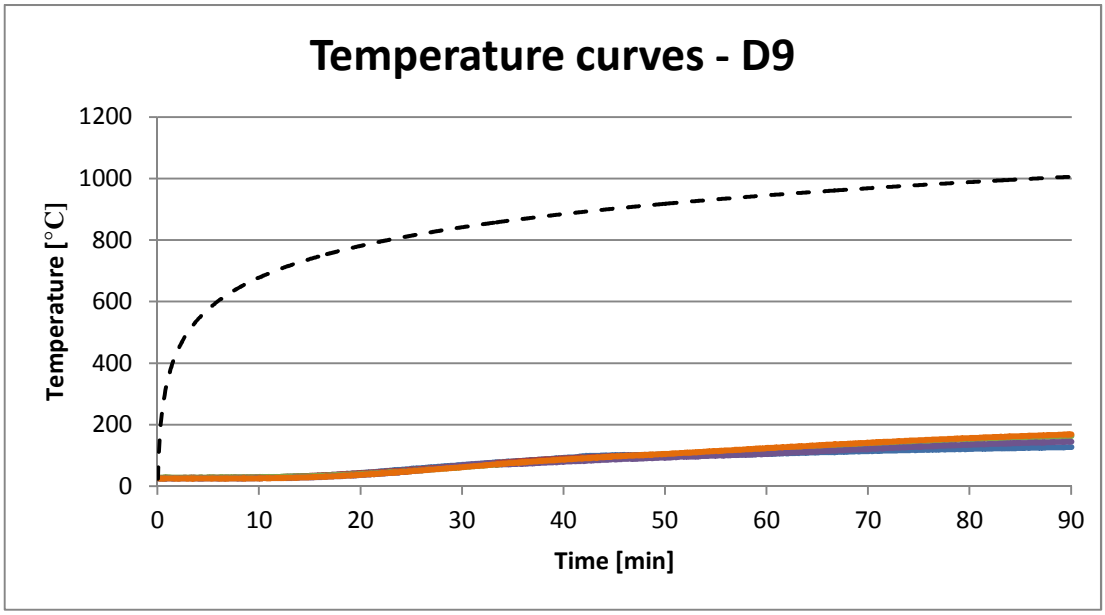

Figure 51: Time-temperature curves in depth 9 cm - detail

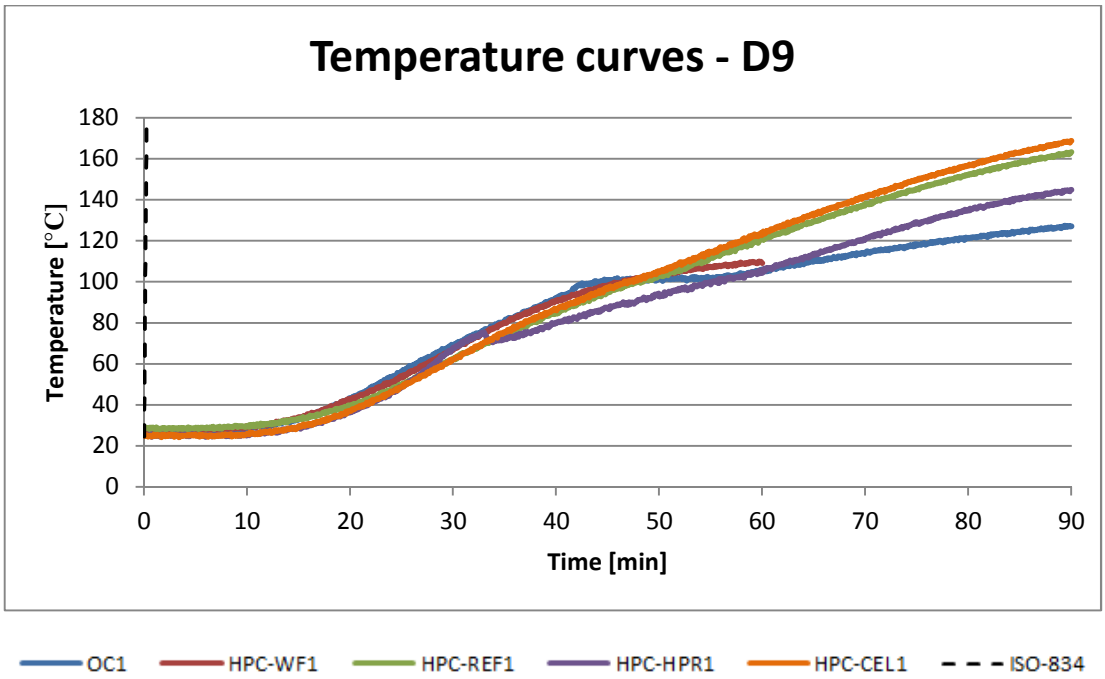

Figure 51, 52: The temperature of all the mixtures were constant until 13 minutes of the fire test. After 13 minutes, the curves start to go up. At 100 °C, there is a significant plateau with the mixture OC1, therefore, OC1 has the lowest temperature curve in depth 9 cm. After the end of the fire test, all the curves were steadily increasing.

Figure 52: Time-temperature curves on surface

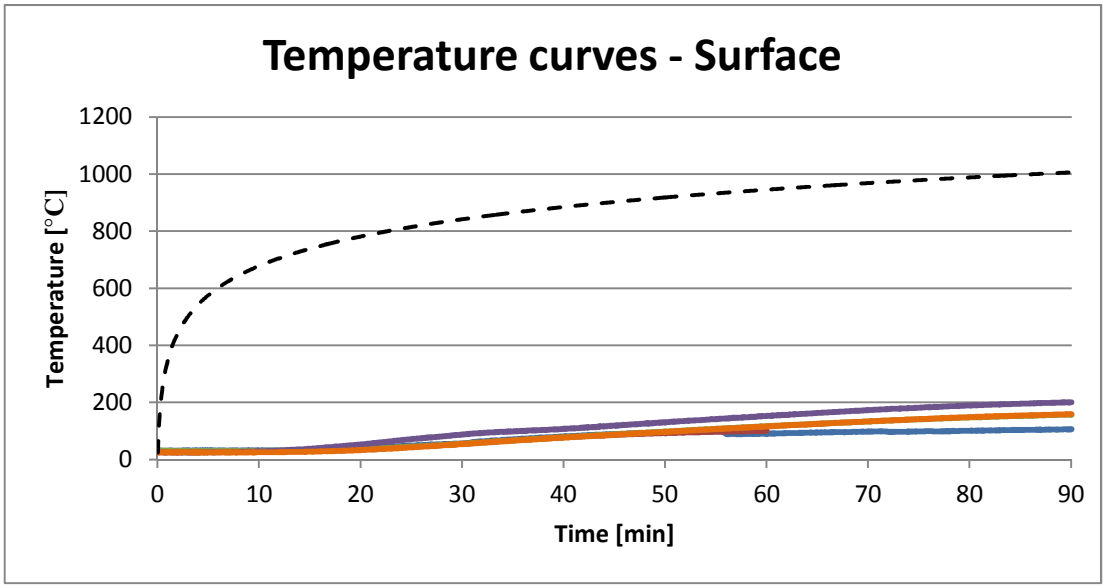

Figure 53: Time-temperature curves on surface - detail

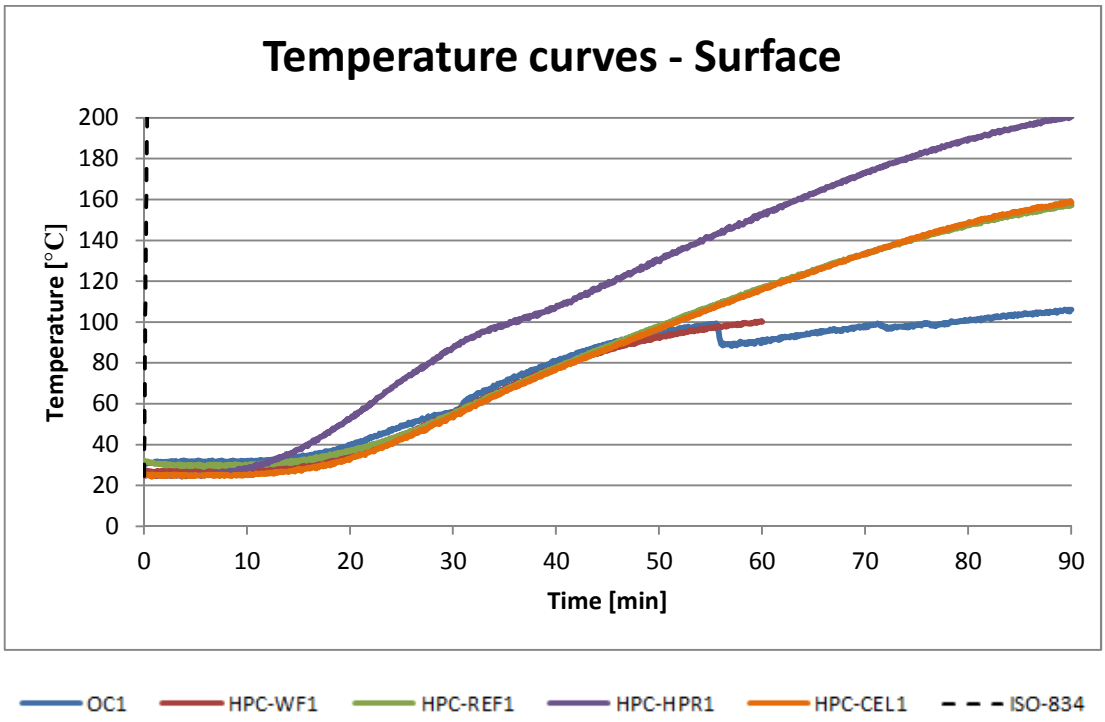

Figure 53, 54: The temperature curve HPC-HPR1 started to rise in 9 minutes and had the highest temperature, approx. 200 °C, at the end of the measuring. In 55 minutes, the temperature curve OC1 suddenly decreased to 10 °C. This can be cause of brief wrong function of thermocouple.

Figure 54: The compressive strength after the fire test related to the mixture

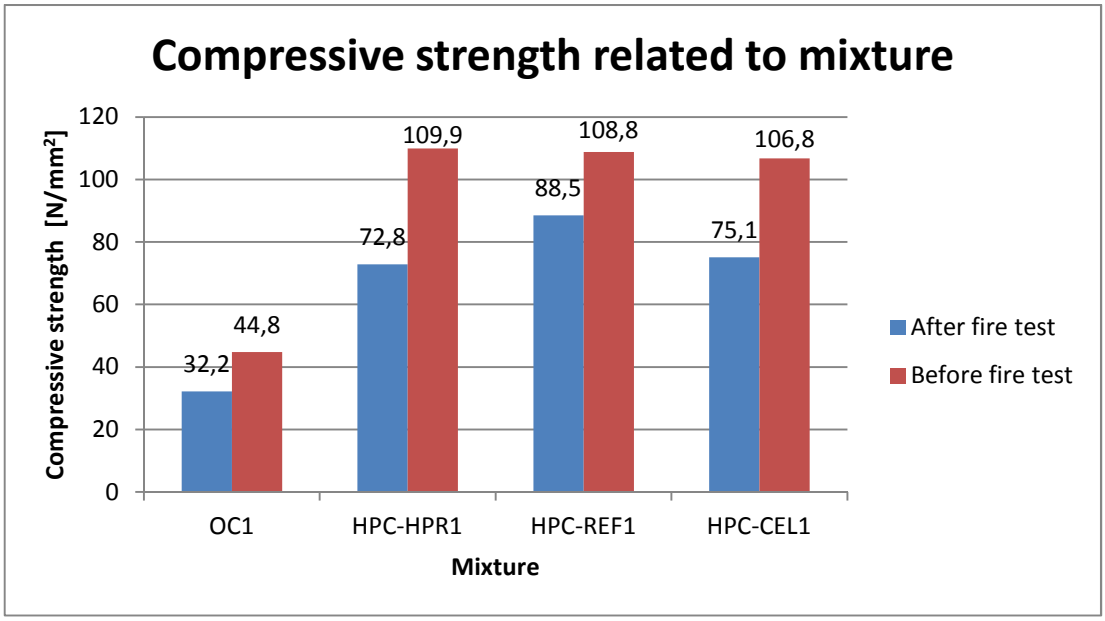

Table 27: Characteristics of specimens before and after the fire test

	Before fire test			After fire test			
	m_1 [kg]	Water content [%]	σ_1 [N/mm^2]	m_2 [kg]	σ_2 [N/mm^2]	Mass loss [%]	Compressive strength loss [%]
OC1	17,585	4,6	44,8	16,913	32,2	3,8	28,1
HPC-WF1	19,361	4,3	121,9	16,231	-	16,2	-
HPC-REF1	18,219	4,4	109,9	17,507	72,8	3,9	33,8
HPC-HPR1	18,329	4,5	108,8	17,587	88,5	4,0	18,7
HPC-CEL1	18,337	4,4	106,8	17,621	75,1	3,9	29,7

Table 27: The mass loss was the highest in the mixture HPC-WF1 16,2 %. This mixture was the only one where explosive spalling occurred. The mass loss of other mixtures was almost comparable, the mixture OC1 had the lowest mass loss – 3,8 %. The compressive strength after the fire test was not measured in the case of the specimen HPC-WF1 due to explosive spalling. The highest compressive strength loss was observed in the case of the mixture of high performance concrete with reference (standard) fibers HPC-REF1, the compressive strength decreased from 109,9 N/mm^2 to 72,8 N/mm^2. The lowest decrease was with the mixture of high performance concrete with modified polypropylene fibers – 18,7 %.

In the pictures of the specimens (except for the mixture of high performance concrete without fibers - HPC-WF1) there are visible small changes 24 hours after the fire test. This

is the result of the reaction of the specimens and the aggregate with CO_2 from the air. The heating material containing $CaCO_3$ leads to calcination. CaO is not stable and therefore reacts with CO_2 from the air. These changes are described by the following equations:

Calcination of calcium carbonate (ca. 825°C): $CaCO_3 \rightarrow CaO + CO_2$

Carbonation of calcium oxide: $CaO + CO_2 \rightarrow CaCO_3$

The mixture HPC-WF1 had no changes of the heated surface after the fire test, this was caused by a short duration of the fire test and explosive spalling of the specimen.

2.4.2 Hydrocarbon curve

Specimens of each mixture were heated for 60 minutes according to hydrocarbon curve (Figure 56) and afterwards, the measuring continued for 30 minutes. The specimens were left to cool down to room temperature and samples were taken to measure porosimetry. 3 samples were taken from each specimen from a different depth (from the fire exposed surface 0-2 cm, 4-6 cm and 8-10 cm).

Figure 55: Time-temperature hydrocarbon curve [6]

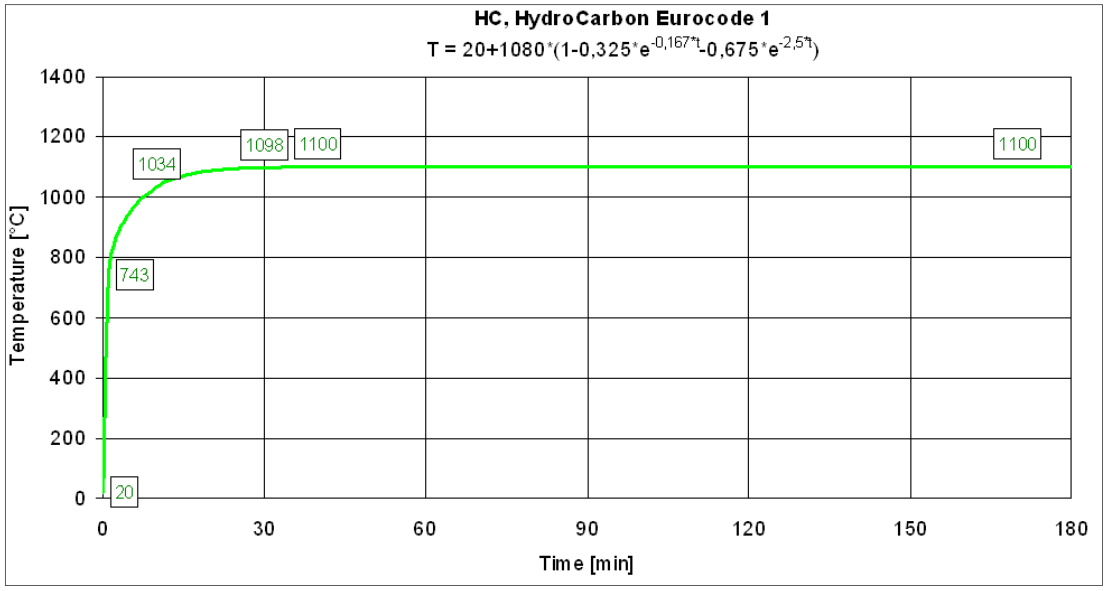

Specimen OC2

Observation of the fire test

- Room temperature: 25 °C Oven temperature: 165 °C
- 5 min. First cracks
- 8 min. Appearance of other cracks; water coming out of the specimen
- 60 min. End of the fire tests

Figure 56: Time-temperature curves of the specimen OC1

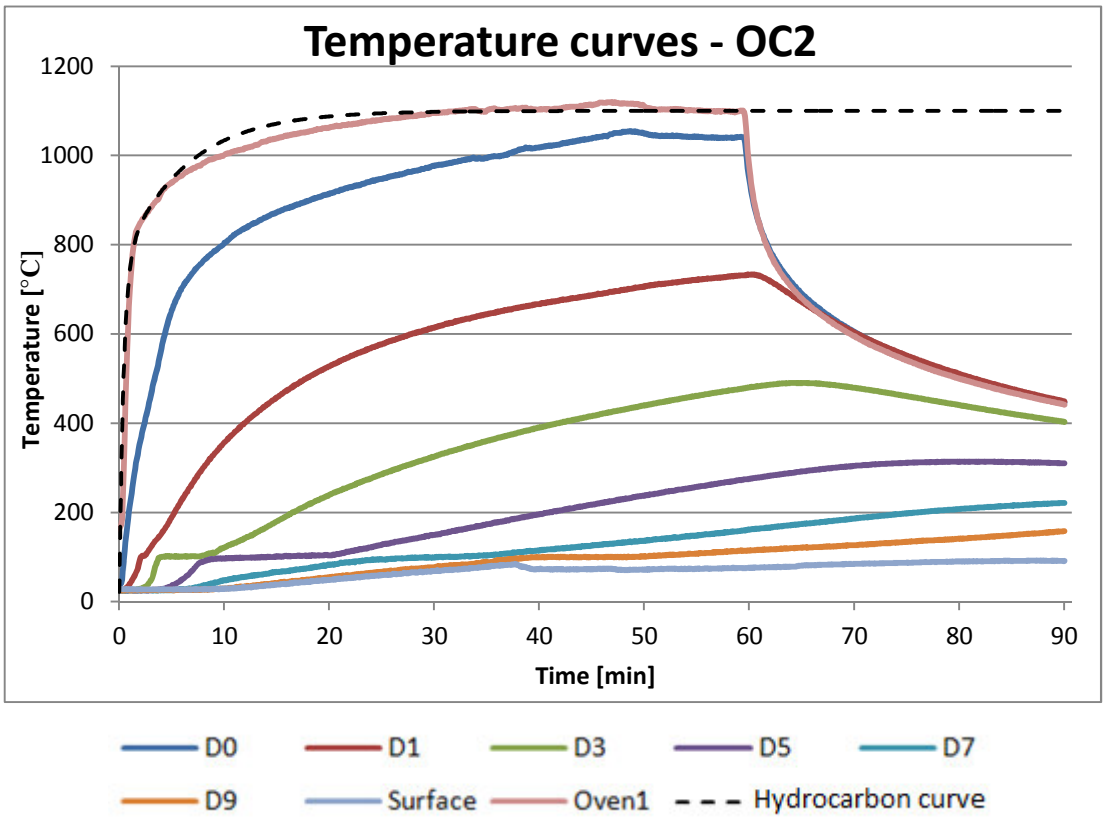

Figure 57: There are visible plateaus in the graph, significant plateaus can be observed especially in depths 5 cm, 7 cm and 9 cm. A smaller plateau is at the temperature curve D3. The maximum temperature 1054 °C was recorded in 49 minutes (D0) which responds to a slight increase of the oven temperature. The temperatures in the depths D5, D7, D9 and on the surface of concrete were rising steadily.

Temperatures at time 60 minutes (end of the fire test)

- D0 ca. 1041 °C
- D1 ca. 733 °C
- D3 ca. 482 °C
- D5 ca. 277 °C
- D7 ca. 160 °C
- D9 ca. 115 °C
- Surface ca. 77 °C

Figure 57: Specimen OC2 during the fire test

Figure 58: Specimen OC2 24 hours after the fire test

Figure 59: Porosity of specimen OC2

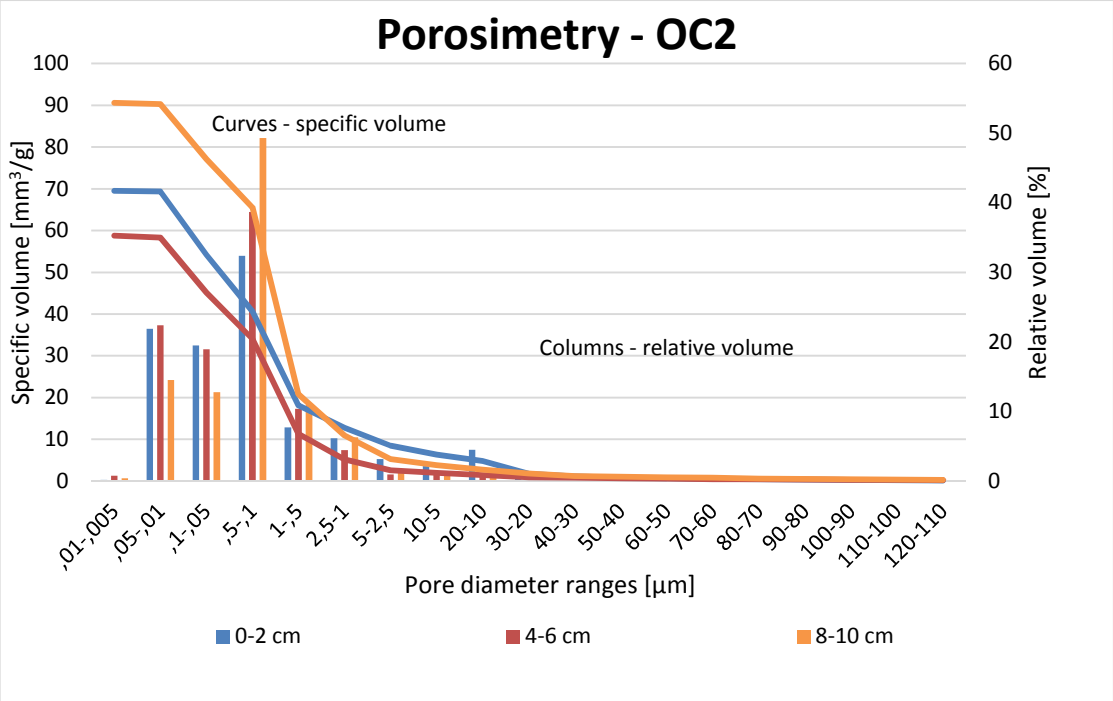

Figure 60: Ordinary concrete had the highest porosity in depth 8-10 cm, then 0-2 cm and the lowest porosity was recorded in depth 4-6 cm. This could have been caused by wrong preparation of the samples (for depths 0-2, 4-6 cm), since bigger part of the aggregate might have been present in the samples, resulting in smaller porosity.

Specimen HPC-WF2

Observation of the fire test

- Room temperature: 28 °C Oven temperature: 280 °C
- 2 min. First spalling
- 3 min. First cracks
- 5 min. Water coming out of the cracks
- 22min. Specimen destroyed
- 60 min. End of the fire test

Figure 60: Time-temperature curves of the specimen HPC-WF2

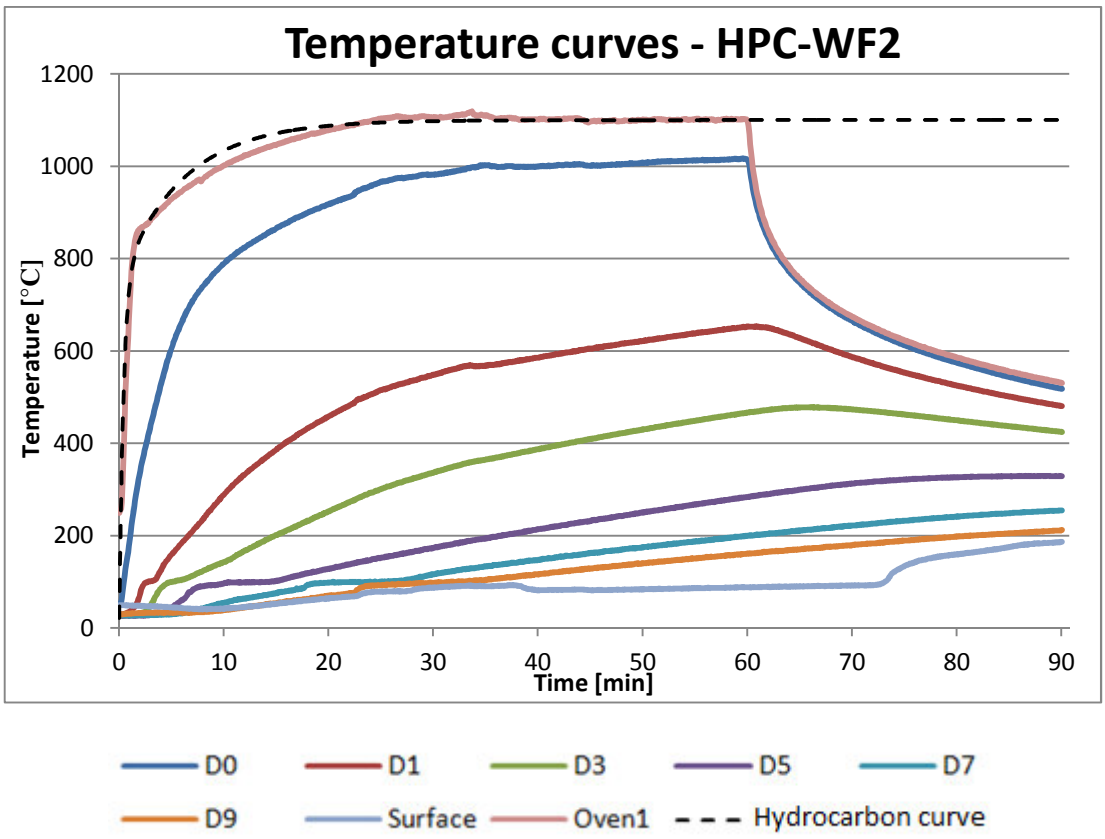

Figure 61: The specimen was split into two pieces ca. 22 minutes after the beginning of the test so results after 22 minutes should not be evaluated. Heating continued, because break occurred in place of wires and was not noticed.

Temperatures at time 60 minutes (end of the fire test)

- D0 ca. 1016 °C
- D1 ca. 653 °C
- D3 ca. 467 °C
- D5 ca. 285 °C
- D7 ca. 201 °C
- D9 ca. 162 °C
- Surface ca. 88 °C

Figure 61: Specimen HPC-WF1 - 24 hours after the fire test

Figure 62: Porosity of specimen HPC-WF2

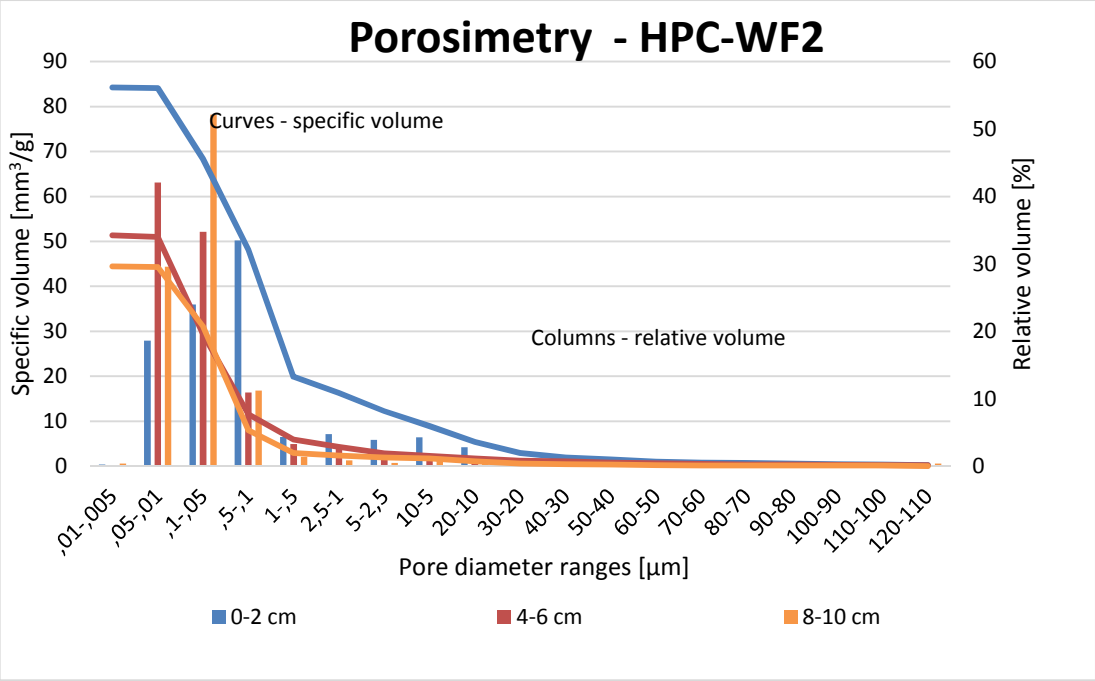

Figure 63: The results of mercury porosimetry showed the expected effect; the highest porosity was in depth 0-2 cm (temperatures reached approx. 900 °C), the part which had the highest temperatures. After that, porosity went equally down. The second highest porosity was 4-6 cm (around 280 °C), and the next lowest porosity was 8-10 cm (around 160 °C).

Specimen HPC-REF2

Observation of the fire test

- Room temperature: 25 °C Oven temperature: 160 °C
- 3 min. First cracks in the frontal part of the specimen
- 4 min. Second cracks, water coming out of the cracks
- 60 min. End of the fire test

Figure 63: Time-temperature curves of the specimen HPC-REF2

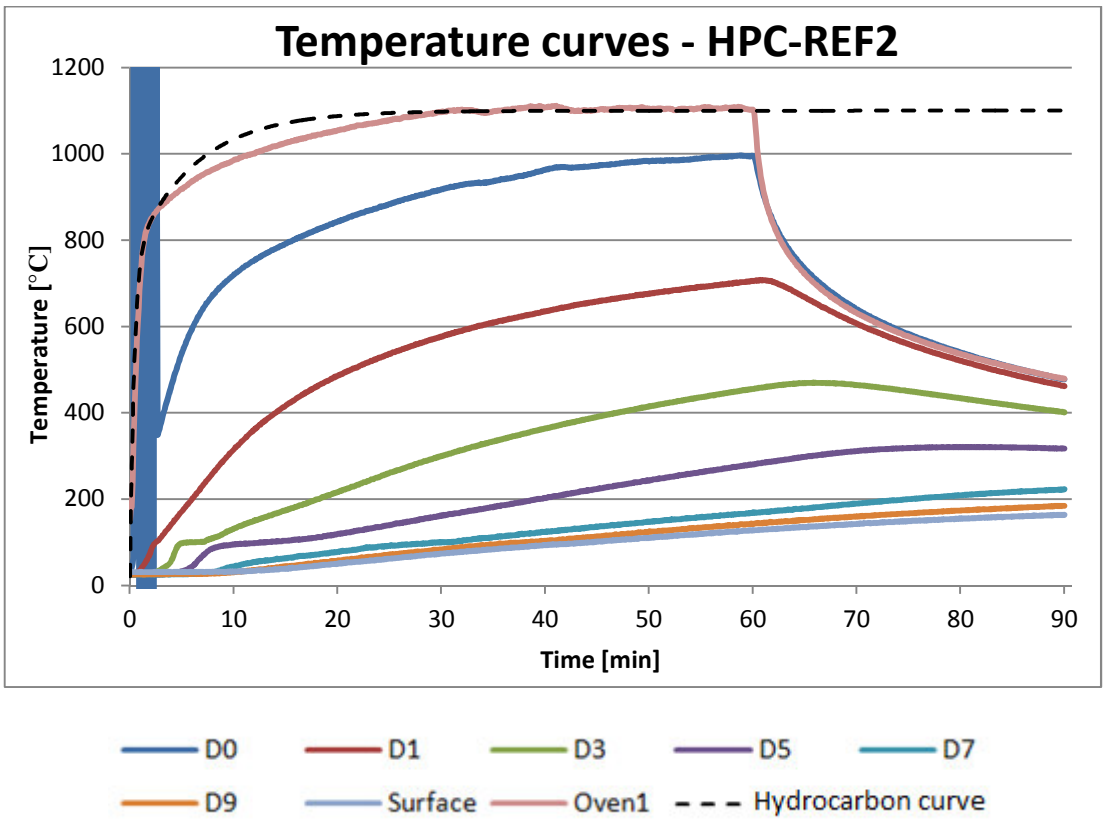

Figure 64: Thermocouple on the heated surface of the specimen was not measuring the right values at the beginning of the fire test. After three minutes, it started to measure values which can be presumed to be correct. The maximum temperature was ca. 1000 °C at the end of the test. A small plateau is visible at D3, other curves have no sign of plateau. After 60 minutes, the temperatures were dropping in depths 0, 1 and 3 cm. Then, the temperatures were rising after 60 minutes at D5-9 including the surface of the concrete.

Temperatures at time 60 minutes (end of the fire test)

- D0 ca. 996 °C
- D1 ca. 707 °C
- D3 ca. 458 °C
- D5 ca. 284 °C
- D7 ca. 170 °C
- D9 ca. 144 °C
- Surface ca. 129 °C

Figure 64: Specimen HPC-REF2 24 hours after the fire test

Figure 65: Cut of specimen HPC-REF2 24 hours after the fire test

Figure 66: On the picture can be seen color changes. Heated surface of concrete get whitish, due to calcination process $CaCO_3$ turns to lime and give pale shades of white and grey. Black part is approximately 0,5-2,5 cm. Reddish part of concrete is roughly 3-5 cm, where temperatures reached max. 470 °C. This part of concrete is caused by iron contained in the fine aggregate or the coarse aggregate, and the hydrate starts to dissolve and the iron starts to get oxidized at this temperature. Almost no color changes were visible in depths 8-10 cm, temperature were not that high to cause color changes.

Figure 66: Porosity of specimen HPC-REF2

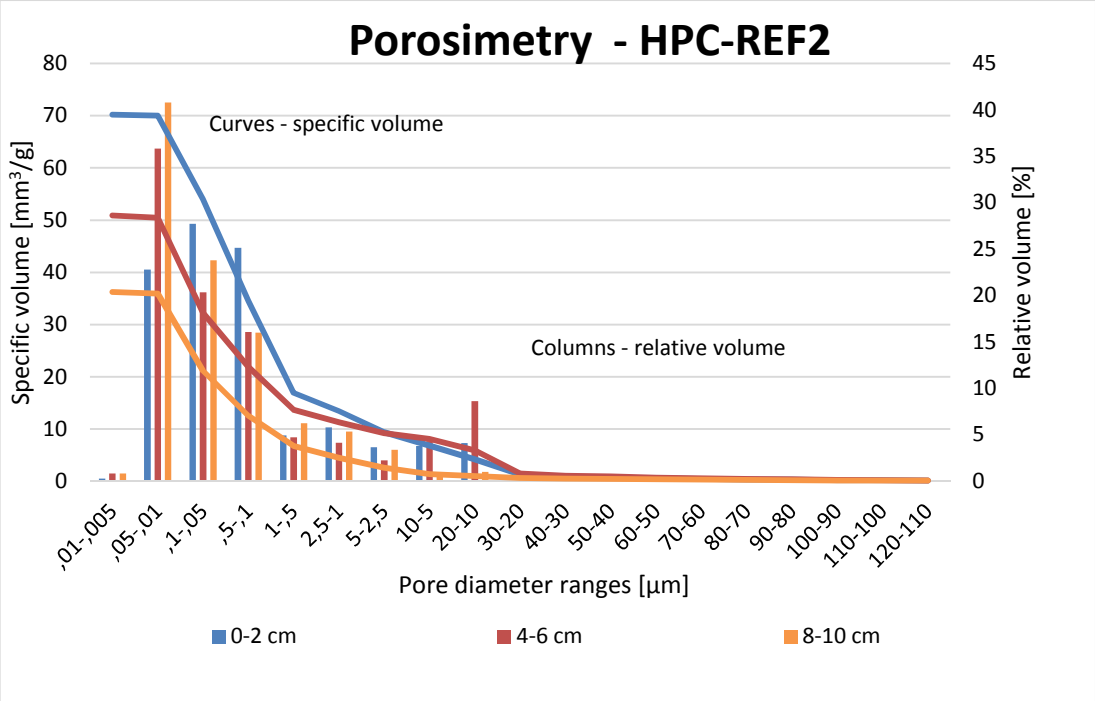

Figure 67: The results of mercury porosimetry showed the expected effect; the highest porosity was in depth 0-2 cm (approx. 700 °C), the part which had the highest temperatures. After that, porosity went equally down. The second highest porosity was 4-6 cm, and the next lowest porosity was 8-10 cm where temperature reached 150 °C.

Specimen HPC-HPR2

Observation of the fire test

- Room temperature: 27 °C Oven temperature: 231 °C
- 4 min. First cracks
- 5min. Other cracks; water coming out of the cracks
- 60 min. End of the test

Figure 67: Time-temperature curves of the specimen HPC-HPR2

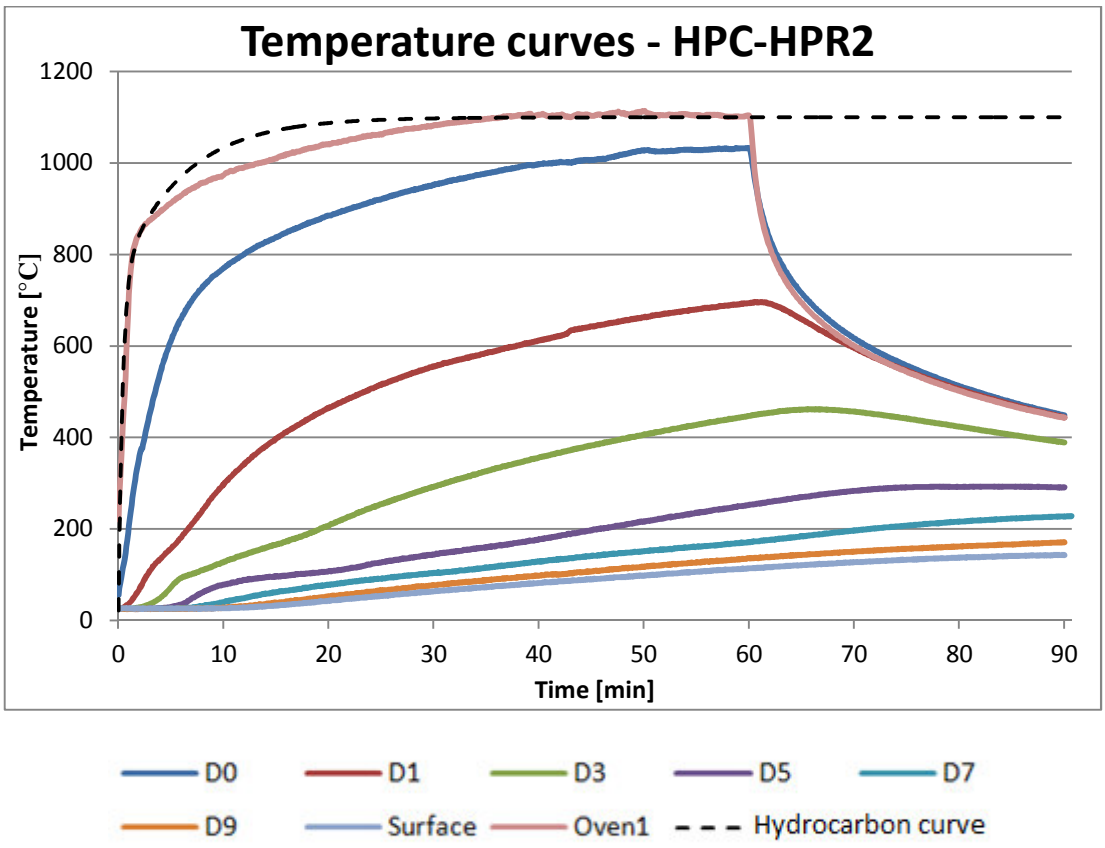

Figure 68: Thermocouples of the specimen HPC-HPR2 did not record any plateaus. Temperature curve D0 is decreasing rapidly after stopping the burner from 1033 °C to 439 °C. The graph shows, that by the end of the measuring, the specimen was not containing any water (temperature above 100 °C).

Temperatures at time 60 minutes

- D0 ca. 1033 °C
- D1 ca. 693 °C
- D3 ca. 447 °C
- D5 ca. 253 °C
- D7 ca. 171 °C
- D9 ca. 135 °C
- Surface ca. 114 °C

Figure 68: Specimen HPC-HPR2 24 hours after the fire test

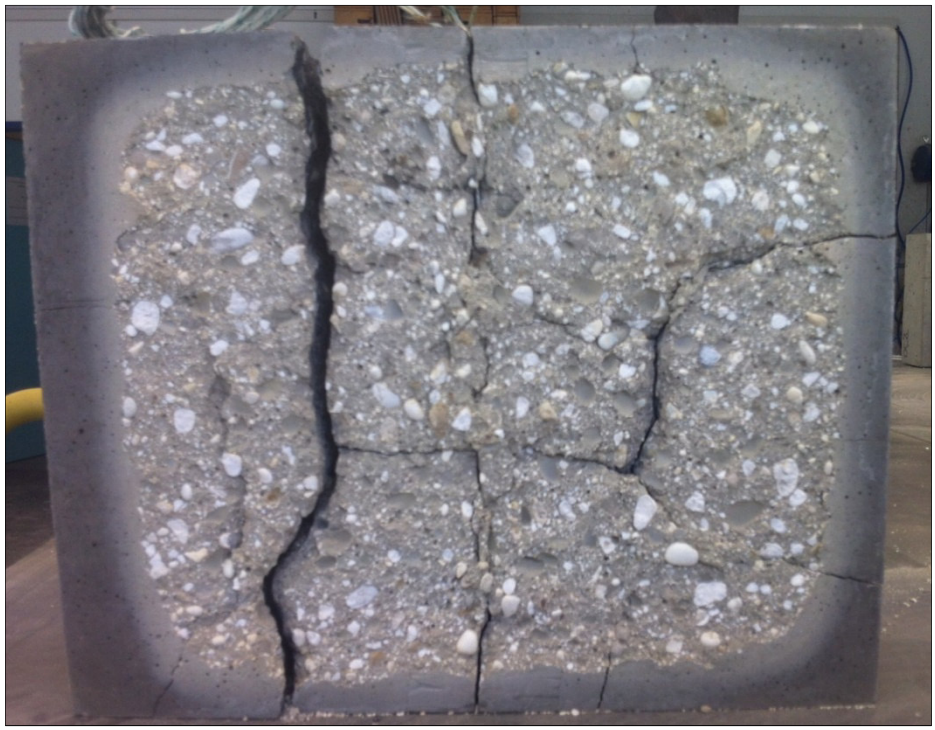

Figure 69: Cut of specimen HPC-HPR2 24 hours after the fire test

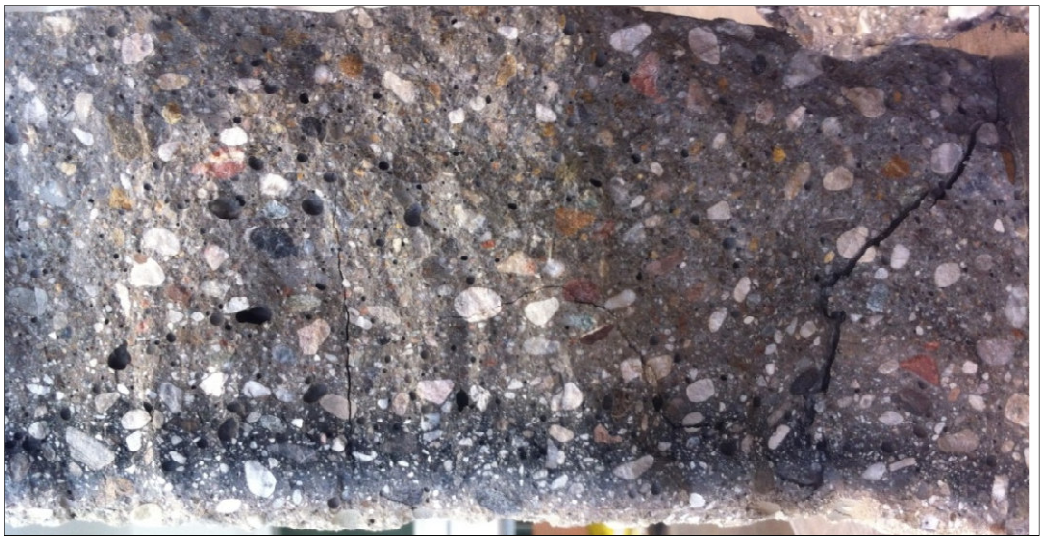

Figure 70: Porosity of specimen HPC-HPR2:

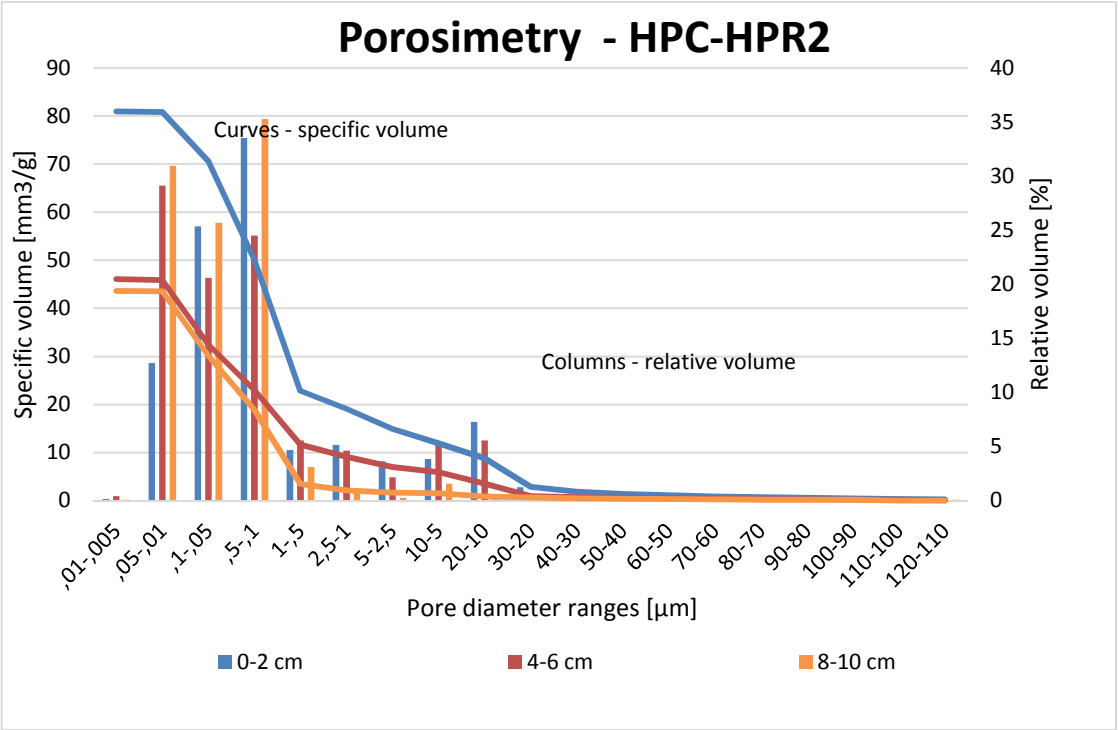

Figure 71: The results of mercury porosimetry showed the expected effect; the highest porosity was in depth 0-2 cm, the part which had the highest temperatures – 690 °C. After that, porosity went equally down. The second highest porosity was 4-6 cm (around 250°C), and the next lowest porosity was 8-10 cm.

Specimen HPC-CEL2

Observation of the fire test

- Room temperature: 26 °C Oven temperature: 240 °C
- 3 min. First cracks
- 4 min. Appearance of more cracks
- 6 min. Water coming from cracks
- 60 min. End of the fire test

Figure 71: Time-temperature curves of the specimen HPC-CEL2

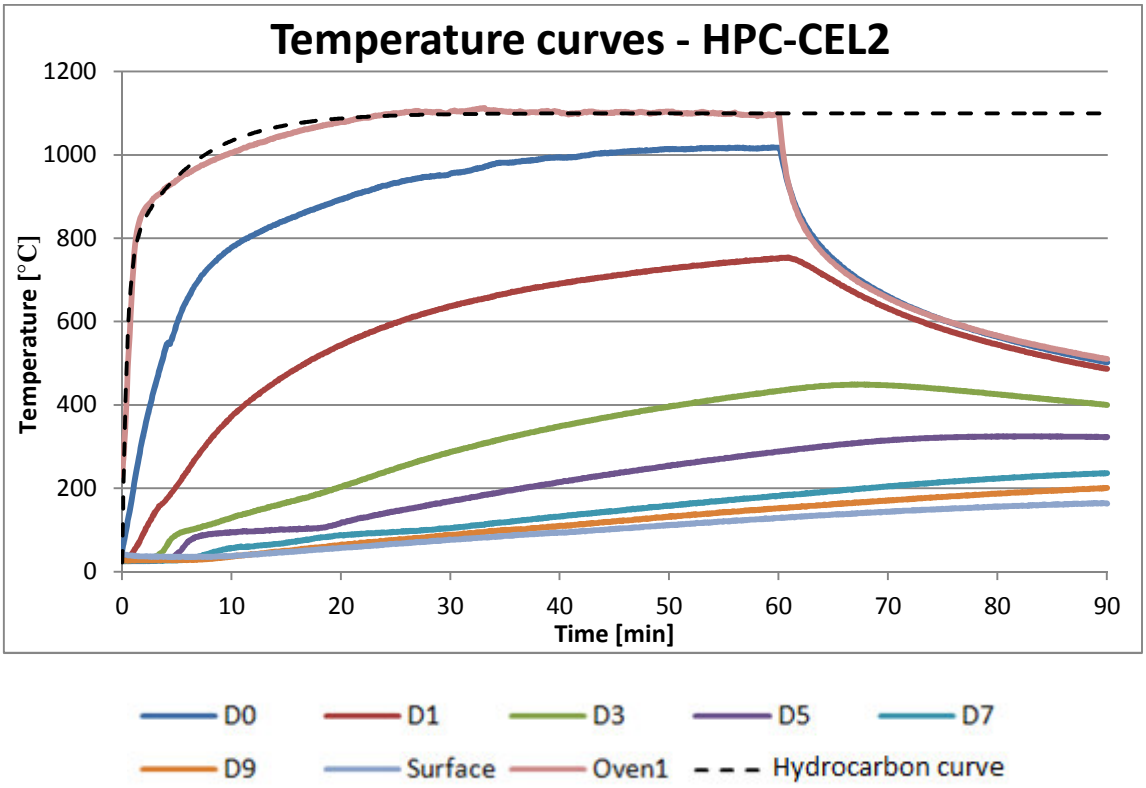

Figure 72: Thermocouple D5 recorded plateau at 100 °C. The maximum temperature was above 1000 °C. This was measured directly on the heated surface of the concrete at time 60 minutes (end of the heating of the specimen).

Temperatures at time 60 minutes (end of the fire test)

- D0 ca. 1018°C
- D1 ca. 753°C
- D3 ca. 435°C
- D5 ca. 288°C
- D7 ca. 181°C
- D9 ca. 153°C
- Surface ca. 130°C

Figure 72: The specimen HPC-CEL 24 hours after the fire test:

Figure 73: Cut of specimen HPC-CEL2 24 hours after the fire test

Figure 74: Porosity of specimen HPC-CEL2

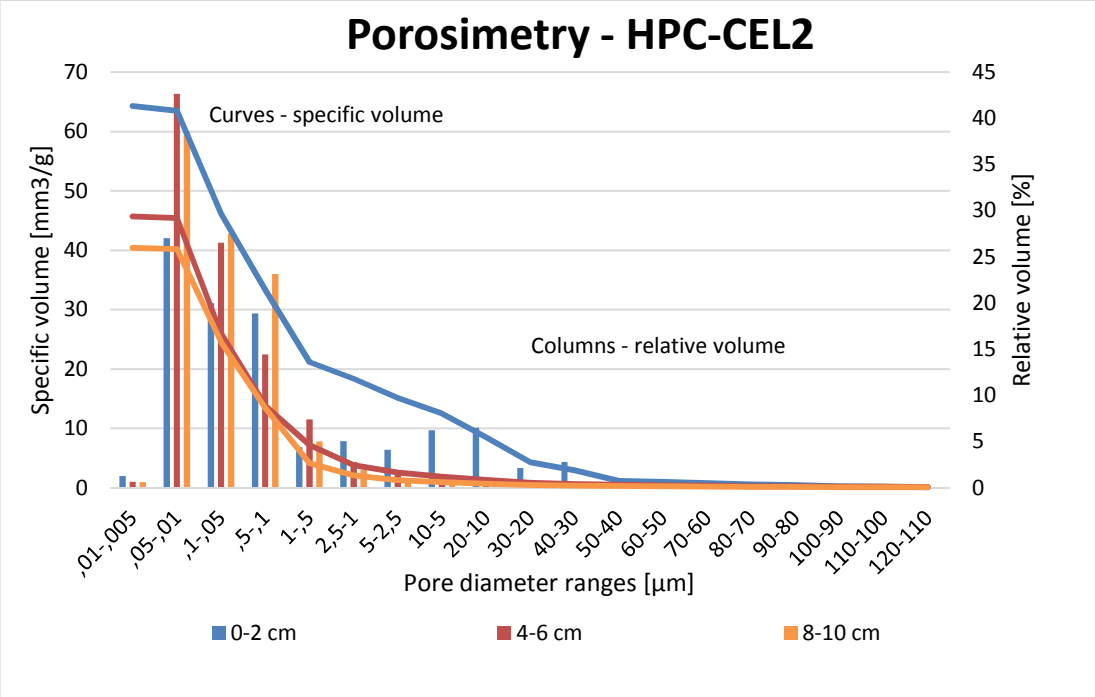

Figure 75: The results of mercury porosimetry showed the expected effect; the highest porosity was in depth 0-2 cm (temperatures around 750 °C), the part which had the highest temperatures. After that, porosity went equally down. The second highest porosity was 4-6 cm, and the next lowest porosity was 8-10 cm where temperature reached 150 °C.

Evaluation

Figure 75: Time-temperature curves in depth 0 cm

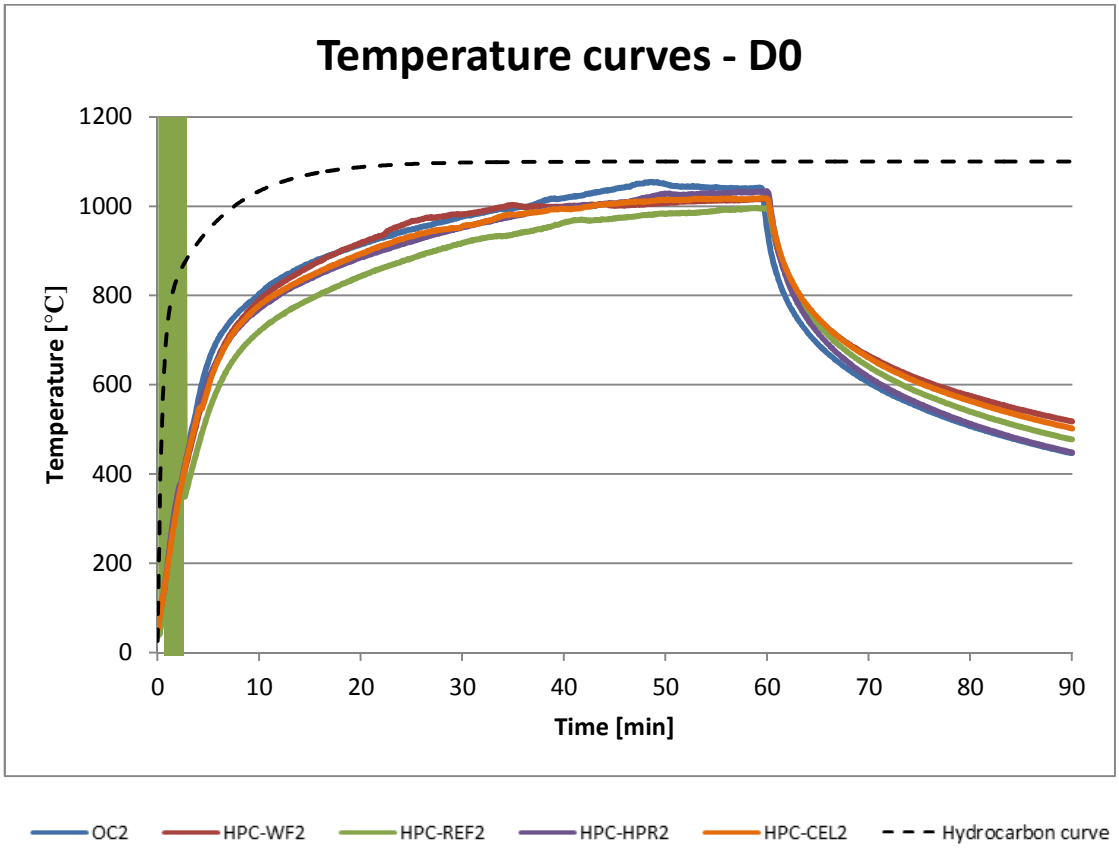

Figure 76: Thermocouple of OC2 measured the highest temperature 1054 °C before the end of the heating (49 minutes). This was the highest temperature of all mixtures. Overall, mixture HPC-REF2 had the lowest temperatures during the heating. Nevertheless, in the cooling part, it was the mixture OC2 that had the lowest temperatures.

Figure 76: Time-temperature curves in depth 1 cm

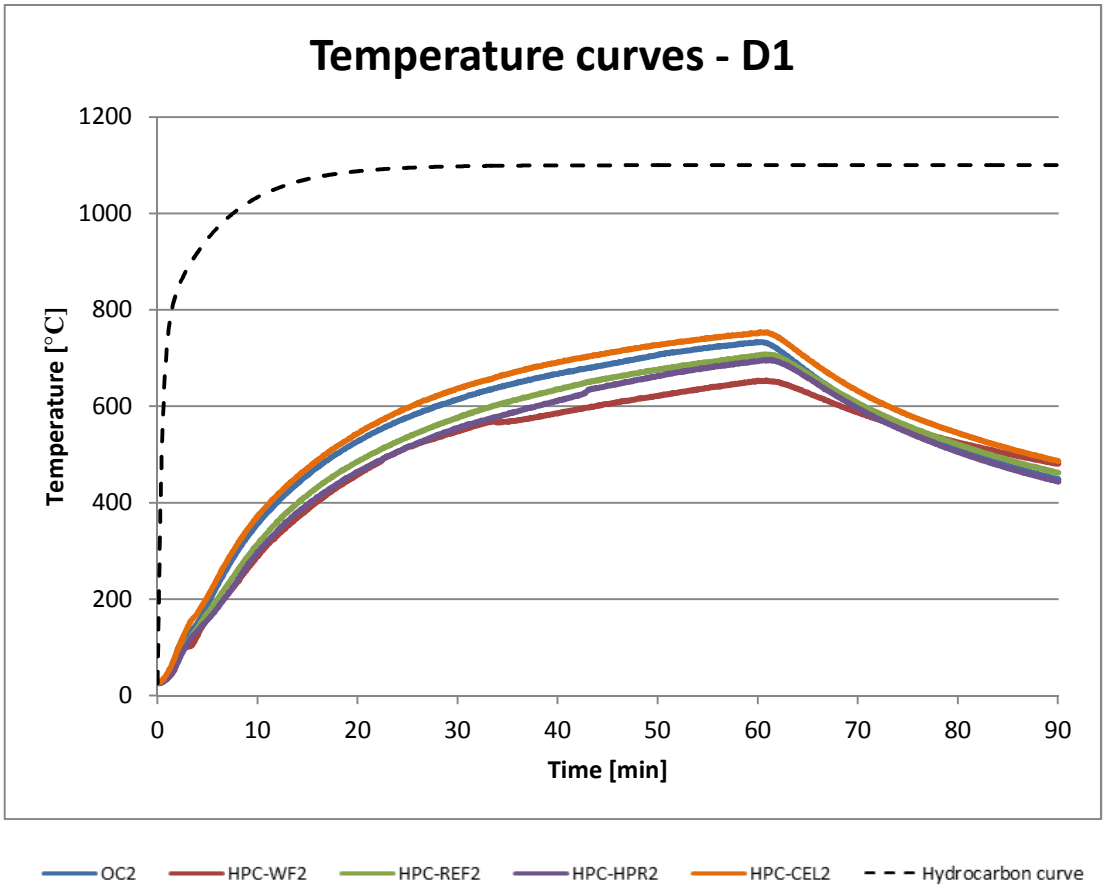

Figure 77: The highest temperature 752 °C was measured with the mixture HPC-CEL2, whereas the lowest temperature was recorded by thermocouple HPC-WF2.

Figure 77: Time-temperature curves in depth 3 cm

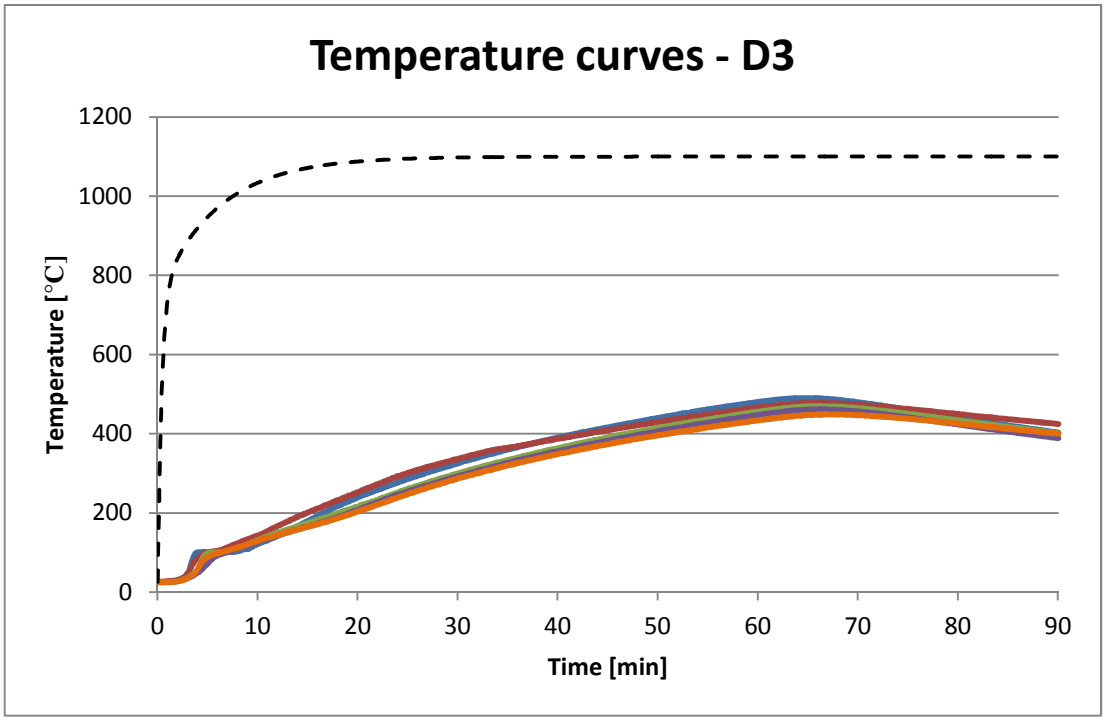

Figure 78: Time-temperature curves in depth 3 cm - detail

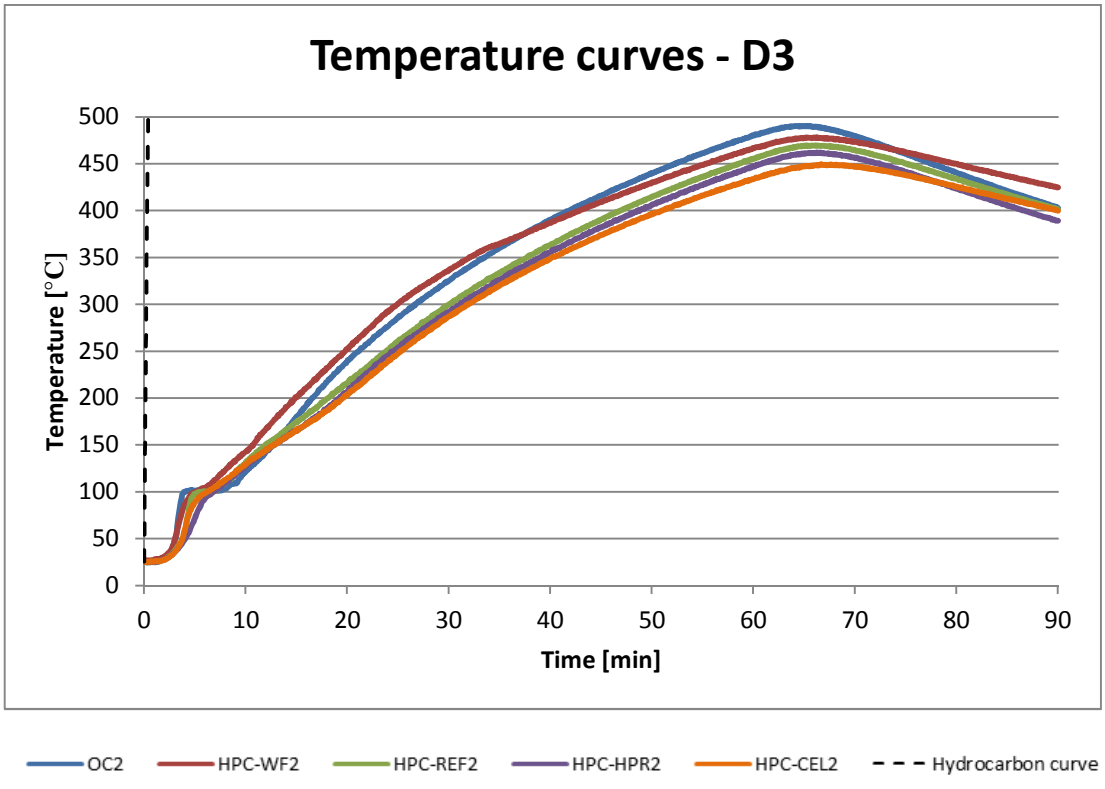

Figure 78, 79: At 100 °C there are small plateaus visible with the mixtures of HPC-REF2 and OC2. The highest temperature 490 °C is reached with the mixture OC2. In 40 °C, the difference is the lowest temperature HPC-CEL2.

Figure 79: Time-temperature curves in depth 5 cm

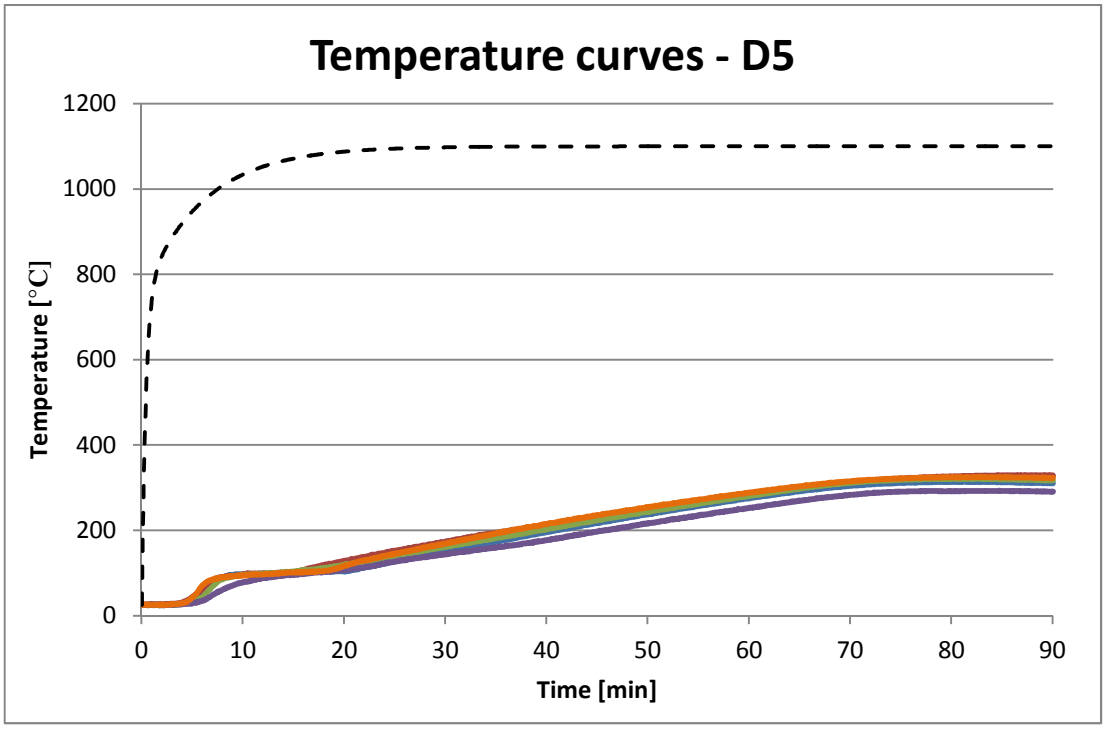

Figure 80: Time-temperature curves in depth 5 cm - detail

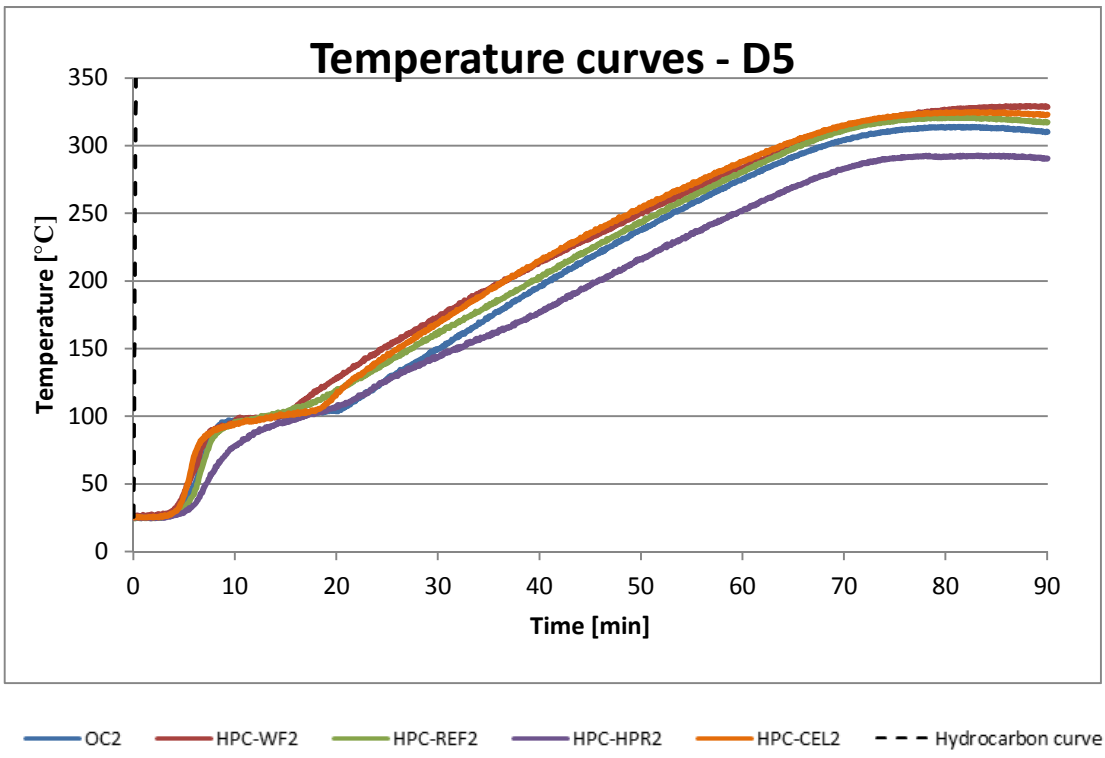

Figure 80, 81: Even though no plateaus with cooling effect appeared at HPC-HPR2, it has the lowest temperatures in depth 5 cm. Large plateau at 100 °C occurred by mixture OC2 it lasted for 10 minutes. All curves were rising for 10 minutes, but then, after stopping the heating part, they remained almost constant.

Figure 81: Time-temperature curves in depth 7 cm

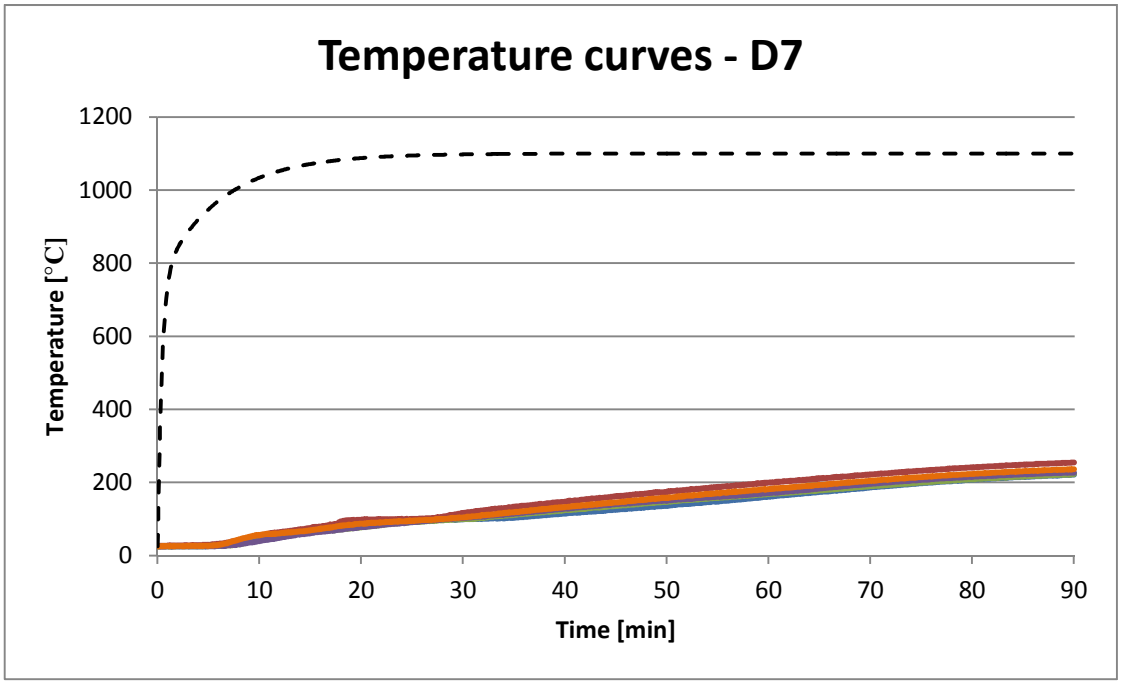

Figure 82: Time-temperature curves in depth 7 cm - detail

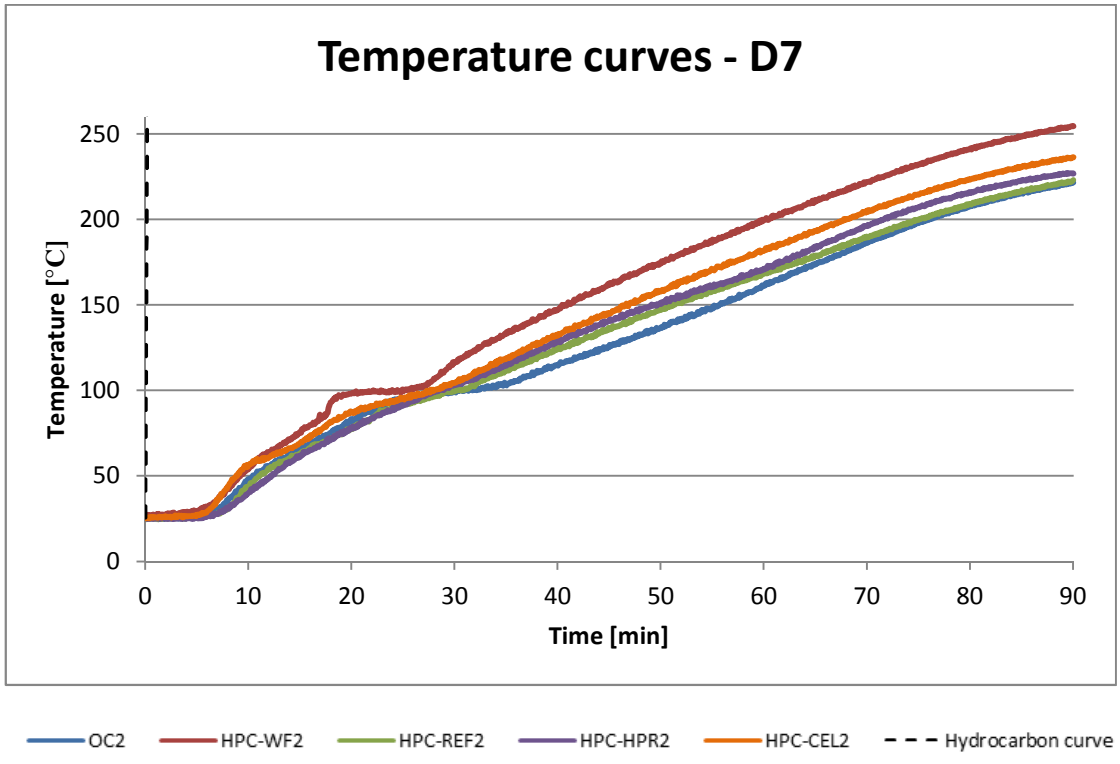

Figure 82, 83: Mixture HPC-WF2 has plateau at 100 °C. After the end of the heating, all temperature curves were constantly increasing.

Figure 83: Time-temperature curves in depth 9 cm

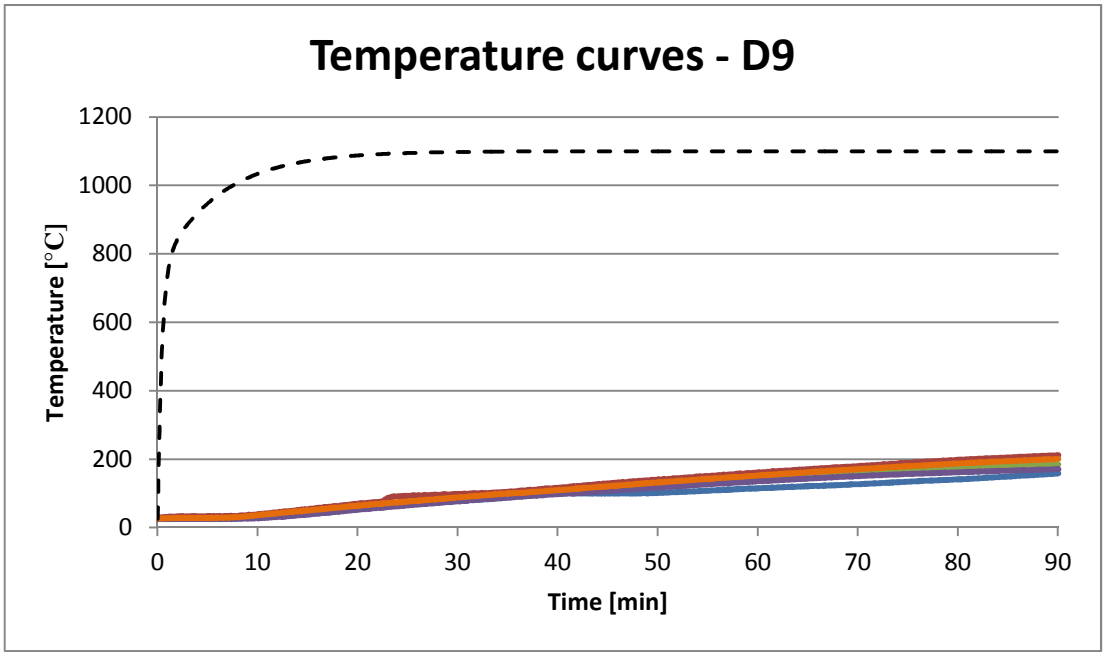

Figure 84: Time-temperature curves in depth 9 cm - detail

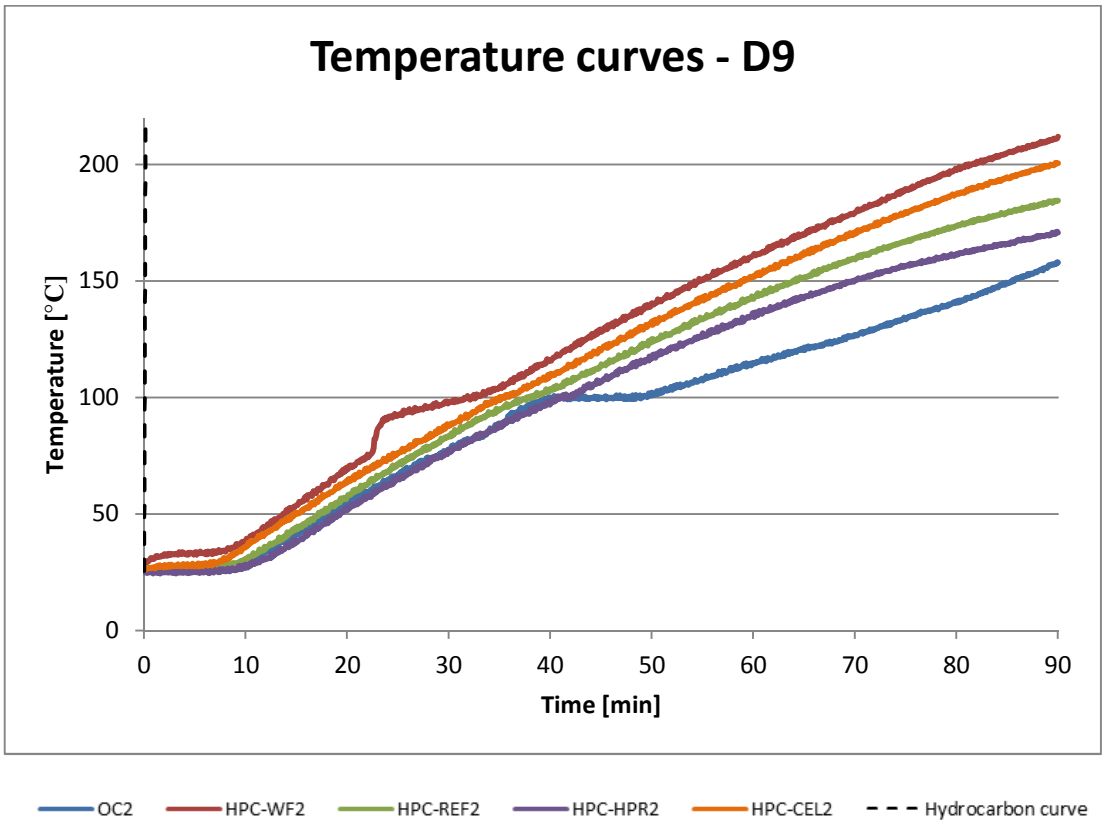

Figure 84, 85: Temperature curve of OC2 has plateau at 100 °C, therefore it had lowest temperature progress of all mixtures. Thermocouple HPC-WF2 has sudden increase of 10 °C in 23 minutes after test begin, this increase may be explained that thermocouple was not working properly for brief period of time.

Figure 85: Time-temperature curves on surface

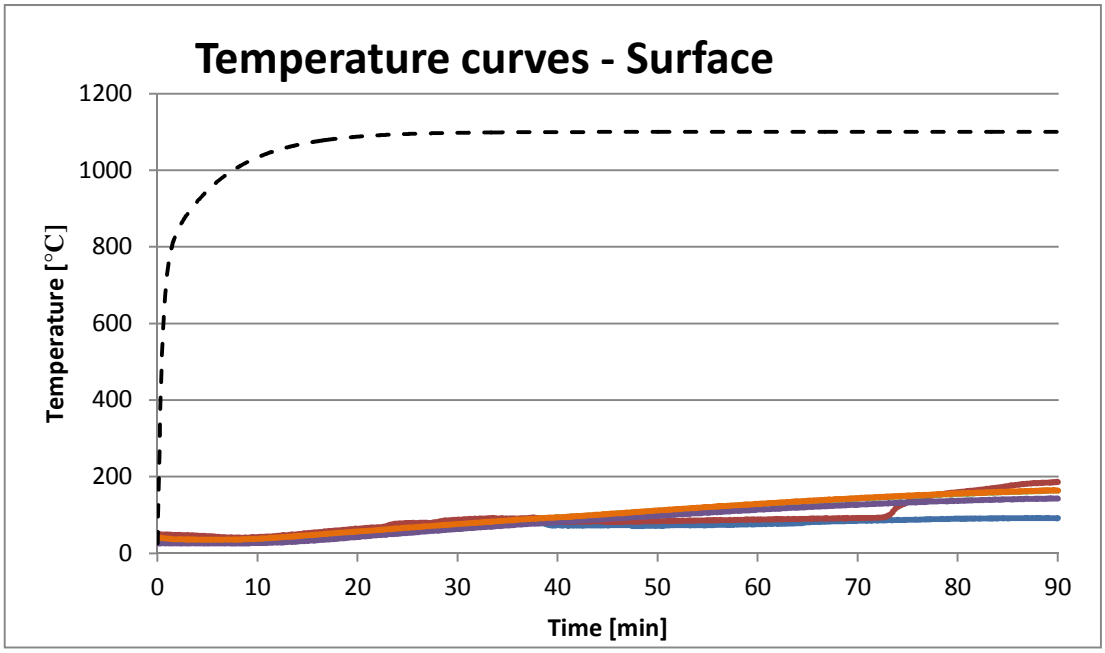

Figure 86: Time-temperature curves on surface - detail

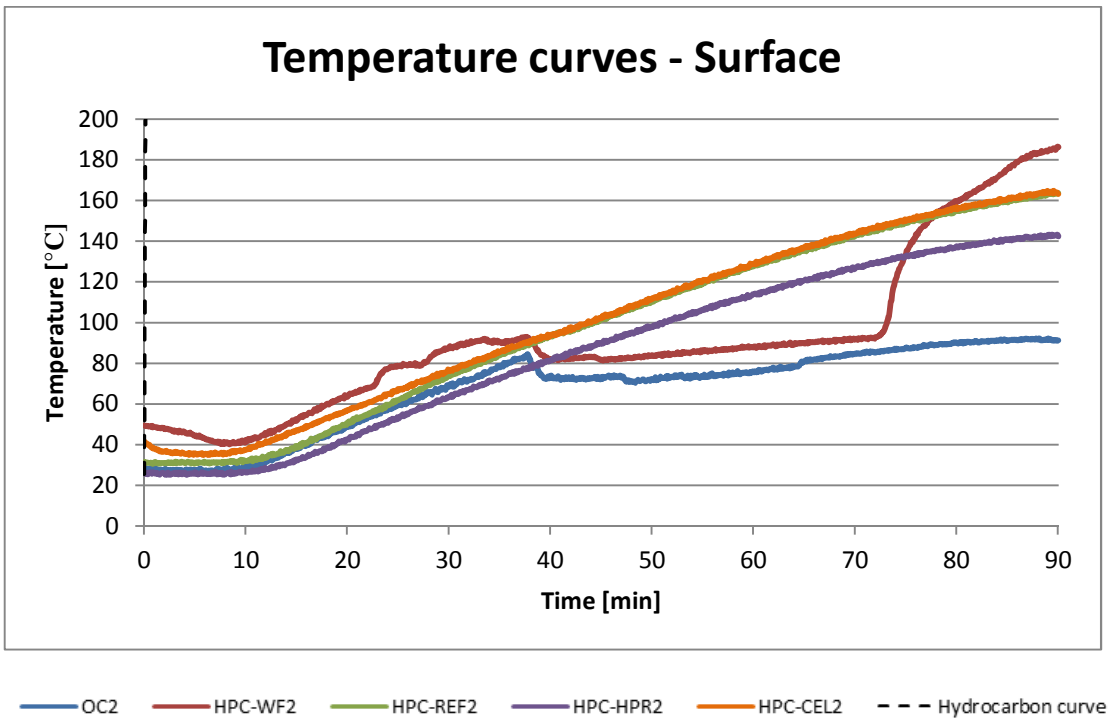

Figure 86, 87: Thermocouples HPC-CEL2 and HPC-WF2 were measuring from the beginning of fire test higher temperature of surface than expected. Thermocouple for measuring surface temperature was probably close to oven, which was pre-heated (approx. 260 °C) to reach hydrocarbon curve or thermocouples were not measuring right values. Thermocouple HPC-WF2 started to measure after 23 minutes temperatures, which cannot

be presume correct. After 38 minutes thermocouple OC2 was also measuring false temperature.

Table 28: Mass loss

	m_1 [kg]	m_2 [kg]	Mass loss [%]
OC2	17,704	16,768	5,3
HPC-WF2	18,426	-	-
HPC-REF2	18,241	17,261	5,4
HPC-HPR2	18,538	17,495	5,6
HPC-CEL2	18,529	17,53	5,4

Table 28: Mass loss of the specimen HPC-WF2 was not recorded because the specimen fell apart into many pieces during manipulation after the fire test. Otherwise, mass loss of the others fluctuated around 5,5 %.

2.4.3 Discussion of results

When you compare the ISO-curve and the hydrocarbon curve, the hydrocarbon curve is steeper and reaches higher temperature of 1100 °C. This fact influences in many ways all of the results after the fire test.

Volume density was as expected the lowest with ordinary concrete (OC), the mixture of high-performance concrete HPC-WF had the highest volume density 2400 kg/m^3, due to its dense structure. The mixtures of high performance concrete with polypropylene fibers had slightly lower volume density. Tensile strength was highest at HPC-WF (9,1 N/mm^2), fibers used in the thesis have no major function in increase of tensile strength, therefore fiber-reinforced concrete had lower tensile strength of 7,1 N/mm^2. The ordinary concrete also had similar results.

Compressive strength was again the highest in the mixture HPC without fibers 121,9 N/mm^2. Compressive strength of the fiber-reinforced concrete fluctuated around 107 N/mm^2. The ordinary concrete mixture was designed to reach a strength class C30/37, but the final compressive strength was 44,8 N/mm^2, which can be classified as C32/40. To compare, a test of compressive strength was made after the fire test. For this test, specimens heated according to ISO-834 were used. It was not possible to obtain a figure in proper dimension for the test of compressive strength from the specimens heated by hydrocarbon curve. Specimen HPC-WF1 was also not possible to use due to explosive spalling. Loss of the compressive strength was the highest in the mixture HPC-REF1 33,8 % and the lowest in high-performance concrete with modified polypropylene fibers 18,7 %. The bad results of mixture HPC-REF1 can have been also influenced by possible cracks after the test in the specimen.

Time-temperature curves were overall higher in the hydrocarbon curve. Massive explosive spalling appeared only with HPC-WF1, where spalling depths reached up to 4,2 cm. Spalling did occur to minor extent with the same mixture. However, the heating occurred according to the hydrocarbon curve. Depths of spalling were not possible to measure, due to the falling apart of the specimen. However, by observing with naked eye, the spalling depths were not as high as with HPC-WF1. With each spalling, one could notice slight decreases of temperature in the oven, which resulted in the heat being spent for heating of the newly exposed layer of concrete. After the heating has finished, temperatures to depths 3 cm were decreasing. In depths 7-10 cm, the temperatures were

still rising from residual heat. In 5 cm, the temperatures remained constant which was again due to residual heat coming from the specimen. In some depths, plateaus appeared at 100 °C. The appearance of plateaus indicates the possibility of almost no spalling due to the reduction of pressure in the concrete. Interesting fact is that HPC-WF1 had plateaus, but the spalling still occurred.

The mass loss was the highest in the mixture HPC-WF1 16,2 %. This mixture was the only one where explosive spalling occurred. Therefore, the mass loss is the highest of all mixtures. The mass loss of other mixtures was almost comparable. The mixture OC1 had the lowest mass loss – 3,8 %. On the other hand, specimens heated according to the hydrocarbon curve had mass losses around 5,5 %. Only the specimen of high-performance concrete without fibers had no value, because the specimen had fallen apart to too many pieces. Higher mass loss of specimen heated according to the hydrocarbon curve was in total higher than heated ISO-834 probably for longer and intense heat, therefore water bonded in any form had more possibility to leave.

Significant color changes did not occur with any specimen heated according to the ISO-curve. Color changes showed up at every specimen heated according to the hydrocarbon curve. The surface that was exposed to the heat was whitish and due to calcination process $CaCO_3$ it turns to lime and gives pale shades of white and grey. After the lime is exposed to CO_2 from the air, it goes back to whitish $CaCO_3$. This effect can be seen in all pictures, 24 hours after the exposure to high temperature. It is more significant with the specimen heated according to the hydrocarbon curve, since the temperatures were higher (around 800 °C). Black part, which occurred 0,5-2,5 cm, cannot be acceptable explained. Another color changes that were observed was a part of concrete, also roughly 3-5 cm, that turned reddish. This part of concrete was influenced by iron contained in the fine aggregate or the coarse aggregate. The hydrate starts to dissolve and the iron starts to get oxidized at this temperature. Almost no color changes were visible in depths 8-10 cm, since the temperature was not that high to cause color changes. Because of the higher temperatures reached by hydrocarbon curve, these samples were chosen for mercury porosimetry.

The results of mercury porosimetry showed the expected effect; the highest porosity was in depth 0-2 cm, the part which had the highest temperatures. After that, porosity went equally down. The second highest porosity was 4-6 cm, and the next lowest porosity was 8-10 cm. Ordinary concrete had the highest porosity in depth 8-10 cm, then 0-2 cm and the lowest porosity was recorded in depth 4-6 cm. This could have been caused by wrong

preparation of the samples (for depths 0-2, 4-6 cm), since bigger part of the aggregate might have been present in the samples, resulting in smaller porosity. The highest porosity of all specimens had mixture with modified polypropylene fibers. This is a result of creating more pores after fibers burned out of specimen. Lowest porosity was recorded with cellulose fibers. All results of mercury porosimetry could have been influenced by possible presence of aggregate.

CONCLUSION

The master's thesis was concerned with a study of the behavior of concrete at high temperatures and with given processes in each element of concrete at high temperature. The theoretical part also included explosive spalling of concrete which occurred especially with high performance concrete. Explosive spalling was intensively studied during the last decade. Spalling of concrete, especially in the case of high performance concrete (HPC), may be prevented by technological measures based on the addition of small amounts of PP-fibers or cellulose fibers. The effect of fibers was explained in the theoretical part. Due to our experience, we propose the following that emerged from the experiments carried out to eliminate explosive spalling of concrete structures exposed to elevated temperature:

- Modified polypropylene fibers with lower melting point has better influence on preventing of explosive spalling than ordinary polypropylene fibers of the same dosage (2 kg per m^3)
- Cellulose fibers give positive results as an alternative to prevent explosive spalling, but the results are not as remarkable as with the specimens with polypropylene fibers

For further and wider research, it might be beneficial to include different curing treatment of the concrete before the test and after the test with shocking cooling of the specimen. Other tests can be also included, such as measuring permeability and more tests for each material of the concrete mixtures. The behavior of concrete subjected to high temperatures is not entirely understood nowadays and an attempt to clarify this issue is still in process. Even though many experiments have already been released, it is still difficult to interpret the results due to the facts that the tested concretes are different, the test procedures are different, the test condition are not comparable, the interpretation of results is not clear enough, the description of the test procedures are incomplete, and size and shape of specimens are incomparable.

LIST OF REFERENCES

[1] http://www.ita-aites.cz [online]. [cit. 2017-11-29].

http://www.ita-aites.cz/files/tunel/2007/1/tunel-0701-6.pdf

[2] Directive 2004/54/EC of the European Parliament and of the Council on Minimum Safety. Requirements for Tunnels in the Trans-European Road Network, April 2004, Brussels, Belgium

[3] Eurocode 1: Actions on structures - Part 1-2: General actions - Actions on structures exposed to fire; German version EN 1991-1-2:2002 + AC:2009

[4] Eurocode 2: Design of concrete structures- Part 1-2: General rules-Structural fire design; German version EN 1992-1-2:2004 + AC:2008

[5] EN 13501-1:2007: Fire classification of construction products and building elements - Part 1: Classification using test data from fire reaction to fire tests

[6] *Types of fire exposure* [online]. , 1 [cit. 2017-01-10]. Available from: http://www.promat-tunnel.com/en/advices/fire-protection/fire%20curves

[7] EUREKA-Bericht zu EU 499 Firetun: Fire inTransport Tunnels, Report on Full- Scale Tests, Studiengesellschaft für Stahlanwendung, Düsseldorf, 1996.

[8] BRADÁČOVÁ, I. *Stavby z hlediska požární bezpečnosti*. 1. vyd. Brno: ERA group, 2007. ISBN 978-80-7366-090-1.

[9] HELA, R, L BODNÁROVÁ, K KŘÍŽOVÁ a J VÁLEK. Vytvoření postupů a receptur pro použití betonu s vyšší trvanlivostí vůči působení vysokých teplot v konstrukcích. *Dílčí výzkumná zpráva za rok 2010, CIDEAS – Centrum integrovaného navrhování progresivních stavebních konstrukcí.* november 2010.

[10] HELA, R, L BODNÁROVÁ A I HAGER. *New generation cement concretes*. Košice, june 2009. ISBN 978-80-214-388-3.

[11] HAGER, I.:Behavior of high performance concretes at high temperature – evolution of mechanical properties, disertační práce, Národní škola mostů a silnic, november 2004, 182 s.

[12] BODNÁROVÁ, Lenka, Jaroslav VÁLEK, Libor SITEK a Josef FOLDYNA. *Effect of high temperatures on cementious composite materials in concrete stuctures*. Acta Geodyn. Geomater [online]. 2012, (2) [cit. 2015-05-24]. DOI: 10.13168/AGG.2013.0017. Available from: https://www.irsm.cas.cz/materialy/acta_content/2013_doi/Bodnarova_AGG_2013_0 017.pdf

[13] FIALA, Jiří. *Studium chování betonů při působení vysokých teplot* [online]. Brno, 2015 [cit. 2015-05-24]. Available from: https://www.vutbr.cz/www_base/zav_prace_soubor_verejne.php?file_id=96863. Diploma thesis.

[14] SCHNEIDER, Ulrich. *Repairability of fire damaged structures*. Kassel: Kassel : Gesamthochsch.-Bibliothek, 1989. ISBN 3-88122-499-8.

[15] International Federation for Structural Concrete Working Party 4.3.1 *Materials Structures and Modelling, Fire design of concrete structures - materials, structures and modelling*. Bulletin 38. 2007, Lausanne: Fédération internationale du béton. 97 P.

[16] Klingsch, E., A. Frangi, and M. Fontana, *Ordinary and High-Performance Concrete: Hot Strength and Residual Strength after cooling from high Temperatures*, in Befestigungstechnik Bewehrungstechnik und... Festschrift zu Ehren von Prof. Dr.-Ing. Rolf Eligehausen anlässlich seines 60. Geburtstages. , W. Fuchs and J. Hofmann, Editors. 2012.

[17] Gary, M., *Brandproben an Eisenbetonbauten: Ausgeführt im königl*. Materialprüfungsamt zu BerlinLichterfelde-West in d. Jahren 1914 u. 1915 - Deutscher Ausschuss für Eisenbeton Heft 33. 1916: Ernst und Sohn.

[18] ISO 834-1-1999 *Fire-resistance test - elements of building construction*. 2002: International Organization for Standardization.

[19] Meyer-Ottens, C., Zur Frage der Abplatzungen an Betonbauteilen aus Normalbeton bei Brandbeanspruchung. 1972, Braunschweig. 90 P.

[20] Connolly, R.J., *The spalling of concrete in fires*., PhD theisis - University of Aston in Birmingham, 1995

[21] Klingsch, E. and M. Fontana, Explosive spalling of concrete cylinders - internal IBK test report (unpublished). 2013.

[22] Mechanical properties of concrete at high temperature—A review. *Construction and Building Materials*. 2015.

[23] Consolazio GR, McVay MC, Rish III JW. Measurement and prediction of pore pressures in saturated

[24] U. Schneider, Research Report vol.9, Vienna University of Technology, Institute for building materials, buildings physic and fire protection, Institute 206.

[25] KLINGSCH, Eike. *EXPLOSIVE SPALLING OF CONCRETE IN FIRE* [online]. Zürich, 2014 [cit. 2017-01-10]. Available from: http://e-collection.library.ethz.ch/eserv/eth:8557/eth-8557-02.pdf

[26] *Passive Fire Protection vs. Active Fire Protection* [online]. [cit. 2017-01-10]. Available from: http://www.lifesafetyservices.com/active-vs-passive-fire-protection-2/

[27] Polypropylen. *Wikipedia: the free encyclopedia* [online]. San Francisco (CA): Wikimedia Foundation, 2001- [cit. 2016-01-10]. Available from: http://cs.wikipedia.org/wiki/Polypropylen

[28] SOVOVÁ, Kateřina. *STUDIUM CHOVÁNÍ CEMENTOVÝCH BETONŮ PŘI PŮSOBENÍ VYSOKÝCH TEPLOT* [online]. 2015, Brno [cit. 2017-01-10]. Available from: https://www.vutbr.cz/www_base/zav_prace_soubor_verejne.php?file_id=108634

[29] P. Kalifa, G. Chéné, C. Gallé, *High temperature behaviour of HPC with polypropylene fibres*: from spalling to microstructure, Cement and Concrete Research 31 (2001) 1487–1499.

[30] DVOŘÁKOVÁ, Michaela. *BEHAVIOR OF CONCRETE AT HIGH TEMPERATURES* [online]. 2015, Brno [cit. 2017-01-10]. Available from:

https://www.vutbr.cz/www_base/zav_prace_soubor_verejne.php?file_id=79830

[31] *What is cellulose?* [online]. [cit. 2017-01-10]. Available from: http://antoine.frostburg.edu/chem/senese/101/consumer/faq/what-is-cellulose.shtml

[32] *ULTRAFIBER 500* [online]. [cit. 2017-01-10]. Available from: http://www.solomoncolors.com/Products/Fiber-Reinforcement/UltraFiber-500/

[33] DER CONTRAGRESS CEM I 52,5 N. *Lafarge* [online]. [cit. 2017-01-10]. Available from: http://www.lafarge.at/zement/produkte/der-contragress-525-n/

[34] Elkem Microsilica® Grade 940 for fibre cement. *Elkem* [online]. [cit. 2017-01-10]. Available from: https://www.elkem.com/silicon-materials/fibre-cement/microsilica-grade-940/

[35] Produktliste. *Bodenkalk* [online]. [cit. 2017-01-10]. Available from: http://bodenkalk.at/Produkte/Produktliste.pdf

[36] Spezialfasern für die Bauindustrie. *Baumhueter-extrusion* [online]. [cit. 2017-01-10]. Available from: http://baumhueter-extrusion.de/content/216/43/produkte/pb-eurofiber

[37] CHRYSO® Fibre UF-500. *Alchelm* [online]. [cit. 2017-01-10]. Available from: https://www.alchem.al/wp-content/uploads/2016/07/Chryso-Fibre-UF-500-EN.pdf

LIST OF FIGURES

FIGURE 1: TEMPERATURE- TIME CURVES FOR FIRE [6] 14

FIGURE 2: THE STRUCTURE OF HPC COMPOSED OF SILICATE-LIME AGGREGATES HEATED UP TO 600 °C (SEM, 50X) [11] 19

FIGURE 3: MODEL OF CSH PHASE [10] 20

FIGURE 4: DIAGRAM OF COMPRESSIVE STRENGTH RELATED TO TEMPERATURE [14] 23

FIGURE 5: EXPLOSIVE SPALLING [25] 26

FIGURE 6: CORNER SPALLING [20] 26

FIGURE 7: POST COOLING SPALLING [21] 27

FIGURE 8: SPALLING OF CONCRETE INDUCED BY PORE VAPOR PRESSURE [22] 28

FIGURE 9: DIFFERENCE OF PRESSURE AND MOISTURE DISTRIBUTION IN ORDINARY CONCRETE AND HIGH PERFORMANCE CONCRETE [24] 29

FIGURE 10: DTA, TGA AND DIFFERENTIAL THERMO-GRAVIMETRIC ANALYSIS (DTG) [29] 33

FIGURE 11: A) MONOFILAMENT FIBERS B) FIBRILLATED FIBERS [28] 34

FIGURE 12: THE AIR CONTENT OF FRESH CONCRETE RELATED TO DOSAGE OF PP FIBERS [30] 34

FIGURE 13: DENSITY OF CONCRETE RELATED TO DOSAGE OF PP FIBERS [30] 35

FIGURE 14: COMPRESSIVE STRENGTH RELATED TO DOSAGE OF PP FIBERS [30] 35

FIGURE 15: SCHEMATIC DESCRIPTION OF "THEORY OF PERMEATION" [24] 36

FIGURE 16: CELLULOSE FIBERS [32] 37

FIGURE 17: PARTICLE SIZE DISTRIBUTION OF LIMESTONE POWDER KSM H 100 [35] 41

FIGURE 18: PREPARED THERMOCOUPLE 44

FIGURE 19: SCHEME OF THERMOCOUPLES D1-D9 IN MOLD 45

FIGURE 20: PREPARED MOLD WITH THERMOCOUPLES 45

FIGURE 21: INTENSIVE MIXER EIRICH R08W 47

FIGURE 22: VOLUME DENSITY OF CONCRETE RELATED TO THE MIXTURE 48

FIGURE 23: COMPRESSIVE STRENGTH AFTER 28 DAYS RELATED TO THE MIXTURE 48

FIGURE 24: TENSILE STRENGTH AFTER 28 DAYS RELATED TO THE MIXTURE 49

FIGURE 25: OVEN 50

FIGURE 26: TIME-TEMPERATURE CURVE ISO – 834 [6] 51

FIGURE 27: TIME-TEMPERATURE CURVES OF SPECIMEN OC1 52

FIGURE 28: SPECIMEN OC1 24 HOURS AFTER THE FIRE TEST 53

FIGURE 29: TIME-TEMPERATURE CURVES OF THE SPECIMEN HPC-WF1 55

FIGURE 30: SPECIMEN HPC-WF1 - AFTER LAST SPALLING 56

FIGURE 31: SPECIMEN HPC-WF1 – DETAIL OF CRACK 56

FIGURE 32: SPECIMEN HPC-WF1 - 24 HOURS AFTER THE FIRE TEST 57

FIGURE 33: SPALLING DEPTHS OF THE SPECIMEN HPC-WF1 57

FIGURE 34: TIME-TEMPERATURE CURVES OF THE SPECIMEN HPC-REF1 59

FIGURE 35: SPECIMEN HPC-REF1 DURING THE FIRE TEST 60
FIGURE 36: SPECIMEN HPC-REF1 24 HOURS AFTER THE FIRE TEST 60
FIGURE 37: TIME-TEMPERATURE CURVES OF THE SPECIMEN HPC-HPR1 62
FIGURE 38: SPECIMEN HPC-HPR1 24 HOURS AFTER THE FIRE TEST 63
FIGURE 39: TIME-TEMPERATURE CURVES OF SPECIMEN HPC-CEL1 64
FIGURE 40: SPECIMEN HPC-CEL DURING FIRE TEST 65
FIGURE 41: SPECIMEN HPC-CEL 24 HOURS AFTER THE FIRE TEST 65
FIGURE 43: TIME-TEMPERATURE CURVES IN DEPTH 0 CM 66
FIGURE 44: TIME-TEMPERATURE CURVES IN DEPTH 1 CM 67
FIGURE 45: TIME-TEMPERATURE CURVES IN DEPTH 3 CM 68
FIGURE 46: TIME-TEMPERATURE CURVES IN DEPTH 3 CM - DETAIL 68
FIGURE 47: TIME-TEMPERATURE CURVES IN DEPTH 5 CM 69
FIGURE 48: TIME-TEMPERATURE CURVES IN DEPTH 5 CM - DETAIL 69
FIGURE 49: TIME-TEMPERATURE CURVES IN DEPTH 7CM 70
FIGURE 50: TIME-TEMPERATURE CURVES IN DEPTH 7CM - DETAIL 70
FIGURE 51: TIME-TEMPERATURE CURVES IN DEPTH 9 CM 71
FIGURE 52: TIME-TEMPERATURE CURVES IN DEPTH 9 CM - DETAIL 71
FIGURE 53: TIME-TEMPERATURE CURVES ON SURFACE 72
FIGURE 54: TIME-TEMPERATURE CURVES ON SURFACE - DETAIL 72
FIGURE 55: THE COMPRESSIVE STRENGTH AFTER THE FIRE TEST RELATED TO THE MIXTURE 73
FIGURE 56: TIME-TEMPERATURE HYDROCARBON CURVE [6] 75
FIGURE 57: TIME-TEMPERATURE CURVES OF THE SPECIMEN OC1 76
FIGURE 58: SPECIMEN OC2 DURING THE FIRE TEST 77
FIGURE 59: SPECIMEN OC2 24 HOURS AFTER THE FIRE TEST 77
FIGURE 60: POROSITY OF SPECIMEN OC2 78
FIGURE 61: TIME-TEMPERATURE CURVES OF THE SPECIMEN HPC-WF2 79
FIGURE 62: SPECIMEN HPC-WF1 - 24 HOURS AFTER THE FIRE TEST 80
FIGURE 63: POROSITY OF SPECIMEN HPC-WF2 81
FIGURE 64: TIME-TEMPERATURE CURVES OF THE SPECIMEN HPC-REF2 82
FIGURE 65: SPECIMEN HPC-REF2 24 HOURS AFTER THE FIRE TEST 83
FIGURE 66: CUT OF SPECIMEN HPC-REF2 24 HOURS AFTER THE FIRE TEST 84
FIGURE 67: POROSITY OF SPECIMEN HPC-REF2 85
FIGURE 68: TIME-TEMPERATURE CURVES OF THE SPECIMEN HPC-HPR2 86
FIGURE 69: SPECIMEN HPC-HPR2 24 HOURS AFTER THE FIRE TEST 87
FIGURE 70: CUT OF SPECIMEN HPC-HPR2 24 HOURS AFTER THE FIRE TEST 88
FIGURE 71: POROSITY OF SPECIMEN HPC-HPR2: 88
FIGURE 72: TIME-TEMPERATURE CURVES OF THE SPECIMEN HPC-CEL2 89
FIGURE 73: THE SPECIMEN HPC-CEL 24 HOURS AFTER THE FIRE TEST: 90

FIGURE 74: CUT OF SPECIMEN HPC-CEL2 24 HOURS AFTER THE FIRE TEST 90
FIGURE 75: POROSITY OF SPECIMEN HPC-CEL2 91
FIGURE 76: TIME-TEMPERATURE CURVES IN DEPTH 0 CM 92
FIGURE 77: TIME-TEMPERATURE CURVES IN DEPTH 1 CM 93
FIGURE 78: TIME-TEMPERATURE CURVES IN DEPTH 3 CM 94
FIGURE 79: TIME-TEMPERATURE CURVES IN DEPTH 3 CM - DETAIL 94
FIGURE 80: TIME-TEMPERATURE CURVES IN DEPTH 5 CM 95
FIGURE 81: TIME-TEMPERATURE CURVES IN DEPTH 5 CM - DETAIL 95
FIGURE 82: TIME-TEMPERATURE CURVES IN DEPTH 7 CM 96
FIGURE 83: TIME-TEMPERATURE CURVES IN DEPTH 7 CM - DETAIL 96
FIGURE 84: TIME-TEMPERATURE CURVES IN DEPTH 9 CM 97
FIGURE 85: TIME-TEMPERATURE CURVES IN DEPTH 9 CM - DETAIL 97
FIGURE 86: TIME-TEMPERATURE CURVES ON SURFACE 98
FIGURE 87: TIME-TEMPERATURE CURVES ON SURFACE - DETAIL 98

LIST OF TABLES

TABLE 1: CHANGES OF CONCRETE RELATED TO TEMPERATURE [10] 18

TABLE 2: COEFFICIENT OF LINEAR THERMAL EXPANSION FOR DIFFERENT TYPES OF ROCKS [9] 21

TABLE 3: PROCESSES IN AGGREGATES DURING THERMAL LOAD [13] 22

TABLE 4: SPALLING CHARACTERISTICS BY KHOURY [15]..... 26

TABLE 5: MATERIAL RELATED PARAMETERS [25] 30

TABLE 6: STRUCTURAL /MECHANICAL PARAMETERS RELATED TO INFLUENCE ON SPALLING [25] 31

TABLE 7: HEATINGS PARAMETERS RELATED TO INFLUENCE ON SPALLING [25]..... 31

TABLE 8: PROPERTIES OF CEMENT CEM I 42,5 N C3A FREI [33] 40

TABLE 9: CHEMICAL AND PHYSICAL PROPERTIES OF MICROSILICA ELKEM 940 U [34]..... 41

TABLE 10: CHEMICAL ANALYSIS OF LIMESTONE POWDER KSM H 100 [35] 42

TABLE 11:MINERALOGICAL ANALYSIS OF AGGREGATE 42

TABLE 12: CHARACTERISTICS PB EUROFIBER HPR..... 43

TABLE 13: CHARACTERISTICS PB EUROFIBER 43

TABLE 14: CHARAKTERISTICS CHRYSO® FIBRE UF-500 [37]..... 44

TABLE 15: MIX DESIGN OF HIGH PERFORMANCE CONCRETE 46

TABLE 16: MIX DESIGN OF CONCRETE C30/37 46

TABLE 17: CHARACTERISTICS BEFORE THE FIRE TEST 47

TABLE 18: CHARACTERISTICS OF SPECIMEN OC1 BEFORE THE FIRE TEST 52

TABLE 19: CHARACTERISTICS OF SPECIMEN OC1 AFTER THE FIRE TEST 53

TABLE 20: CHARACTERISTICS OF SPECIMEN HPC-WF1 BEFORE THE FIRE TEST 54

TABLE 21: CHARACTERISTICS OF SPECIMEN HPC-WF1 AFTER THE FIRE TEST 58

TABLE 22: CHARACTERISTICS OF SPECIMEN HPC-REF1 BEFORE THE FIRE TEST 59

TABLE 23 : CHARACTERISTICS OF THE SPECIMEN HPC-REF1 AFTER THE FIRE TEST 61

TABLE 24: CHARACTERISTICS OF THE SPECIMEN HPC-REF1 BEFORE THE FIRE TEST..... 62

TABLE 25: TIME-TEMPERATURE CURVES OF THE SPECIMEN HPC-HPR1..... **CHYBA! ZÁLOŽKA NENÍ DEFINOVÁNA.**

TABLE 26 : CHARACTERISTICS OF THE SPECIMEN HPC-CEL1 BEFORE THE FIRE TEST 64

TABLE 27: CHARACTERISTICS OF SPECIMENS BEFORE AND AFTER THE FIRE TEST 73

TABLE 28: MASS LOSS..... 99

LIST OF ACRONYMS AND SYMBOLS

OC	Ordinary concrete
HPC	High performance concrete
PP	polypropylene fibers
PCE	polycarboxylate